GL00032-1

UNITED STATES DEPARTMENT OF THE INTERIOR
GEOLOGICAL SURVEY

GEOLOGY AND PORPHYRY COPPER-TYPE ALTERATION-

MINERALIZATION OF IGNEOUS ROCKS AT THE

CHRISTMAS MINE, GILA COUNTY, ARIZONA

By

Randolph Allan Koski

Open-File Report

79-844

This report is preliminary
and has not been edited or
reviewed for conformity with
Geological Survey standards

ABSTRACT

The Christmas copper deposit, located in southern Gila County, Arizona, is part of the major porphyry copper province of southwestern North America. Although Christmas is known for skarn deposits in Paleozoic carbonate rocks, ore-grade porphyry-type copper mineralization also occurs in a composite granodioritic intrusive complex and adjacent mafic volcanic country rocks. This study considers the nature, distribution, and genesis of alteration-mineralization in the igneous rock environment at Christmas.

At the southeast end of the Dripping Spring Mountains, the Pennsylvanian Naco Limestone is unconformably overlain by the Cretaceous Williamson Canyon Volcanics, a westward-thinning sequence of basaltic volcanic breccia and lava flows, and subordinate clastic sedimentary rocks. Paleozoic and Mesozoic strata are intruded by Laramide-age dikes, sills, and small stocks of hornblende andesite porphyry and hornblende rhyodacite porphyry, and the mineralized Christmas intrusive complex.

Rocks of the elongate Christmas stock, intruded along an east-northeast-trending fracture zone, are grouped into early, veined quartz diorite (Dark Phase), biotite granodiorite porphyry (Light Phase), and granodiorite; and late, unveined dacite porphyry and granodiorite porphyry. Biotite rhyodacite porphyry dikes extending east and west from the vicinity of the stock are probably coeval with biotite granodiorite porphyry. Accumulated normal displacement of approximately 1 km along the northwest-trending Christmas-Joker fault

ii

system has juxtaposed contrasting levels (lower, intrusive-carbonate rock environment and upper, intrusive-volcanic rock environment) within the porphyry copper system.

K-Ar age determinations and whole-rock chemical analyses of the major intrusive rock types indicate that Laramide calc-alkaline magmatism and ore deposition at Christmas evolved over an extended period from within the Late Cretaceous ($\sim$75-80 m.y. ago) to early Paleocene ($\sim$63-61 m.y. ago). The sequence of igneous rocks is progressively more alkaline and silicic from basalt to granodiorite.

Early (Stage I) chalcopyrite-bornite (-molybdenite) mineralization and genetically related K-silicate alteration are centered on the Christmas stock. K-silicate alteration is manifested by pervasive hornblende-destructive biotitization in the stock, biotitization of basaltic volcanic wall rocks, and a continuous stockwork of K-feldspar veinlets and quartz-K-feldspar veins in the stock and quartz-sulfide veins in volcanic rocks. Younger (Stage II) pyrite-chalcopyrite mineralization and quartz-sericite-chlorite alteration occur in a zone overlapping with but largely peripheral to the zone of Stage I stockwork veins. Within the Christmas intrusive complex, K-silicate-altered rocks in the central stock are flanked east and west by zones of fracture-controlled quartz-sericite alteration and strong pyritization. In volcanic rocks quartz-chlorite-pyrite-chalcopyrite veins are superimposed on earlier biotitization and crosscut Stage I quartz-sulfide veins. Beyond the zones of quartz-sericite alteration, biotite rhyodacite porphyry dikes contain the propylitic alteration assemblage epidote-chlorite-albite-sphene.

Chemical analyses indicate the following changes during pervasive alteration of igneous rocks: (1) addition of Si, K, H, S, and Cu, and loss of Fe^{3+} and Ca during intense biotitization of basalt; (2) loss of Na and Ca, increase of Fe^{3+}/Fe^{2+}, and strong H-metasomatism during sericitization of quartz diorite; and (3) increase in Ca, Na, and Fe^{3+}/Fe^{2+}, and loss of K during intense propylitization of biotite rhyodacite porphyry dikes. Thorough biotitization of biotite granodiorite porphyry in the Christmas stock was largely an isochemical process.

Fluid-inclusion petrography reveals that Stage I veins are characterized by low to moderate populations of moderate-salinity and gas-rich inclusions, and sparse but ubiquitous halite-bearing inclusions. Moderate-salinity and gas-rich inclusions become less abundant, and halite-bearing inclusions are absent in Stage II veins. The distribution of gas-rich inclusions suggests that fluids were boiling during Stage I mineralization, particularly at higher levels in the porphyry copper system.

A sequential two-stage model for intrusion, alteration, and mineralization at Christmas is proposed. During Stage I, K-silicate alteration, stockwork veining, and chalcopyrite-bornite mineralization were broadly contemporaneous with emplacement of quartz diorite and repeated surges of biotite granodiorite porphyry. The fracture-controlled, predominantly hydrolitic alteration and high total sulfide, pyrite-chalcopyrite mineralization of Stage II probably commenced with the first significant incursion of ground water into the porphyry copper system. A convection cell model may reasonably account for the distri-

bution of Stage II alteration and mineralization.

At Christmas the tendency to form biotite during K-metasomatism of basalt has greatly expanded the dimensions of the K-silicate alteration zone. The recognition and interpretation of secondary biotite in mafic volcanic terranes should be an important contribution to future exploration for porphyry copper deposits in the region.

ACKNOWLEDGMENTS

TABLE OF CONTENTS

TABLE OF CONTENTS-CONTINUED

LIST OF TABLES

LIST OF ILLUSTRATIONS

LIST OF ILLUSTRATIONS-CONTINUED

INTRODUCTION

The Christmas copper deposit is part of the major porphyry
copper province of southwestern North America. The deposit is located
in a steep-sided canyon at the southeast end of the Dripping Spring
Mountains in southern Gila County, Arizona (Figure 1). Christmas and
several other mines in the southeastern Dripping Spring Mountains,
most notably the Seventy Nine, Chilito, and London-Arizona, constitute
the Banner mining district. The closest major porphyry copper deposit
is at Ray, approximately 27 km to the northwest. The nearest communi-
ties, Winkelman and Hayden, are 8 km to the south, and Globe is 37 km
to the north. The mine is accessible by paved secondary road from
State Highway 77 which follows the Gila River canyon north of Winkelman.
Most of the open-pit mine and support facilities at Christmas are
located in the west-central portion of the Christmas 7.5-minute quad-
rangle, but the total map area discussed in this study straddles the
boundary between the Christmas and Hayden quadrangles (Figure 1).

Mining History

The colorful, copper-bearing skarns cropping out at the surface
in an isolated canyon near the Gila River presented an inviting target
for early prospectors. The first mining activity took place in the

1
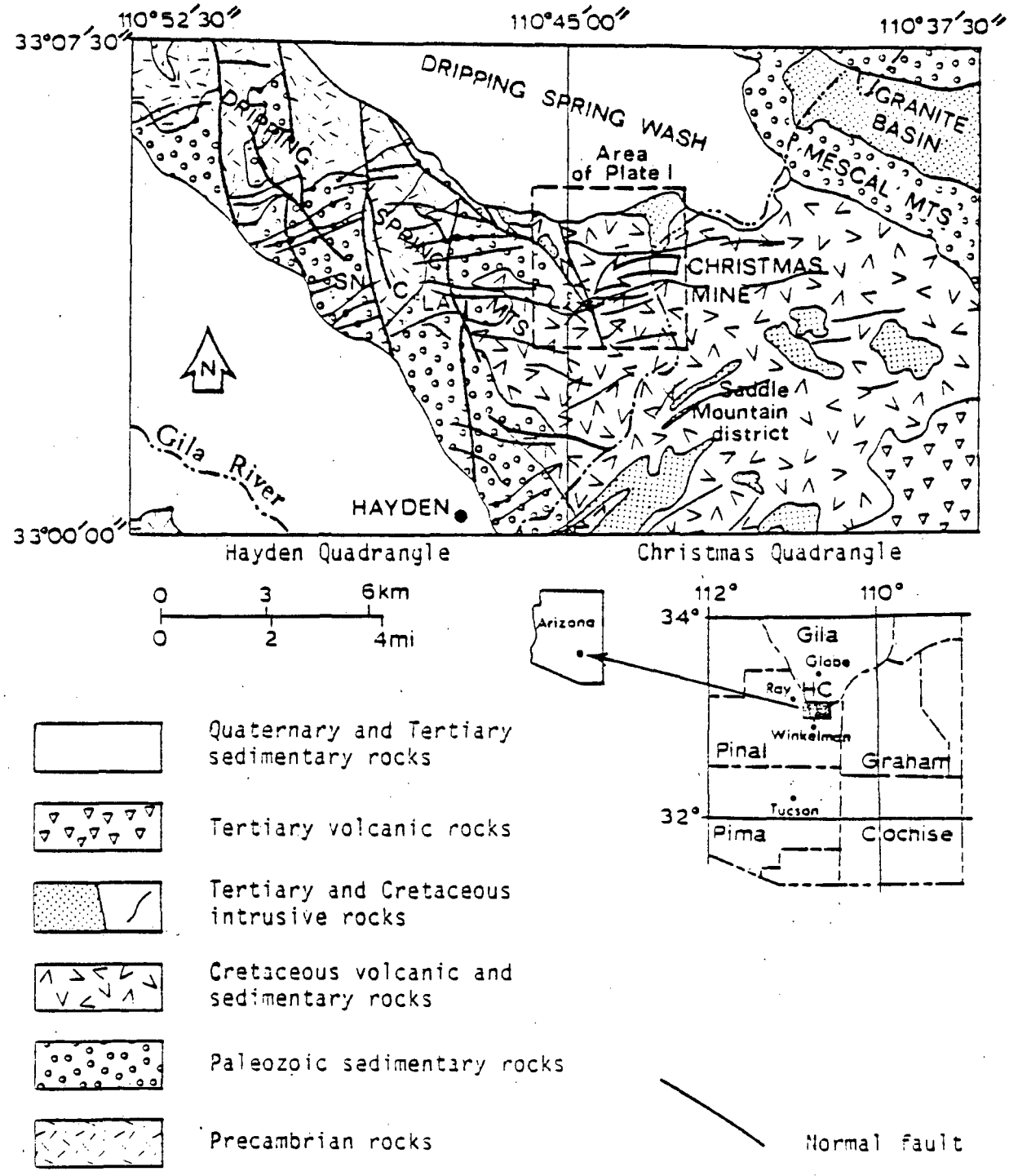
Figure 1. Generalized regional geology near Christmas. Geology of the Hayden quadrangle from Banks and Krieger (1977); geology of the Christmas quadrangle from Willden (1964). SN = Seventy Nine mine; C = Chilito mine; and LA = London-Arizona mine.

early 1880's, but territorial land use disputes prevented any substantial development until the enterprising G. B. Chittendon staked the property for the Saddle Mountain Mining Company on Christmas morning, 1902, the day for which the property was named. Mining activity by a succession of small and short-lived companies was intermittent during the early 1900's, largely due to unstable economic conditions, low copper prices, lack of sufficient working capital, and geographic isolation. After the Depression, production stabilized with the shipment of high lime fluxing ore to the nearby Asarco smelter at Hayden. Ore mined through 1940 came mainly from skarn deposits in the Naco Limestone above the 800-foot mine level.

During World War II the U.S. Bureau of Mines and the U.S. Geological Survey conducted detailed studies of the skarn ore bodies. Deep drilling below the 800 level revealed extensive ore horizons in the Escabrosa and Martin Limestones. Development of deeper levels, however, did not begin until the property was purchased by the Inspiration Consolidated Copper Company in 1955. Additional exploration by Inspiration confirmed the presence of significant ore reserves at depth, particularly in the rich "O'Carroll bed" at the base of the Martin Limestone. Underground workings were extended to the 1,600-foot level by 1962. Inspiration began surface mining above the site of the old underground workings in 1965, and shortly afterward, underground operations were terminated; all production now comes from an elongate open pit centered on the Naco Limestone-Christmas stock contact (Figure 3).

Christmas is the major producer of copper ore in the Banner mining district. From the early 1900's through 1966, underground mining of the skarn ore bodies produced 4.6 million tons of ore yielding 144.5 million pounds of copper. The open pit has produced 15.8 million tons of ore and 160.6 million pounds of copper in the period 1966-1976. Small amounts of gold, silver, and selenium have also been recovered. The open pit ore, a mixture of 95 percent sedimentary and 5 percent intrusive rock, averages 0.60 percent Cu. In early 1977 production was averaging 6,000 tons per day with a stripping ratio of 5:1. Copper concentrates milled at Christmas are trucked to Inspiration's smelter in Miami, Arizona.

The Inspiration Consolidated Copper Company Annual Report for 1975 lists reserves totalling 819 million pounds of copper, 70 percent of which remains unmined underground. Inspiration has also announced (Annual Report, 1974) the discovery of a "large low-grade orebody" located "close to the present Christmas open pit mine." The principal host rocks are intermediate intrusive and mafic volcanic rocks east of the Christmas-Joker fault system. Some of the near-surface ores in this deposit are oxidized necessitating the implementation of a dump leaching recovery process. A small-scale pilot leaching program was initiated at Christmas in 1976.

Previous Work

The geology, ore deposits, and mining activity of the Ray-
Christmas region were first reported by Ransome (1919, 1923) and Ross
(1925). Their excellent field descriptions and detailed mine evalua-
tions are the foundation for all subsequent studies. These early re-
searchers noted the variety of shallow level porphyritic intrusions;
and recognized their genetic importance with respect to ore deposits.
Ransome (1923) observed that these bodies "... have themselves been
altered by the ore-bearing solutions, and, where favorably situated,
have been changed into protore ... and ... it is from these larger and
deeper masses ... that most of the energy and at least part of the
materials were derived to form the protore."

A quadrangle mapping program conducted by the U.S. Geological
Survey in the Ray-Winkelman-San Manuel area provides a regional geo-
logic framework. Willden (1964) mapped and described the geology in
the Christmas 15-minute quadrangle which contains the Christmas mine
area and the contiguous Saddle Mountain mining district to the south-
east (see Figure 1). Near Christmas, several .7.5-minute quadrangles
have been mapped including Hayden (Banks and Krieger, 1977), El Capitan
(Cornwall and Krieger, in press), Winkelman (Krieger, 1974), and
Saddle Mountain (Krieger, 1968).

In a detailed field study of the Saddle Mountain mining dis-
trict, Barrett (1972) established alteration and sulfide mineraliza-
tion patterns along Laramide dikes intruding Cretaceous volcanic rocks.

The Christmas copper deposit has been described in published

reports by Tainter (1948), Peterson and Swanson (1956), Eastlick (1968), and Perry (1969), and unpublished theses by Perry (1968) and McCurry (1971). These studies have emphasized aspects of mineralization in carbonate wall rocks. In a comprehensive report on the geology of the Banner mining district, Eastlick (1968) focused on the form, mineralogy, and paragenesis of the skarn ore bodies at Christmas. Eastlick also recognized "normal porphyry-type alteration" represented by "secondary biotite in the andesite and the alteration of the diorite into an aggregate of sericite and secondary quartz."

In his detailed study of skarn genesis, Perry (1968, 1969) defined three types of skarn: (1) magnesian skarn in dolomitic limestone; (2) calcian skarn in relatively pure limestone; and (3) endoskarn in granodioritic intrusive rocks in contact with altered sedimentary rocks. Perry classified Christmas as a "complex" porphyry copper deposit (after Titley, 1966) with mineralization in both the intrusive and intruded rocks. Much additional information exists on the Christmas deposit in the form of unpublished maps and reports prepared by the geologic staff of the Inspiration Consolidated Copper Company.

Regional Geology

Christmas occurs in a zone of topographic transition within the Mountain subprovince of the Basin and Range physiographic province (Ransome, 1923). To the west and north, upraised Precambrian and

Paleozoic strata form the sharply etched Dripping Spring and Mescal ranges, whereas rolling, subdued topography is characteristic of the terrane developed on overlapping Cretaceous volcanic rocks to the east, south, and southeast. The narrow Gila River canyon is cut perpendicular to the northwest-trending axes of the Dripping Spring and Mescal Mountains, and the intervening Dripping Spring Wash. Elevations in the two quadrangles shown in Figure 1 range from 1,850 feet (560 m) at the Gila River to 4,700 feet (1420 m) along the crest of the Dripping Spring Mountains.

A diagrammatic geologic section for the region is shown in Figure 2. Older Precambrian rocks forming the core of the Dripping Spring Mountains and adjacent ranges consist of highly deformed Pinal Schist and plutons of batholithic proportions, principally the Ruin Granite. Conglomerate, shale, quartzite, limestone, and basalt flows belonging to the younger Precambrian Apache Group, and the Troy Quartzite unconformably overlie the crystalline basement rocks. Diabase, the youngest rock type of Precambrian age, intrudes all of the previously mentioned rocks, commonly occurring as sills dilating the Apache Group or as tabular masses in the Ruin Granite.

Diabase sills from the Sierra Ancha region of Arizona have been dated at 1,150 m.y. using the U-Pb method for zircon (Silver, 1963), and 1,140 m.y. using the K-Ar method for biotite (Damon and others, 1962). However, Banks and others (1972) report a somewhat younger K-Ar age of 1,040 m.y. for biotite from diabase near Miami, Arizona.

A depositional hiatus of approximately 500 m.y. separates the
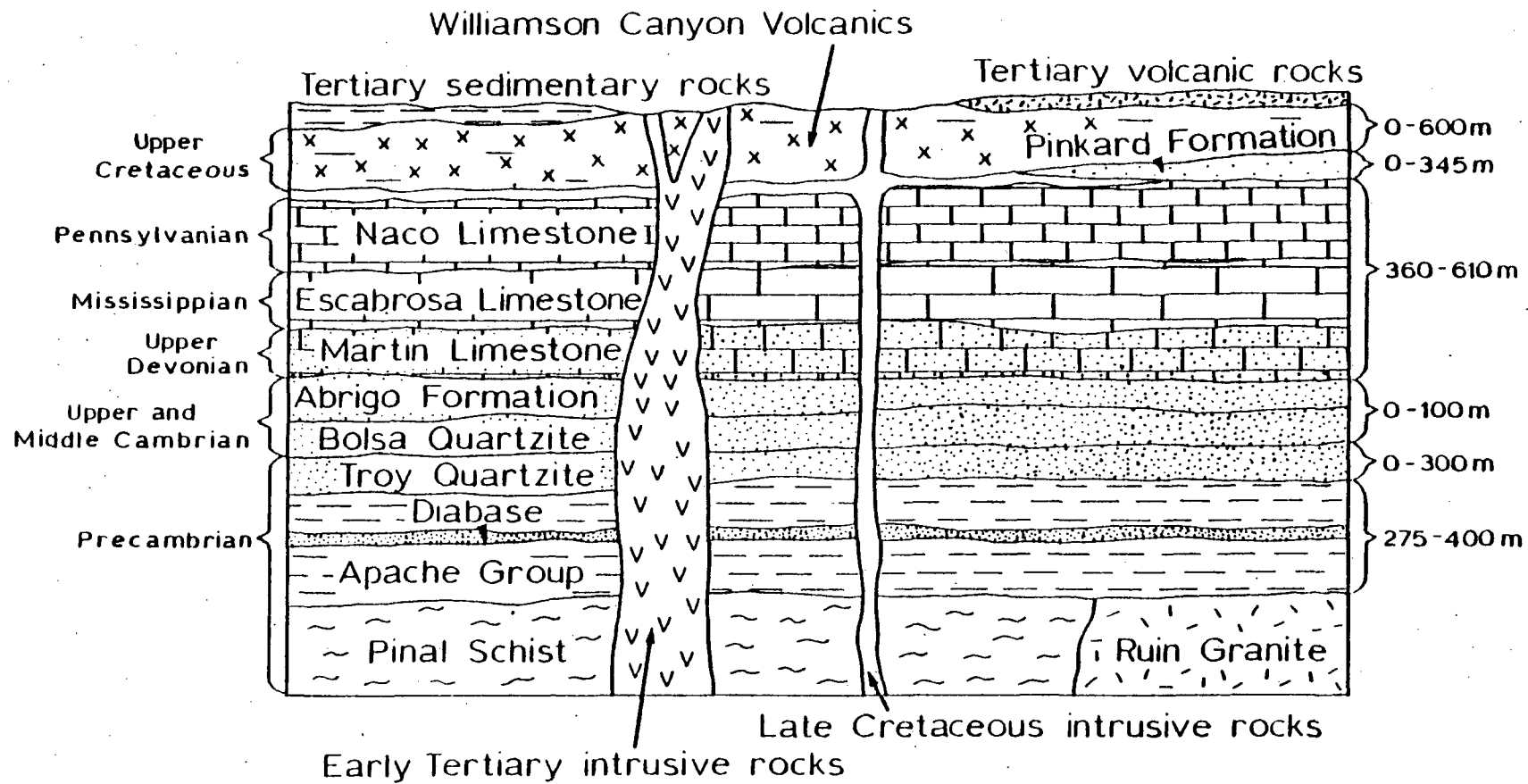
Figure 2. Diagrammatic geologic section for the region around Christmas.

Labels within figure

Williamson Canyon Volcanics

Tertiary sedimentary rocks

Tertiary volcanic rocks

Upper Cretaceous

Pennsylvanian

Mississippian

Upper Devonian

Upper and Middle Cambrian

Precambrian

Naco Limestone

Escabrosa Limestone

Martin Limestone

Abrigo Formation

Bolsa Quartzite

Troy Quartzite

Diabase

Apache Group

Pinal Schist

Pinkard Formation

Ruin Granite

0-600 m
0-345 m
360-610 m
0-100 m
0-300 m
275-400 m

Early Tertiary intrusive rocks

Late Cretaceous intrusive rocks

8

Precambrian Troy Quartzite from the basal Paleozoic formations, the

Middle Cambrian Bolsa Quartzite and overlying clastic sedimentary rocks

of the Middle and Upper Cambrian Abrigo Formation. Ordovician and

Silurian rocks were not deposited in this part of Arizona, or were

removed by pre-Devonian erosion.

The combined thickness of the dolomitic Upper Devonian Martin

Limestone, Mississippian Escabrosa Limestone, and Pennsylvanian

(-Permian?) Naco Limestone varies between 360-610 m in the Dripping

Spring Mountains (Banks and Krieger, 1977) and 600-750 m in the Mescal

Mountains (Willden, 1964; Cornwall and Krieger, in press). Each of

these formations was deposited on an erosion surface developed over

flat-lying or slightly tilted strata. The nearly conformable sequence

of younger Precambrian and Paleozoic strata suggests that the Paleozoic

was an era of relative tectonic stability. However, the variability in

thickness of the Paleozoic section and inclined bedding within the

sequence can be attributed to periodic epeirogenic adjustments result-

ing in the formation of broad warps, basins, and sags (Peirce, 1976).

East of Christmas, Paleozoic rocks are overlain by shallow-water

marine sedimentary rocks of the Pinkard Formation originally described

by Lindgren (1905) in the Morenci, Arizona area. Plant and invertebrate

fossils are thought to indicate an early Late Cretaceous age (Ross,

1925; Hayes, 1970). A sequence of mudstone, shale, sandstone, con-

glomerate, and coal beds described by Willden (1964) 8 km east of

Christmas apparently represents the northern edge of a southward-

thickening wedge of Pinkard Formation. An Inspiration Company drill

hole in the Saddle Mountain district southeast of Christmas intersected 345 m of Pinkard Formation, but a diamond drill hole located on the Gila River 1.5 km east of the Christmas mine intersected only 12 m of conglomerate above the Naco Limestone. Pinkard-equivalent sedimentary rocks appear to be absent within, and west of, the Christmas open pit.

The Pinkard Formation or, where the Pinkard is absent, the Naco Limestone, is overlain by a thick vent- or cone-complex facies accumulation of basaltic flows and volcanic breccia with subordinate graywacke and siltstone. Covering approximately 230 km^2, the volcanic sequence ranges in thickness between 750-900 m in the Klondyke area southeast of the Christmas 15-minute quadrangle (Simons, 1964) and 450-600 m where downfaulted at Christmas, but thins rapidly westward from the Christmas mine. K-Ar age determinations presented in this report indicate a minimum age for the Williamson Canyon Volcanics of 75-80 m.y. before present. The transition from shallow marine sedimentation to subaerial(?) volcanism in Late Cretaceous time is recognized in many areas of southeastern Arizona (Hayes, 1970), and such successions are spatially correlative on a broad regional scale with porphyry copper deposits (Titley, 1972).

Post-Laramide rocks shown in Figures 1 and 2 consist largely of Tertiary basalt-andesite-rhyolite sequences, Miocene and younger basin-filling alluvial and lacustrine deposits, and alluvium deposited along the Gila River drainage.

Precambrian and Paleozoic strata in the Dripping Spring Mountains are folded into a northwest-trending anticline plunging gently

to the southeast (Eastlick, 1968; Banks and Krieger, 1977). This broad arch and numerous parasitic folds are dissected by numerous faults grouped by Banks and Krieger (1977) into: (1) four major north-south fault systems; (2) two northwest-southeast range-front faults; and (3) numerous faults and fractures oriented within 0-35° of east-west. Eastlick (1968) also describes a system of faults striking N15E to N50E and dipping 50-65° northwest. The easternmost major fault structure in the Dripping Spring Mountains, the northwest-trending Christmas-Joker system, displaces the ore body at Christmas.

The Dripping Spring Mountains arch apparently evolved during a period of Laramide compression with maximum stress operating along an east-west to northeast-southwest axis (Banks and Krieger, 1977; Rehrig and Heidrick, 1972, 1976). Differential uplift and northwest-directed tensional stress resulted in a system of east- to northeast-trending fractures. These extensional structures served as avenues for emplacement of Cretaceous and Paleocene calc-alkaline intrusions, several of which are spatially associated with base metal deposits.

The presence of thick Miocene valley-fill deposits indicates a shift from Laramide to basin-range tectonics and sedimentation by middle Tertiary time. Although Banks and Krieger (1977) cite evidence for Precambrian, Laramide, and post-Laramide movement along normal range-front faults in the Dripping Spring Mountains, modern basin and range physiography in the region reflects, in large part, post-middle Tertiary block faulting.

Objectives and Method of Study

This study is a contribution to a decade-long investigation conducted by the U.S. Geological Survey of the geology and ore deposits at Ray, Arizona and the surrounding region. Notwithstanding occasional changes in approach and design, it was the objective at Christmas to: (1) describe the geology and geochronology of the igneous rocks; (2) determine the nature, distribution, and paragenesis of hypogene silicate-sulfide mineral assemblages; and (3) construct a space-time model for intrusion and mineralization. Initially, the porphyry-related mineralization in both igneous and carbonate host rocks was to be considered. However, when the complex alteration pattern in volcanic wall rocks became more apparent, the focus of study shifted to the igneous rock environment.

During the first phase of the study, an area of approximately 11 km^2 around the Christmas open pit was mapped at a scale of 1:4800. Spot mapping in the open pit (scale 1:1200) and recent company mine maps provided information on internal relationships in the multiphase Christmas stock. Numerous surface and drill core samples collected at that early stage were essential for determination of subtle variations in the mafic volcanic sequence and in the recognition and classification of the many intrusive rock types in the map area. K-Ar age dates were obtained to develop the geochronology of magmatic and hydrothermal events. Whole rock chemical analyses provided a second basis for comparison and classification of the igneous rocks.

Early mapping and sampling provided the background for topical alteration-mineralization studies. Additional surface and drill hole samples were collected in an attempt to ascertain both large- and small-scale distribution patterns for secondary minerals. Selected rocks were submitted for chemical analysis in order to evaluate chemical changes during alteration.

In total, approximately 500 surface samples along with core samples from 70 diamond drill holes were collected for petrographic, chemical, and X-ray diffraction analyses. Core samples were particularly valuable because of the destructive effects of weathering and oxidation at the surface, and the large area covered by surficial deposits. Nearly all of the samples were slabbed, polished, and stained to check alteration and textural features. Mineral modes were obtained by point counting polished slabs and thin sections. Mineral identifications and compositions were determined by X-ray diffraction and electron microprobe.

The model for intrusion of the Christmas stock and alteration-mineralization of igneous rocks was developed from: (1) textural relationships in coexisting mineral assemblages; (2) the distribution and style of rock fractures and veins; (3) crosscutting features seen in outcrops, hand specimens, and thin sections; (4) distribution patterns for hypogene alteration minerals and sulfides; and (5) fluid inclusion petrography.

GEOLOGY OF THE CHRISTMAS MINE AREA

A detailed geologic map and cross section of the Christmas mine and vicinity are presented as Plates I and II, respectively. Major contacts and faults in the mine area are also illustrated in Figure 3. Plates I and II show that gently-tilted, Pennsylvanian Naco Limestone, the uppermost formation in the Paleozoic section at Christmas, lies stratigraphically above the Mississippian Escabrosa Limestone. The Naco is, in turn, overlain by the westward-thinning Williamson Canyon Volcanics of Cretaceous age. These Paleozoic and Mesozoic strata are intruded by numerous Laramide stocks, sills, and dikes ranging in composition from andesite to aplite. A sill of hornblende andesite porphyry, 5-15 m thick, is emplaced along or just below the unconformity between limestone and volcanic rocks. Combined offset of nearly 1 km on high angle normal faults in the northwest-trending Christmas-Joker fault system juxtaposes the Williamson Canyon Volcanics and Naco Limestone within the open pit and along the range front northwest of Christmas.

Approximately 25 percent of the map area (Plate I) is covered by surficial deposits. Stratified, partly consolidated gravels of Dripping Spring Wash, probably of Middle Miocene or Miocene-Pliocene age (Banks and Krieger, 1977), overlie bedrock north of the mine area. On gentle slopes developed over Williamson Canyon Volcanics, a thin veneer of volcanic rubble thickens toward, and merges with, alluvial deposits in the major drainages. Narrow talus piles are present on

Figure 3. Low altitude aerial photograph and sketch map of the Christmas mine and vicinity. View is toward the south with the Hayden smelter visible at the top just to the right of center. Christmas townsite is left of center near the middle of the photograph. Primary crusher, concentrator plant, and McDonald shaft are at bottom center. The Naco Limestone in the far wall of the open pit and right middleground (bedded, light gray) is unconformably overlain by the Williamson Canyon Volcanics (massive, dark gray). The northwest-trending Christmas and Joker faults downdrop the Williamson Canyon Volcanics (left and bottom) against Naco Limestone. The long axis of the Christmas stock, which underlies the near side of the open pit, trends approximately N80E. Biotite rhyodacite porphyry dikes extend east-northeast from near the Christmas stock. Photograph courtesy of the Inspiration Consolidated Copper Company.

Williamson Canyon Volcanics

Open pit

No. 4 Shaft Fault

Rhyodacite porphyry

dikes

Christmas stock

Naco Limestone

Christmas Fault

Williamson Canyon Volcanics

Joker Fault

N
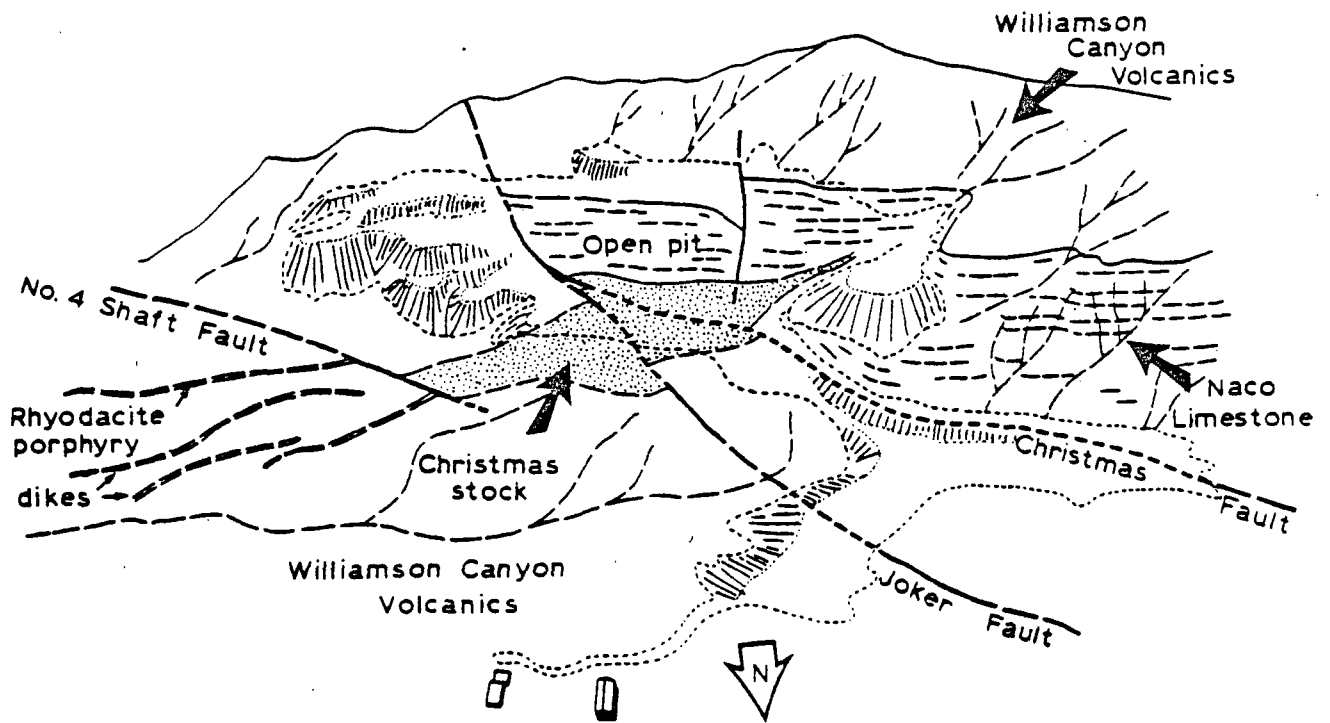
steeper slopes. Unconsolidated sand and gravel deposits occur along the Gila River and principal tributary drainages. Man-made overburden, a bane to detailed mapping in mine areas, includes mine dumps, tailings ponds, and road fill.

Naco Limestone

The oldest rock unit exposed at the surface in the mine area, the Naco Limestone, is characterized by thin to medium beds of fossiliferous cherty gray limestone and thin but persistent beds of finely laminated calcareous shale and siltstone. Elongate nodules and discontinuous layers of gray, black, and red chert help to define bedding planes where beds are otherwise massive. Strata generally strike northwest to east-west and dip 12-25° to the south. Locally, however, minor flexures and fault-related drag have produced other orientations.

I briefly examined forty thin sections from three stratigraphic sections of Naco Limestone in the Dripping Spring Mountains loaned to me by N. G. Banks. The Naco in these samples is predominantly biomicrite (lime wackestone) and micrite (lime mudstone). Allochem constituents include fossils, both macrofossil fragments and microfossils, calcite grains, quartz grains, and rare lithic fragments. X-ray diffraction of uncovered thin sections revealed the presence of a minor amount of dolomite in samples with a large micritic component. Detailed lithologic and paleontologic descriptions of the Naco Limestone in the southeastern Dripping Spring Mountains can be found in Reid (1966),

Perry (1968), and Banks and Krieger (1977).

Sections of Naco Limestone measured by previous workers along the prominent cliffs 1-1.5 km northwest of the mine range from 260 to 330 m in thickness. Assuming a thickness of 300 m for the highly altered Pennsylvanian limestone in the Christmas mine would place the Naco-Escabrosa Limestone contact approximately 200 m below the present pit bottom.

Within the metamorphic aureole adjacent to the Christmas stock, relatively pure limestone beds in the Naco Limestone are recrystallized to white marble or converted to andradite exoskarn; shale and siltstone are thermally metamorphosed to diopsidic hornfels. Garnetization of favorable beds extends northwest in the footwall of the Christmas fault for a distance of 750-775 m from the Christmas stock. A roughly-defined limit of intense garnetization is shown on Plate I.

Individual skarn ore bodies in the Naco are typically thin-bedded replacements of limestone, 0.5-18 m in thickness, sandwiched between layers of hornfels and granodioritic sills (Perry, 1968, 1969). The principal hypogene sulfide minerals in Naco skarn are chalcopyrite, bornite, pyrite, and sphalerite, with lesser amounts of molybdenite and galena; magnetite is often abundant in garnet-sulfide-rich zones near the intrusive contact. For details of skarn mineralogy and genesis the reader should consult publications by Eastlick (1968) and Perry (1969).

Williamson Canyon Volcanics

The Williamson Canyon Volcanics is a monotonous, westward-thinning sequence of dark-gray to greenish-gray basaltic volcanic breccias and flows, and subordinate clastic sedimentary rocks. The volcanic pile has a thickness of 450-600 m east of the Joker fault and approximately 250-350 m along the ridge south of the mine, but tapers out 1.5 km west of the Christmas open pit. Strike and dip measurements on sedimentary beds in the Williamson Canyon Volcanics are roughly conformable (northwest to east-west strikes, shallow southwest to northeast dips) with attitudes in the Naco Limestone, providing evidence that the volcanic rocks were also folded during Laramide compression. The wedging out of the volcanic sequence may then be attributed, in part, to erosional beveling along the axis of the southeast plunging Dripping Spring Mountains anticline.

Clastic sedimentary rocks were not observed along the Naco-Limestone-Williamson Canyon Volcanics contact west of the mine, but within the open pit a meter or two of impure fine-grained sandstone and siltstone occurs locally along the base of the volcanic section. This bed is lithologically similar to sedimentary rocks within the Williamson Canyon Volcanics, and is not extensive enough to distinguish a Pinkard-type stratigraphy. Thus, this unit is included with the Williamson Canyon Volcanics, and no Pinkard Formation is shown in Plate I.

The more resistant volcanic rocks have a dense and brittle

quality, and give a distinctive metallic ring when struck with a hammer. Freshly broken surfaces are usually dark tones of gray. In contrast, weathered surfaces often develop a greenish-gray, orange-brown, or buff patina, and in some areas, a distinctive reddish-brown or purple hue related to the presence of hematite or other iron oxides. Shades of green reflect varying degrees of epidotization.

Volcanic breccia

Although the details of an internal stratigraphy are obscured by alteration and poor exposure, pyroclastic rocks appear to be more abundant than lava flows in the volcanic section at Christmas. In many cases, a dark volcanic rock with visible plagioclase phenocrysts appeared to be a homogeneous flow rock in the field, but proved to be a volcanic breccia when observed as a polished slab or thin section.

Fragmental volcanic rocks in the Cretaceous volcanic pile can be broadly classified as volcanic breccia following the definition of Wright and Bowes (1963). They (1963, p. 80) consider a volcanic breccia to be a "rock composed predominantly of angular volcanic fragments greater than 2 mm in size set in a subordinate matrix of any composition and texture, or with no matrix; or composed of fragments other than volcanic set in a volcanic matrix." Volcanic breccia may then include mudflow and water-worked tuff deposits described by Willden (1964) in the Williamson Canyon Volcanics east of the Christmas mine, which were unrecognized or only tentatively identified during this study.

Thoroughly indurated pyroclastic rocks at Christmas are generally poorly sorted, unstratified lapilli tuffs and tuff-breccias. Lapilli tuff and tuff-breccia are terms applied to mixtures of fragments according to size, and are used in the manner described by Fisher (1966). Subangular to subrounded blocks and lapilli, many of accessory volcanic origin, are enclosed in a crystal-rich tuffaceous matrix (Figure 4a). The fragments are typically undeformed and non-vesicular, with porphyritic or pilotaxitic textures. Subhedral tablets of calcic plagioclase up to 2 mm in length, rounded equant grains and cumulophyric clusters of clinopyroxene (or uralite), and granular magnetite are embedded in an intergranular or isotropic brown to black glassy matrix. Embayed and corroded brown hornblende is a frequent constituent of some rock fragments and relict olivine outlines are visible in others. Fragments with diabasic textures are common. Lapilli- and ash-sized chips and grains of plagioclase, clinopyroxene (or uralite), hornblende, and, rarely, quartz are packed into interstices between lithic fragments.

Coarse plagioclase grains in pyroclastic rocks of the Williamson Canyon Volcanics often exhibit normal growth zoning; compositions based on variation in extinction angles range from An_{73} (core) to An_{48} (rim). Measurements of unzoned plagioclase yielded an approximate composition of An_{60}. Alteration products are invariably present and include epidote, albite, chlorite, calcite, sericite, and montmorillonite.

Clinopyroxene is usually pseudomorphed by a fibrous, blue-green amphibole. The pleochroic scheme (Z = light bluish green, Y = light green, and X = pale yellowish green), small extinction angle (14-15°),
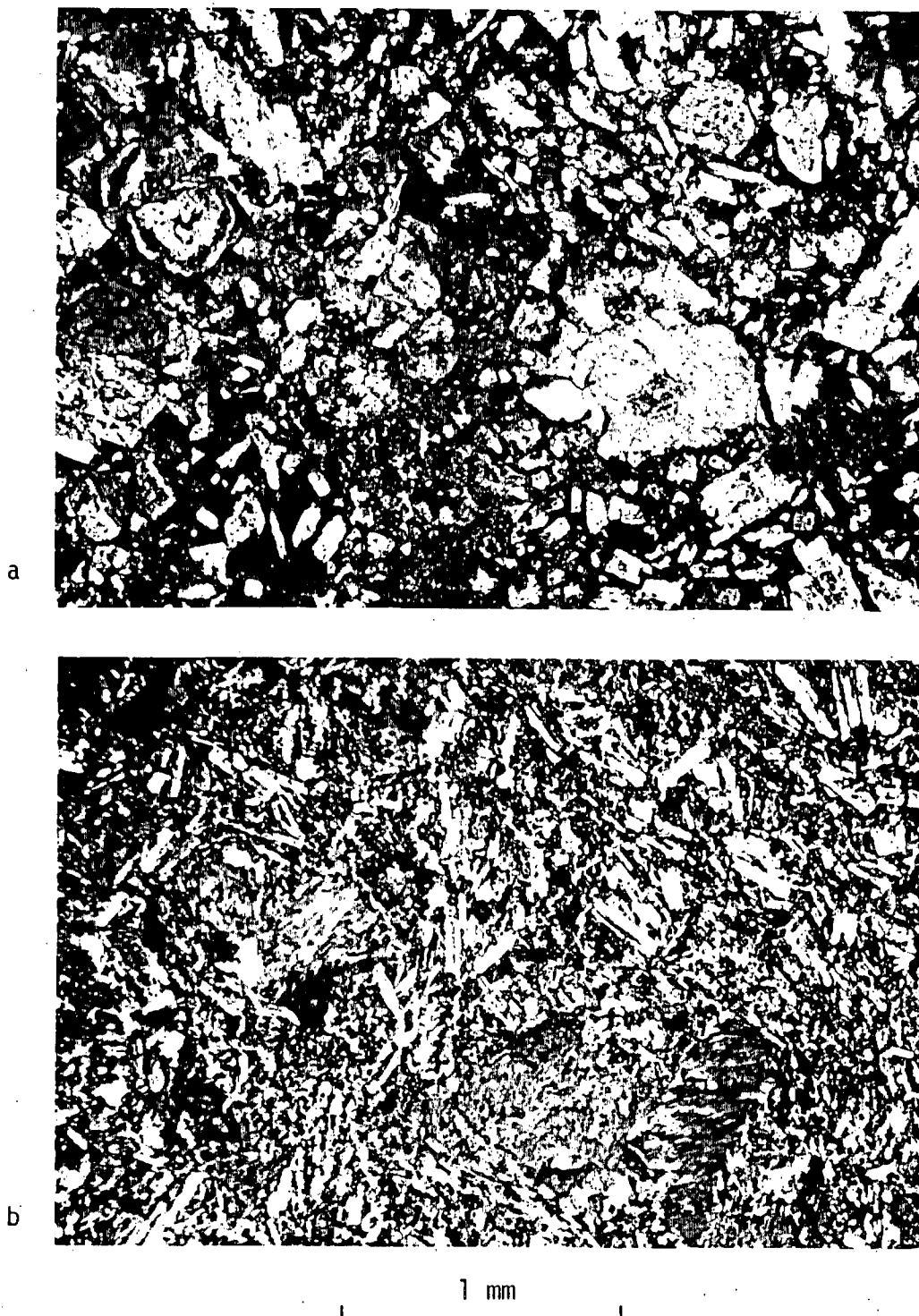
Figure 4. Photomicrographs of basaltic rocks from the Williamson
Canyon Volcanics. (a) Lapilli tuff (plane polarized light) showing
accessory volcanic rock fragments in crystal-rich tuffaceous matrix.
(b) Porphyritic basalt (crossed polarizers) with intergranular ground-
mass. Phenocrysts of clinopyroxene are completely altered to uralite.

fibrous habit, and mode of occurrence suggest that the mineral, commonly referred to as uralite, is actinolite (Deer and others, 1963). In contrast to clinopyroxene, hornblende in volcanic breccia generally appears fresh with the following optical properties: 2V near 80°; $Z \wedge c \sim 28°$; and moderate pleochroism with X = yellow brown, Y = medium brown, and Z = dark greenish, or, in some cases, reddish brown. In a few samples, hornblende grains have well-developed opacitic rims.

The matrix of pyroclastic rocks is largely altered dust or fine ash; feldspar microlites and granules of magnetite are visible under high magnification. An arbitrary particle size separation of 0.02 mm can be made between fine crystal debris and tuffaceous matrix, but a continuum of sizes exists between blocks and ash.

Lava flows

Lava flows in the Williamson Canyon Volcanics are generally holocrystalline rocks with porphyritic textures. Well-formed phenocrysts consisting of rectangular 1-3-mm grains of labradorite and equant grains and glomeroporphyritic aggregates of pale-yellow augite are set into an intergranular groundmass of randomly oriented calcic plagioclase laths (0.1-0.2 mm in length) with interstitial clinopyroxene and magnetite granules (Figure 4b). Plagioclase exhibits normal-oscillatory zoning between core (An_{58-72}) and rim (An_{42-49}). Even in the freshest samples examined, plagioclase grains are weakly saussuritized or cut by veinlets of albite, chlorite, sericite, calcite, montmorillonite, and zeolite (laumontite). Unaltered pyroxene is pale-yellow non-pleochroic

augite ($2V \sim 60°$, $Z \wedge c = 41-45°$), but in most samples pyroxene is com-pletely uralitized (Figure 4b). Fibrous amphibole frequently encloses patches of yellow epidote and pale-green chlorite, and small subhedral granules of pale-brown sphene.

Phenocrysts of olivine are not preserved, but relict crystal outlines contain intimate decomposition mixtures of chlorite-quartz-epidote-sphene or epidote-hematite-smectite.

Vesicular rocks suggestive of flow tops or bottoms are not prevalent near Christmas, probably because of the predominance of pyroclastic deposits in the section. Locally, however, circular to irregular cavities and gashes are made conspicuous by amygdules com-posed of one or more of epidote, chlorite, quartz, calcite, actinolite, prehnite, albite, sphene, and laumontite; K-feldspar, clinozoisite, pyrite, and chalcopyrite are rare cavity-filling constituents.

Table 1 presents chemical data for the principal igneous rock types described in this investigation. Chemical analyses for two flow rocks and a hornblende-bearing lithic lapilli tuff from Christmas are included. Also shown (Table 1, no. 4) is the average for 21 analyses (L. B. Clayton, Kennecott Exploration, Inc. company report, 1975) of flows and breccias from a section of Williamson Canyon Volcanics 3 km southeast of the Christmas mine.

According to these analyses, the volcanic rocks are quartz-normative, high-alumina ($Al_2O_3 \geq 17$ percent) basalts. The basalts from Christmas are also subalkaline, and nearly indistinguishable chemically. This basaltic lithology contrasts with the type section of Williamson

Table 1. Chemical data for volcanic and major intrusive rock types.

Chemical analyses* (oxides and S in weight percent; Cu in parts per million)

	Williamson Canyon Volcanics				Hornblende andesite porphyry			Hornblende rhyodacite porphyry			Phases of the Christmas stock		
Description number	1	2	3	4	5	6	7	8	9	10	11	12	13
Sample number	39AB74	1AB75	74AB75	K-1	72AB74	54AB75	AB68-73	AB64-73A	83AB75	GB-1	D99-430	AB77F-73	D256-148
SiO_2	49.4	49.4	50.8	50.0	56.8	59.0	57.7	61.9	63.1	62.4	63.2	66.5	67.0
Al_2O_3	17.4	18.6	16.8	18.2	17.2	16.7	16.4	15.8	16.0	16.0	16.5	15.1	16.3
Fe_2O_3	4.6	4.3	4.3	5.6	4.1	3.7	4.0	2.5	2.5	2.5	2.2	2.1	1.3
FeO	5.1	4.9	5.4	3.4	2.8	2.8	3.6	2.0	1.8	1.7	2.6	1.9	1.8
MgO	5.8	6.0	5.8	5.2	2.4	2.3	2.9	2.6	2.3	2.7	3.6	2.3	2.4
CaO	9.5	9.5	10.0	7.5	6.6	6.5	5.2	4.2	4.0	3.3	3.4	3.6	3.5
Na_2O	2.2	2.6	2.6	3.3	3.8	4.0	4.9	4.2	4.5	4.5	4.1	4.1	4.0
K_2O	.90	.48	.89	1.5	2.0	1.6	1.0	2.4	2.1	2.5	2.1	2.1	2.2
H_2O^+	2.1	1.2	.97	3.4	1.8	2.0	1.4	2.0	1.6	1.6	1.6	.95	1.3
H_2O^-	.34	.12	.13		.34	.17	.40	.80	.76	.72	.95	.55	.76
TiO_2	.95	1.1	1.1	.7	.95	.72	.79	.74	.69	.49	.80	.36	.34
P_2O_5	.22	.21	.14	.1	.40	.28	.26	.17	.17	.27	.22	.26	.22
MnO	.10	.16	.12	.09	.10	.11	.05	.06	.06	.00	.04	.00	.00
CO_2	.02	.03	.06	1.02	.08	.02	.04	.17	.10	.07	.02	.07	.08
Total	99	99	99	100	99	100	99	100	100	99	101	101	101

Table 1 (continued). Chemical data for volcanic and major intrusive rock types.

Description number	1	2	3	4	5	6	7	8	9	10	11	12	13
Sample Number	39AB74	1AB75	74AB75	K-1	72AB74	54AB75	AB68-73	AB64-73A	83AB75	GB-1	D99-430	AB77F-73	D256-148
S	0.0025	0.145	0.010	0.087	0.0025	0.0025	0.031	0.003	0.0007	0.0025	0.014	0.0025	0.028
Cu	20	50	50	80	20	20	100	70	50	20	1500	50	300

Partial CIPW Norms (weight percent) and Differentiation Index**

Q	4.7	3.2	3.6	1.8	11.7	14.2	10.9	16.7	17.9	16.7	18.5	23.8	24.2
Or	5.7	3.0	5.5	9.5	12.0	9.5	6.0	14.4	12.5	15.1	12.4	12.4	12.9
Ab	19.8	23.0	22.9	30.4	32.5	33.9	42.2	36.0	38.5	38.8	34.6	34.6	33.7
An	37.2	39.4	32.8	32.9	24.2	22.9	20.2	17.4	17.4	14.4	15.3	15.7	15.4
D.I.	30.2	29.2	32.0	41.7	56.2	57.6	59.1	67.1	68.9	70.6	65.5	70.8	70.8

* Oxides by rapid rock method; analysts: L. Artis, H. Smith, Z. A. Hamlin, and F. Brown. S by X-ray spectroscopy; analysts: L. Espos, B. P. Fabbi. Cu by semiquantitative spectrographic analysis; analysts: C. Heropoulos, R. E. Mays. All analyses performed in laboratories of the U.S. Geological Survey.

** Differentiation Index = Σnormative quartz + orthoclase + albite (Thornton and Tuttle, 1960).

1. Basalt flow. 2. Basalt flow. 3. Hornblende-bearing lithic lapilli tuff. 4. Average of 23 chemical analyses (20 pyroclastic rocks, 3 flow rocks) furnished by Kennecott Exploration, Inc. (L. B. Clayton, company report, 1975). 5. Coarse-grained variety. 6. Fine-grained variety. 7. Fine-grained variety. 8. McDonald stock. 9. McDonald stock. 10. Granite Basin pluton. 11. Quartz diorite (Dark Phase). 12. Biotite granodiorite porphyry (Light Phase). 13. Granodiorite.

Sample locations and descriptions are given in Appendix I.

Canyon Volcanics described by Simons (1964) in the Klondyke area which reportedly ranged in composition from hornblende latite to andesite. I have not recognized volcanic rocks with andesitic or more felsic compositions at Christmas.

Clastic sedimentary rocks

Sedimentary deposits within the Williamson Canyon Volcanics include massive to thinly laminated siltstone, impure feldspathic graywacke and grit, and boulder conglomerate. In thin section, a representative sample of graywacke is poorly sorted and consists of subrounded to subangular grains of plagioclase (40 percent of the rock), quartz and chert (15 percent), opaque minerals, mostly magnetite (5 percent), and dark rock fragments, predominantly volcanic (10 percent); all are enclosed in a phyllosilicate-rich matrix (30 percent). The coarser-grained sandstones contain appreciable amounts of detrital K-feldspar.

Narrow ledges and bars of boulder conglomerate in the south-eastern part of the map area and along Highway 77 just beyond the map area to the south contain subrounded, ellipsoidal clasts of Precambrian granite, red sandstone, white quartzite, diabase, basalt, and conglomerate up to one meter in diameter. The texture and composition of the matrix is not unlike that of the sandstone described in the previous paragraph.

The restricted vertical and lateral extent and extreme textural variation of these thoroughly indurated epiclastic rocks suggest that they represent shallow basin- and channel-fill deposits interspersed

within the volcanic pile. Barrett (1972), however, described a more widespread "continuous sequence" of shale, silty sandstone, and conglomerate in the Saddle Mountain district. The abundance of quartz, chert, K-feldspar, and heterogeneous rock fragments, particularly in the coarse-grained sedimentary facies, indicates that much detritus was derived from source areas beyond the limits of the volcanic pile; these deposits appear to be only minimally volcaniclastic.

Intrusive Rocks

Sedimentary and volcanic rocks at Christmas are intruded by numerous Laramide-age calc-alkaline dikes, sills, and small stocks (Plate I). The most prominent of these hypabyssal intrusions, in order of decreasing age, are hornblende andesite porphyry, hornblende rhyodacite porphyry, and the various facies of the granodioritic Christmas intrusive complex. The whole-rock chemical analyses of intrusive rocks listed in Table 1 and the chemical variation diagrams shown in Figures 16 and 17 illustrate the regular and progressive trend of calc-alkaline differentiation in the southeastern Dripping Spring Mountains. The most differentiated rocks, phases of the Christmas intrusive complex, are emplaced along an east-west fracture zone and are spatially related to copper mineralization. Minor intrusive rocks at Christmas include quartz latite porphyry, plagioclase porphyry, aplite, and post-Laramide andesite and basalt porphyry dikes.

Hornblende andesite porphyry

Greenish-gray dikes, sills, and irregular pluglike masses of
hornblende andesite porphyry (Kap) are the oldest rocks intruding the
Williamson Canyon Volcanics. Intrusions of Kap become more abundant
south and east of the mine, and these bodies are probably equivalent to
the swarm of shallow-level andesitic intrusions described in the Saddle
Mountain mining district (Willden, 1964; Barrett, 1972). Intrusive
rocks of this composition are less common beyond the limits of the
volcanic pile west of Christmas.

Two mutually crosscutting textural varieties of hornblende
andesite porphyry, a coarse porphyritic type (Kap_1) and a relatively
fine-grained type (Kap_2), were mapped separately (Plate I). Represen-
tative modal data (Table 2) and chemical data (Table 1) for Kap_1 and
Kap_2 indicate a close petrologic affinity.

The coarse-grained variety occurs mainly as narrow (1-5 m)
upright dikes, and is characterized by large spindly phenocrysts of
black hornblende up to 2 cm in length, and much less conspicuous pale-
yellow to greenish-gray grains of plagioclase, 1-3 mm across, all set
in a dull, aphanitic groundmass (Figure 5a). The hornblende prisms
frequently show a well-developed flow lineation subparallel to the
dike margins, but no obvious chill or alteration borders are apparent
along contacts with basaltic country rock.

The fine-grained variety forms thick discontinuous dikes,
small plugs, and the sills emplaced along and just below the uncon-
formity between Naco Limestone and Williamson Canyon Volcanics. Kap_2

Table 2. Modal data* for hornblende andesite porphyry.

Coarse-grained variety:	Average for 3 thin sections
Groundmass	71.1
Phenocrysts	
Plagioclase	17.7
Hornblende	6.6
Augite	0.6
Opaque	3.6
Other	
Apatite	0.1
Quartz	0.1
Secondary[1]	0.2
Total	100.0

Fine-grained variety:	Average for 6 thin sections
Groundmass	60.4
Phenocrysts	
Plagioclase	23.8
Hornblende	10.2
Augite	0.3
Opaque	2.5
Other	
Apatite	0.1
Quartz	1.1
Secondary[2]	1.6
Total	100.0

*Calculated from 700 or more points counted per thin section.

1. Includes calcite, chlorite, and epidote.
2. Includes epidote, calcite, and quartz.

has a fine- to medium-grained equigranular appearance megascopically (Figure 5a), but is somewhat porphyritic in thin section (Figure 5b); hornblende phenocrysts are commonly 1-5 mm, and rarely 10 mm, in length.

Microscopically, the hornblende in both varieties of hornblende andesite porphyry is a dark-brown variety (Z = dark brownish green, Y = olive brown, and X = yellowish brown) with $Z \wedge c$ = 17-19° and a 2V of about 70°. Oscillatory-zoned plagioclase (An_{54-62}) is blocky or tabular, rarely exceeding 3 mm in longest dimension. Accessory minerals are pale-green augite, magnetite, quartz, and apatite. The groundmass, constituting 55-70 percent of the rock volume, consists of a felty (occasionally pilotaxitic in Kap_1) mixture of feldspar and disseminated opaque granules, and averages less than 0.05 mm in grain size. Polished slabs of hornblende andesite porphyry stained with sodium cobaltinitrite reveal a moderate amount of groundmass K-feldspar.

Secondary minerals are sericite, calcite, clinozoisite, epidote, and albite clouding and replacing plagioclase; chlorite and epidote webbing hornblende and augite; and quartz-epidote aggregates that are in part cavity fillings, and, to a lesser extent, replacements of groundmass minerals. Magnetite is slightly oxidized to hematite.

Small plugs of Kap_1 in the southeast corner of the map area contain inclusions of quartzite, limestone, argillite, granite, basalt, and hornblendite. The latter rock appears to be a hornblende-magnetite cumulate consisting of 75 percent cumulus hornblende, 8 percent cumulus magnetite, 1 percent cumulus plagioclase, 1 percent magnetite included

a

b

1 mm
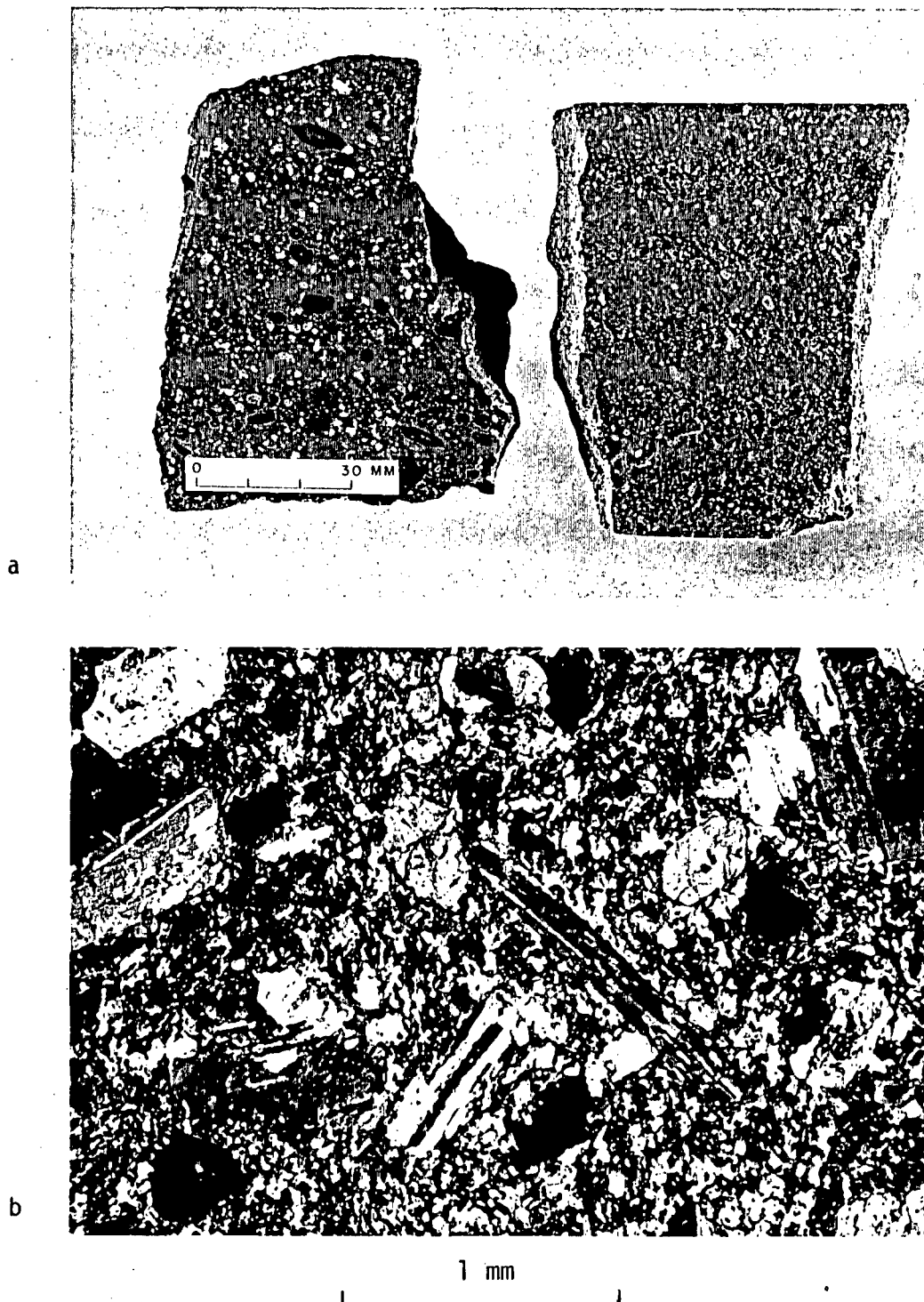
Figure 5. Hornblende andesite porphyry. (a) Hand samples of coarse-grained (left) and fine-grained varieties. (b) Photomicrograph (crossed polarizers) of fine-grained variety showing relatively fresh hornblende and plagioclase phenocrysts in feldspathic groundmass.

within hornblende, and 15 percent intercumulus matrix. The original matrix material is altered to an intergrown mixture of quartz, chlorite, epidote, prehnite, calcite, and greenish-brown montmorillonite(?). The cumulus hornblende is optically similar to phenocrystic hornblende in the porphyry host.

The relative ages of Kap_1 and Kap_2 and their genetic relationship with the Williamson Canyon Volcanics are uncertain. I observed, as did Barrett (1972), dikes of coarse-grained hornblende andesite porphyry cutting the finer-grained variety, and, in other localities, the reverse relation. Although K-Ar age determinations (Table 6) on hornblendes separated from these rocks fail to resolve this ambiguity, the field and petrographic evidence suggests that Kap_1 and Kap_2 have a comagmatic origin. Dikes of both varieties intruded the volcanic pile and crosscut each other over a prolonged period of time.

Andesitic intrusives may represent, at least in part, exhumed feeders for extrusive rocks, perhaps from the upper, more differentiated parts of the Williamson Canyon Volcanics now removed by erosion. A section of Cretaceous volcanic rocks described by Simons (1964) does include "hornblende latite" and "porphyritic hornblende andesite or dacite" petrographically similar to Kap. Moreover, volcanic breccia in the Williamson Canyon Volcanics at Christmas occasionally contains hornblende-bearing fragments resembling Kap suggesting that volcanism continued after emplacement of some hornblende andesite porphyry. Strong evidence for possible consanguinuity from a regional point of view is the close spatial correlation of Kap intrusions and the Williamson Canyon Volcanics.

The emplacement of hornblende andesite porphyry appears to predate copper mineralization at Christmas, and throughout the region.

Hornblende rhyodacite porphyry

Hornblende rhyodacite porphyry (Krp) forms two stocks and interconnecting east-west-trending dikes intruding the Williamson Canyon Volcanics in the northern third of the map area (Plate I). Diamond drill and water well records indicate that the triangular stock northeast of Christmas, referred to as the McDonald stock, represents only the upper portion of a much larger pluton which extends under volcanic and alluvial cover to the north, east, and southwest. The McDonald stock may be directly linked to the petrographically similar laccolithic pluton of hornblende rhyodacite porphyry intruding Naco Limestone in Granite Basin (Willden, 1964) 8 km northeast of Christmas (Figure 1).

Areas underlain by Krp are marked by gently rounded grus-covered slopes littered with spherical, partially decayed boulders. Freshly broken rock specimens have a light-gray to greenish-gray color which becomes grayish brown to brown as mafic minerals are oxidized during weathering. In hand samples an aphanitic groundmass encloses conspicuous phenocrysts of white or pale-pink plagioclase and subordinate amounts of dark greenish-black chloritized ferromagnesian minerals (Figure 6a). Quartz phenocrysts are sparse and K-feldspar phenocrysts are absent. Stained slabs, however, indicate a high percentage of groundmass K-feldspar (Figure 6a).
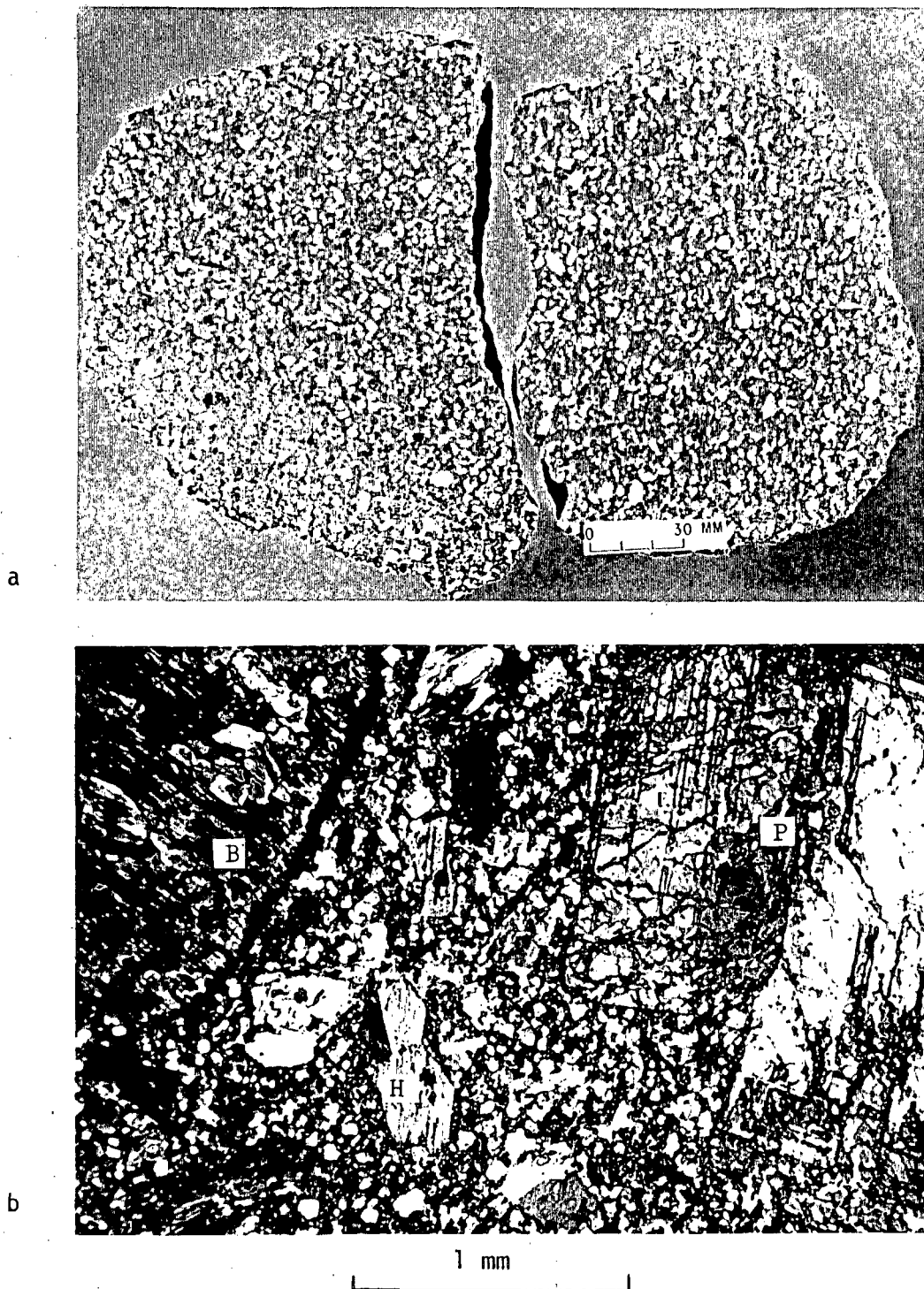
Figure 6. Hornblende rhyodacite porphyry. (a) Hand samples showing phenocrysts of plagioclase, hornblende, and biotite in aphanitic groundmass. Stain (sample with scale) indicates high percentage of groundmass K-feldspar. (b) Photomicrograph (crossed polarizers) showing plagioclase (P), hornblende (H), and biotite (B) phenocrysts in microcrystalline groundmass. Biotite is pseudomorphed by chlorite which hosts lenses of epidote.

Whole rock chemical data for the McDonald stock and Granite Basin pluton, presented in Table 1, reflect the characteristic textural and mineralogical homogeneity of hornblende rhyodacite porphyry intrusions. Modal compositions for Krp stocks and dikes are presented in Table 3. In thin section (Figure 6b), 2-10-mm-plagioclase phenocrysts exhibit strong oscillatory zoning over the compositional range An_{27-44}. Plagioclase appears cloudy and weakly albitized in Krp dikes, but is flecked with sericite, epidote, quartz, calcite, clinozoisite(?), and clay in samples from larger intrusions. Smaller prismatic phenocrysts of pleochroic green hornblende are susceptible to patchy replacement by epidote and chlorite.

Pseudohexagonal books of brown biotite up to 3 mm in width are partially to totally replaced by chlorite occasionally interleaved with with flat lenses of prehnite. The prehnite lenses have produced some distortion by bulging the enclosing mica cleavages. Where alteration of Krp is more advanced, chlorite is interleaved with epidote (Figure 6b). This chlorite-prehnite and chlorite-epidote alteration of biotite also generates a small amount of granular sphene, calcite, and quartz. The rather unusual mineral association biotite-prehnite has been described elsewhere in plutonic rocks (e.g., Ross, 1976; Moore, 1976; and Phillips and Rickwood, 1975), and may result from deuteric alteration reactions (Phillips and Rickwood, 1975).

Partly resorbed phenocrysts of clear quartz, 0.25-3.0 mm across, many with squarish outlines, constitute about one percent of the rock volume. Minor accessories include magnetite, prismatic apatite, and

Table 3. Modal data* for hornblende rhyodacite porphyry.

Hornblende rhyodacite porphyry stocks:	Average for 6 thin sections
Groundmass	52.8
Phenocrysts	
Plagioclase	31.3
Hornblende	9.1
Biotite	3.8
Quartz	1.4
Opaque	1.2
Other[1]	
Apatite	0.1
Secondary[2]	0.3
Total	100.0

Hornblende rhyodacite porphyry dikes:	Average for 3 thin sections
Groundmass	59.3
Phenocrysts	
Plagioclase	27.0
Hornblende	6.9
Biotite	4.3
Quartz	1.0
Opaque	0.4
Other[1]	
Apatite	0.1
Secondary[2]	0.9
Total	99.9

*Calculated from 700 or more points counted per thin section.

1. Includes trace quantities of sphene and zircon.
2. Includes epidote, calcite, chlorite, and sphene(?).

sparse subhedral zircon. The groundmass of Krp is aplitic or micro-
crystalline in thin section, but often appears fuzzy or cloudy because
of alteration. The average grain size is 0.02-0.05 mm in samples from
stocks, and 0.01-0.02 mm in dikes. The groundmass consists of approxi-
mately subequal amounts of quartz, plagioclase, and K-feldspar with
minor amounts of hornblende and opaque dust.

Quartz:hornblende:biotite phenocryst ratios plotted in Figure 7
show that hornblende rhyodacite porphyry intrusions can be distinguished
from megascopically similar porphyritic phases of the Christmas stock-
dike complex by greater homogeneity, higher hornblende/biotite ratios,
and lower quartz contents. Additional geological characteristics of
the McDonald and Christmas stocks are compared in Table 4. In summary,
hornblende rhyodacite porphyry stocks and dikes near Christmas are
homogeneous masses barren of porphyry-type mineralization or alteration.
Weak propylitic alteration appears to be the result of pervasive deuteric
processes. Rare veins are composed of brown calcite and manganese
oxides. Carbonate and volcanic wall rocks along the margins of these
plutons display only minor thermal effects and no evidence of additive
metasomatism. According to Willden (1964), emplacement of the 600-m-
thick hornblende rhyodacite porphyry laccolith into Naco Limestone at
Granite Basin produced only 16 m of marblization.

These observations suggest that magmas crystallizing to form
hornblende rhyodacite porphyry stocks were relatively dry in comparison
to the Christmas intrusions and lacked suitable internal plumbing sys-
tems necessary for transport of fluids, metals, sulfur, and so forth.
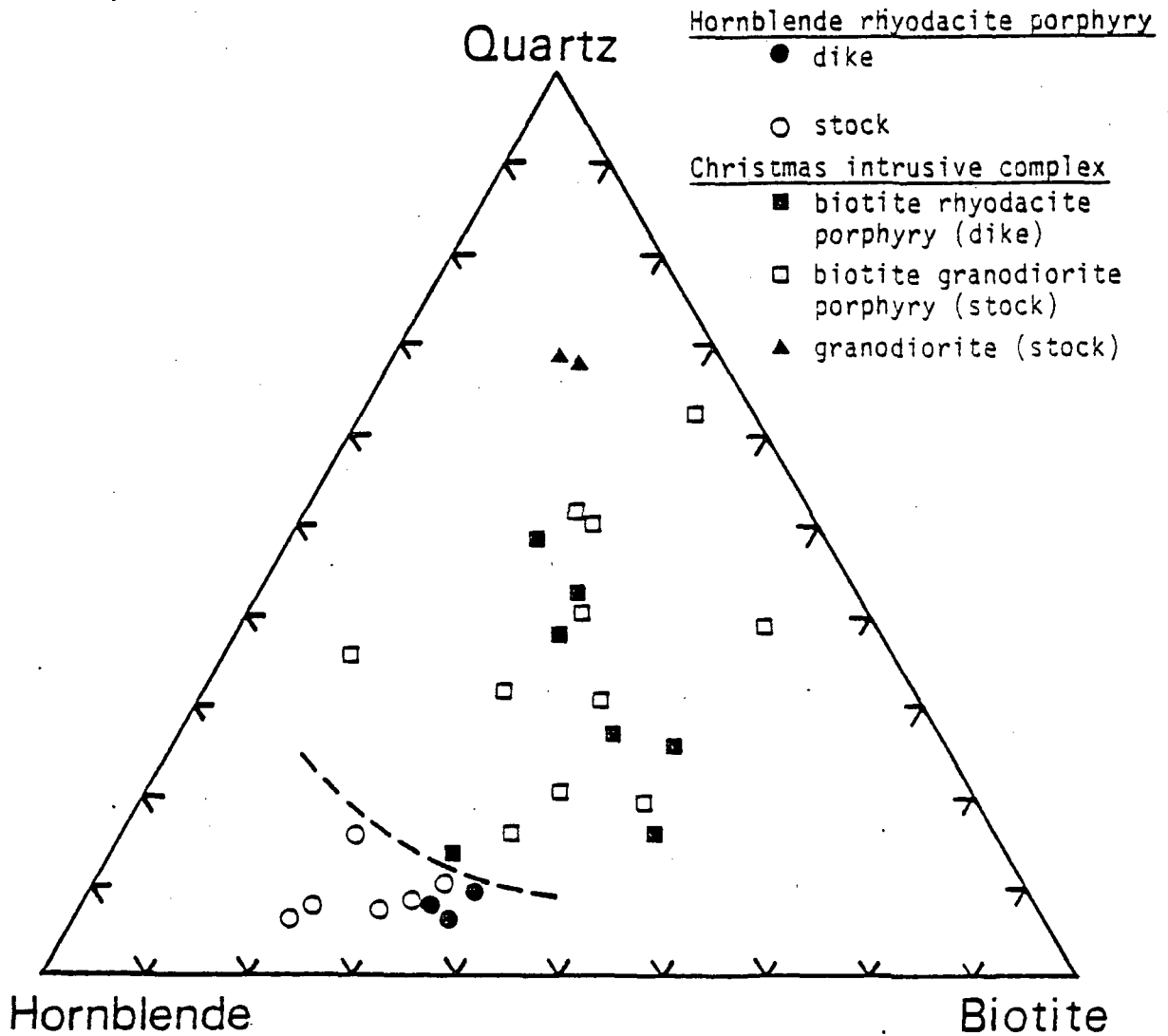
Figure 7. Triangular diagram showing relative proportion of quartz, hornblende, and biotite phenocrysts in hornblende rhyodacite porphyry and porphyritic phases of the Christmas intrusive complex. Ratios for the granodiorite phase of the Christmas stock also included.

Table 4. Summary of characteristics of the McDonald and Christmas stocks.

	McDonald stock	Christmas stock
Form:	irregular	elongate or dikelike
Nature of intrusion:	largely a single homogeneous phase	multiphase
Type of emplacement:	passive(?)	passive
Structural control of emplacement:	(?)	east-northeast fracture zone
Texture of intrusive phases:	porphyritic	porphyritic, seriate-porphyritic, granitoid
Age:	∿70 m.y.	∿62 m.y.
Trend of related dikes:	N80E	N80E
Pervasive alteration:	propylitic	K-silicate (biotitization), propylitic
Veining:	calcite, chlorite (rare)	quartz-K-feldspar, quartz-sericite
Sulfide mineralization:	pyrite (rare)	pyrite, chalcopyrite, bornite, molybdenite
Alteration in volcanic wall rock:	slight development of hornfels	strong K-metasomatism, development of secondary biotite

Furthermore, it is apparent that the fundamental structural control over porphyry-type mineralization in the Christmas vicinity is exerted by deep-seated(?) east- to east-northeast-trending fractures. In view of the observation, however, that Krp dikes also inhabit fractures striking N80E, additional parameters such as time and environment of magma generation must also be critical to ore formation. The close proximity in many mining districts of mineralized and barren hypabyssal intrusive bodies of like composition and texture continues to be a vexing problem for students of hydrothermal ore deposits.

Christmas intrusive complex

The Christmas intrusive complex includes a composite granodioritic stock and peripheral, east-west-striking porphyry dikes which intrude Paleozoic sedimentary and Cretaceous volcanic rocks (Figure 8). The elongate stock, positioned at the geometric center of the Christmas porphyry copper system, is rather small, measuring approximately 900 m by 450 m at the present level of exposure; the long horizontal axis has a trend subparallel to that of the dikes, about N80E. Two northwest-striking normal faults, the Christmas and Joker, bisect the stock with displacements of approximately 400 m and 580 m, respectively, east sides down. Therefore, rocks in the triangular block between the Christmas and Joker faults, and further east (in the hanging wall) of the Joker fault, represent successively higher levels within the stock and the porphyry copper system.

The stock is best exposed in the open pit and along north-south

Figure 8. Geologic map of the Christmas stock and related dikes generalized from Plate I.

Cover
Granodiorite porphyry
Dacite porphyry
Biotite granodiorite porphyry and rhyodacite porphyry dikes
Quartz diorite
Hornblende andesite porphyry
Williamson Canyon Volcanics
Naco Limestone

^{70} ....Normal fault with dip, dotted where concealed
....Contact with dip, dotted where concealed

Christmas Fault

Joker Fault

Christmas stock

Pit Limit

No. 4 Shaft Fault

10,000 N

5,000 N

20,000 E

0   1000   2000 ft
0   250   500 m

43

haulage drifts in the underground workings west (in the footwall) of the Christmas fault. It forms a north-plunging wedge-shaped mass tapering westward into two dikelike projections separated by a screen of altered country rock. The south contact has an overall steep northward dip of 80 degrees, but is interrupted by numerous sills and apophyses of intrusive rock penetrating the Paleozoic sedimentary section to the south. The north contact between intrusive and sedimentary rocks is more irregular. The northward dip is moderate until it flattens out over a chamber of interconnected sills and dikes approximately 100 m below the present surface.

Several large isolated blocks of silicated and mineralized limestone up to 5400 m^2 in area, and many smaller ones, are engulfed in the western tip of the stock. Relict bedding within xenoliths, even those of relatively small size, is conformable to bedding in the Paleozoic section surrounding the western half of the stock. This feature, along with cleanly truncated, unbrecciated contacts with country rocks, argues strongly for passive emplacement of the Christmas stock by magmatic stoping and, perhaps, partial assimilation.

Although the area northeast of the open pit is covered largely by mine waste and alluvium (Figure 8), drill hole information indicates that at or near the surface the stock narrows eastward from the Joker fault, and then flares out into several dikes. A salient of inter-digitating intrusive and volcanic rocks extends beneath surficial cover at least 300 m northeast of the central stock. The prophyry/volcanic rock ratio and mineralization decrease rapidly in drill holes beyond

this "northeast salient." Occurrences of volcanic rock within the projected surface limits of the stock may represent roof pendants or country rock partitions between closely spaced dikes.

Rocks of the composite Christmas stock can be grouped into early, veined quartz diorite (Dark Phase), biotite granodiorite porphyry (Light Phase), and granodiorite; and late, unveined granodiorite porphyry and dacite porphyry. Biotite rhyodacite porphyry dikes extending eastward and westward from the Christmas stock are probably coeval with Light Phase. Chemical analyses of the major phases of the Christmas stock are given in Table 1. The data show that biotite granodiorite porphyry and granodiorite in the Christmas stock are the most silicic and differentiated of the major Laramide calc-alkaline igneous rocks at Christmas.

Quartz diorite (Dark Phase). Quartz diorite, or Dark Phase, represents the first injection of magma along the east-west fracture zone. It forms a discrete phase, 45-90 m wide, along the south margin of the stock, and is intersected in several drill holes along the projected northern contact with volcanic wall rocks. Quartz diorite also forms the bulk of the eastern end of the stock, but the dimensions and distribution of Dark Phase east of the Christmas fault are not well known.

The medium- to dark-gray color of quartz diorite (hence the convenient field term, Dark Phase) reflects the presence of varying amounts of pervasive secondary biotite pseudomorphing hornblende, and

to a lesser degree, replacing primary biotite. The megascopic appearance of quartz diorite (Figure 9a) is moderately porphyritic, but the texture in thin section ranges between seriate-porphyritic and allotriomorphic-granular (Figure 9b). Least altered samples consist of blocky subhedral plagioclase phenocrysts up to 1 cm in length, oscillatory-zoned over the narrow range An_{38-41}, prismatic hornblende, and sparse, corroded biotite books set into an anhedral-granular aggregate of hornblende, plagioclase, quartz, biotite, and minor K-feldspar. Books of primary biotite are strongly pleochroic with Y = Z = dark reddish brown, and X = light golden brown. Phenocrystic biotite margins are ragged due to encroachment by groundmass minerals and partial recrystallization to fine-grained mica.

Prisms of moderately pleochroic green hornblende up to 2 mm in length are preserved in drill core samples of quartz diorite from the Christmas stock west of the Christmas fault. Phenocrysts of quartz are absent in Dark Phase. However, interstitial quartz with sutured or scalloped grain boundaries constitute 5-15 percent of the rock volume. Magnetite and apatite are common accessory minerals.

Biotite granodiorite porphyry (Light Phase). Light-gray biotite granodiorite porphyry, or Light Phase, forms the well-veined core of the composite stock, and similar rocks crop out in small and irregular pluglike masses 1-1.5 km east of the mine. This phase is closely related to, but slightly later than, quartz diorite; dikes of Light Phase penetrate quartz diorite with sharp contacts, but without chilled
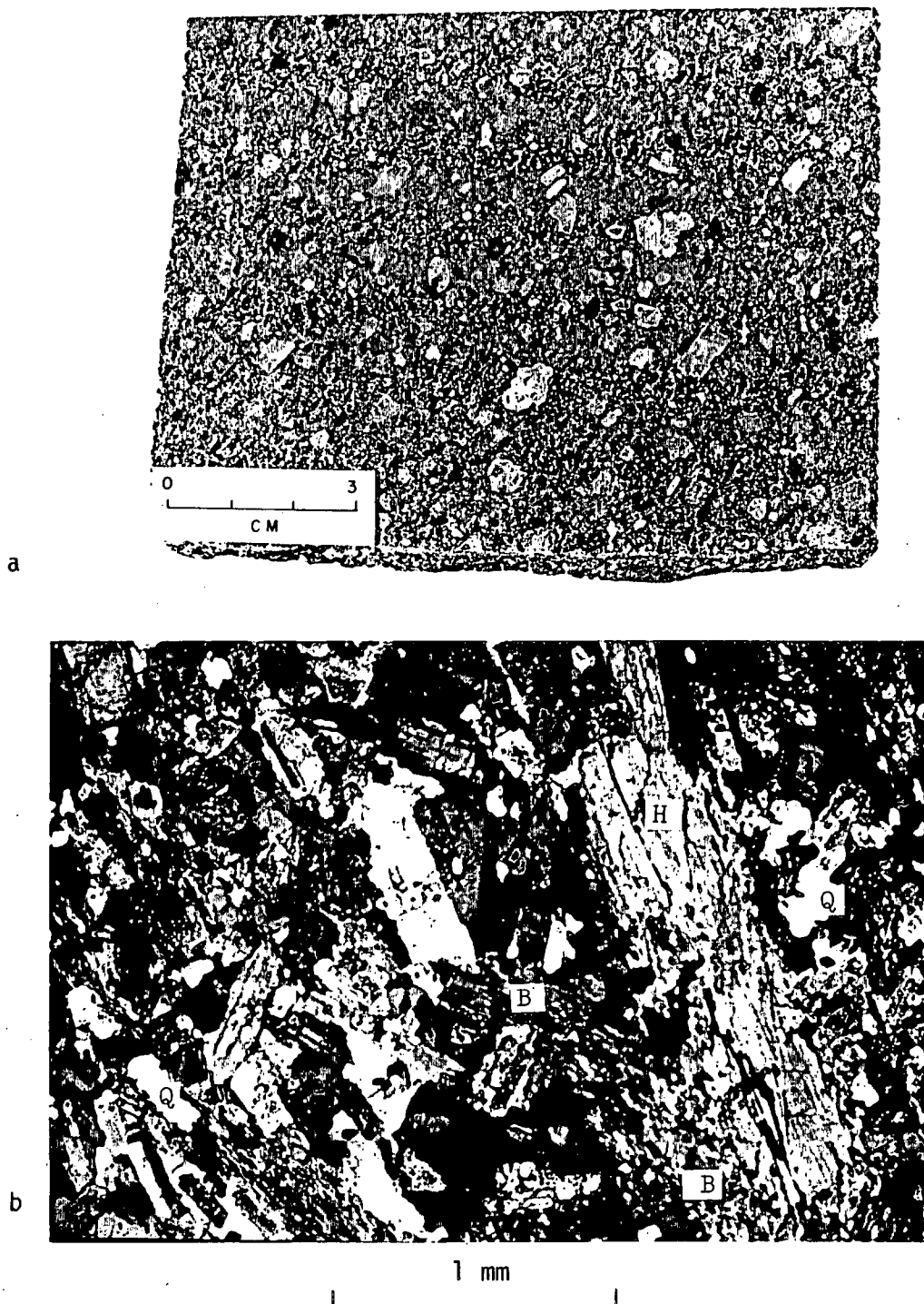
Figure 9. Quartz diorite (Dark Phase) of the Christmas stock. (a)
Hand sample has moderate dark-gray color due to presence of fine-
grained secondary biotite. Stained slab contains very minor ground-
mass K-feldspar. (b) Photomicrograph (crossed polarizers) showing
seriate-porphyritic texture. H = hornblende, P = plagioclase, Q =
quartz. Hornblende is partly replaced by ragged flakes of biotite (B).

margins. Within the open pit the contact between Dark Phase and Light Phase roughly parallels the south boundary of the stock, but is locally broken and irregular due to diking by the younger phase, minor offset along numerous north-south faults, the presence of limestone blocks, and truncation by still younger intrusive phases. Sills and irregular apophyses of biotite granodiorite porphyry also invade Naco Limestone south and northwest of the central intrusive mass.

.The porphyry core itself has many internal contacts between what appear to be individual units or "pulses" of biotite granodiorite porphyry magma. Compositional heterogeneity within the core is manifested by subtle variations in color index, quartz content, and grain size of the groundmass, and is demonstrated by the spread in quartz:hornblende:biotite phenocryst ratios plotted in Figure 7. The internal contacts within biotite granodiorite porphyry are difficult to trace for more than a few meters, but are inhabited locally by quartz veins. Veins composed of quartz and K-feldspar are also truncated at these contacts (Figure 10).

Biotite granodiorite porphyry is a distinctly porphyritic rock with prominent phenocrysts of milky-white plagioclase and shiny black biotite, and less conspicuous hornblende and quartz, all crowded into an aplitic groundmass (Figure 11). The average modal composition is presented in Table 5. Blocky subhedral plagioclase grains, 0.5-10 mm in long dimension, exhibit normal-oscillatory zoning between An_{44-46} at the cores and An_{33-36} near the rims; the average composition is sodic

Figure 10. Internal contact between "pulses" of biotite grano-
diorite porphyry with truncated quartz-K-feldspar veins.

1 mm

Figure 11. Texture of biotite granodiorite porphyry (Light Phase).
Photomicrograph (crossed polarizers) shows phenocrysts of biotite
and zoned plagioclase in aplitic "quenched" groundmass composed of
quartz, plagioclase, and K-feldspar. Scalloped grain edges suggest
that suspended crystals reacted with surrounding melt prior to
consolidation.

Table 5. Modal data* for biotite granodiorite porphyry (Light Phase), granodiorite, and biotite rhyodacite porphyry dikes in the Christmas intrusive complex.

	Biotite granodiorite porphyry--average for 12 thin sections	Biotite rhyodacite porphyry--average for 7 thin sections
Groundmass	43.5[1]	48.2
Phenocrysts		
Plagioclase	42.0	35.8
Biotite	4.6	5.5
Hornblende	4.2	4.6
Quartz	4.3	4.7
Opaque	0.4	0.5
Other		
Apatite	trace	trace
Zircon	trace	trace
Secondary[2]	1.0	0.7
Total	100.0	100.0

	Granodiorite--average for 2 thin sections
Plagioclase	53.5
K-feldspar	9.4
Quartz	24.1
Biotite	6.0
Hornblende	5.3
Opaque	0.8
Apatite	0.2
Anhydrite	0.4
Sphene	0.1
Secondary[2]	0.2
Total	100.0

*Calculated from 600 to 800 points counted per thin section. Data from least altered rocks.
1. Composition of groundmass approximately 40 percent quartz, 28 percent plagioclase, 26 percent K-feldspar, and 6 percent biotite. 2. Includes epidote, chlorite, calcite, and zeolite.

andesine. The barrel-shaped tablets of biotite up to 5 mm in thickness are pleochroic from yellow (X) to dark reddish or chocolate brown (Y = X), and commonly contain inclusions of apatite, magnetite, and quartz. Curved cleavage planes in coarse biotite grains as well as undulose extinction in quartz phenocrysts suggest post-consolidation deformation.

Pleochroic green hornblende (ZΛc ∿ 14°) occurs as subhedral to euhedral prisms reaching 3 mm in length, and is subordinate to biotite. In contrast to the nearly complete biotitization of amphibole in quartz diorite, hornblende in biotite granodiorite porphyry is frequently preserved. Rounded, blebby quartz phenocrysts occasionally show crude dipyramidal forms modified by prominent embayments of groundmass minerals. Accessory minerals include magnetite-ilmenite, apatite, zircon, and disseminated sulfides.

A common characteristic of all phenocrysts in Light Phase is scalloped grain edges (Figure 11) which probably formed as suspended crystals reacted with the surrounding melt. However, tiny anhedral inclusions of quartz within margins of some plagioclase phenocrysts may have been trapped during late growth of feldspar at hypersolidus conditions following emplacement (Theodore and others, 1973).

The groundmass of biotite granodiorite porphyry consists of a simple equigranular "quenched" mosaic of 40 percent quartz, 30 percent plagioclase, and 30 percent K-feldspar (and small amounts of biotite and apatite). Grain size of the groundmass is the principal textural

variable of Light Phase, the average ranging between 0.05 and 0.2 mm. Rocks with coarser groundmasses are gradational in texture with quartz diorite.

Granodiorite. Granodiorite is distinguished from biotite granodiorite porphyry by its coarser-grained hypidiomorphic-granular texture, abundant quartz content, interstitial K-feldspar, and the paucity of secondary biotite. A representative modal analysis is presented in Table 5. Despite textural dissimilarities between granodiorite and biotite granodiorite porphyry, their chemical compositions are nearly identical (Table 1).

Although not present at the surface, granitoid-textured rock is exposed underground at the 1600 level near the No. 6 shaft (370 m below minimum pit elevation), and was intersected in a drill hole in the north-central part of the pit less than 50 m below the present surface. The approximate distribution of granodiorite is shown on the cross section in Plate II. No sharp contacts with other intrusive phases have been observed, and granitoid rocks have not been found in higher levels of the intrusive complex east of the Christmas fault.

The granodiorite is relatively free of sulfide mineralization but is cut by veins of pink K-feldspar and, therefore, appears to have been emplaced before cessation of mainstage K-silicate hydrothermal alteration. Away from veins, alteration is minimal, but plagioclase (sodic andesine) is frequently flecked with sericite and mafic minerals may be partially altered to chlorite plus sphene. Samples obtained

from underground drill core at a level 540 m below the present pit bottom contain a moderate amount of disseminated anhydrite.

This granitoid phase may represent the cupola of a large phaneritic granodiorite pluton of the type thought by some workers (e.g., Sillitoe, 1973) to underlie and grade upward into mineralized porphyritic stocks. Alternatively, granodiorite at Christmas may represent a deep-seated, and therefore more slowly cooled and coarser-grained body of biotite granodiorite porphyry.

Biotite rhyodacite porphyry dikes. Several east- to northeast-trending biotite rhyodacite porphyry dikes extend latitudinally from near the Christmas stock to the limits of the map area. On a regional scale this dike swarm follows the prominent east-west fracture zone across the Dripping Spring Mountains, and is related to copper mineral-ization at the New Year and Chilito mines, 2.5 km and 4 km west of Christmas, respectively (Banks and Krieger, 1977). At Christmas the dikes cannot be traced directly into the central stock, but their occurrence, modal compositions (Table 5), and textural characteristics (Figure 12) imply a close genetic relationship to biotite granodiorite porphyry.

The steeply dipping porphyry dikes are grayish green where propylitically altered, and tan to reddish brown in variably oxidized portions of the quartz-sericite zone. The phenocryst content of the dike interiors constitutes 45-50 percent of the rock volume and con-sists of well-formed plagioclase (An_{35-47}), and biotite, hornblende,
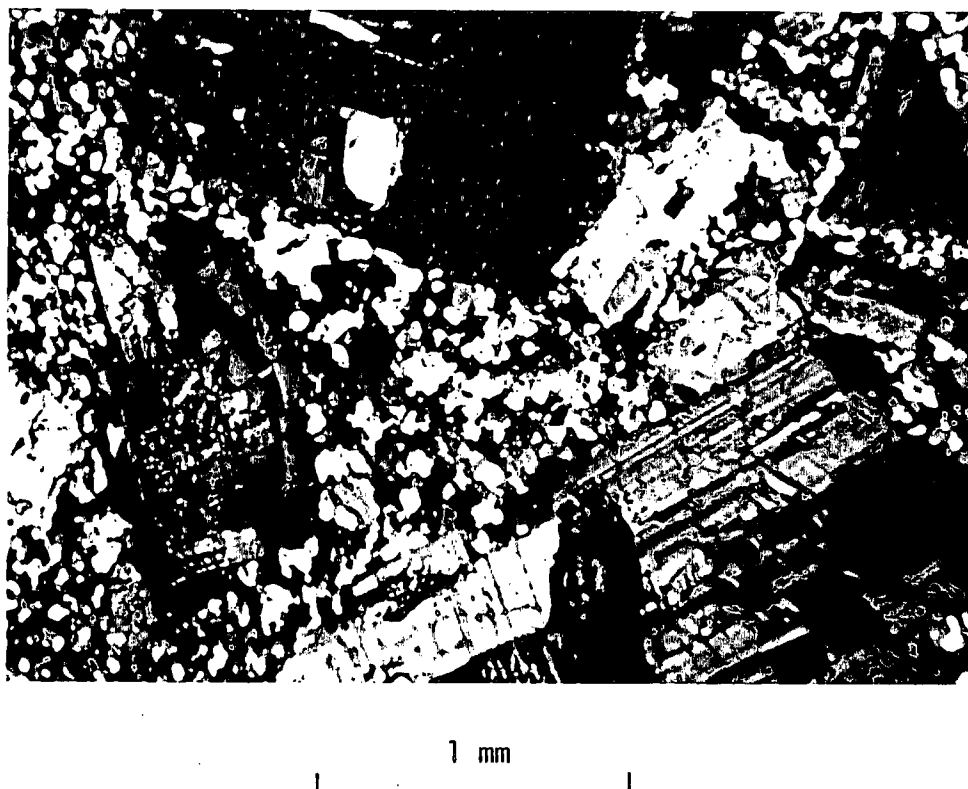
1 mm
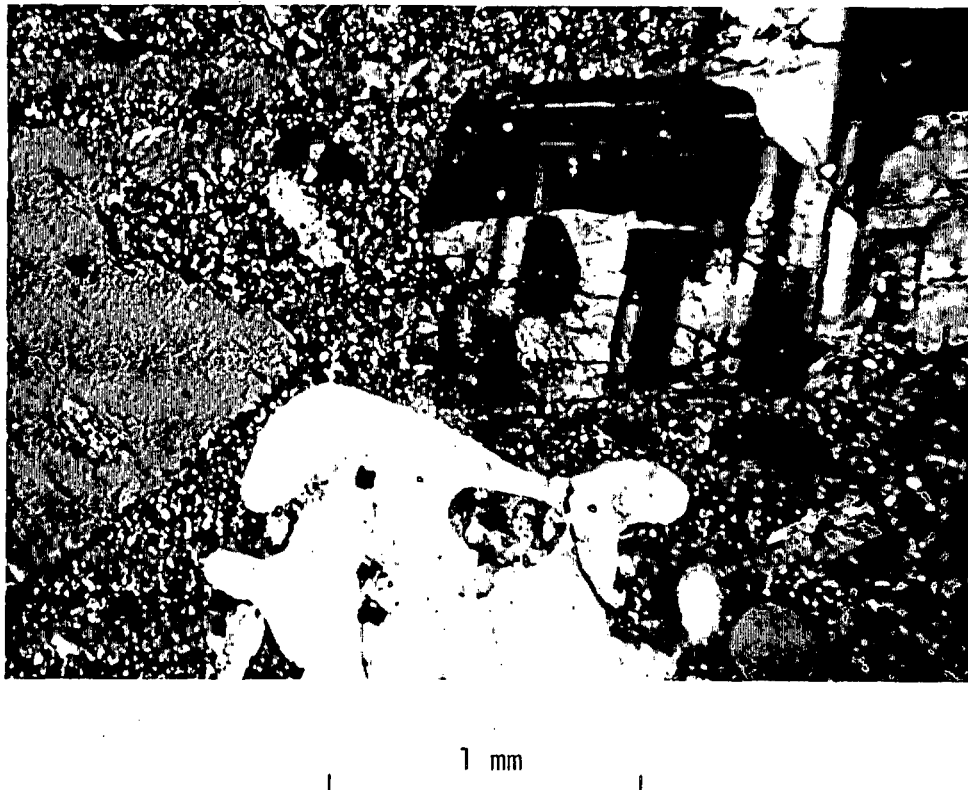
Figure 12. Texture of biotite rhyodacite porphyry dike. Photo-
micrograph (crossed polarizers) shows phenocrysts of zoned plagioclase,
book biotite, and strongly resorbed quartz in turbid feldspathic
groundmass.

and anhedral quartz in roughly the same proportions as in Light Phase
in the stock (see Figure 7). Chilling along dike margins diminishes
the biotite:hornblende ratio, quartz content, and phenocryst:groundmass
ratio. The principal accessory minerals are magnetite and apatite with
rare zircon and sphene.

In contrast to the simple mosaic groundmass texture of biotite
granodiorite porphyry in the stock, least altered biotite rhyodacite
porphyry groundmasses are very fine-grained (0.02-0.05 mm) turbid
aggregates of interlocked quartz, feldspar, and chlorite. K-feldspar
does not occur as phenocrysts in biotite rhyodacite porphyry dikes,
but may constitute up to 50 percent of the total groundmass producing
a strong yellow color in slabs stained with sodium cobaltinitrite.
Grain boundaries are ragged and irregular. The cloudiness results
both from alteration and myriads of tiny inclusions in quartz and
feldspar, some of which appear solid and others that contain fluid.

Unveined intrusive phases. Recent exposures in the Christmas
open pit reveal small, unveined bodies of light-gray to grayish-green
granodiorite porphyry and dacite porphyry intruding quartz diorite and
biotite granodiorite porphyry along the south margin of the stock (see
Figure 8 and Plate I). Granodiorite porphyry occurs in two somewhat
elongate masses penetrating quartz diorite. The larger of the two
masses is also in contact with dacite porphyry to the north and altered
Naco Limestone to the south. The smaller mass is in contact with a
small, pipelike body of intrusion breccia. Dacite porphyry forms a

series of narrow (less than 3-m-wide) north-trending dikes which merge southward into an elliptical mass bordering granodiorite porphyry. Where the granodiorite and dacite porphyry phases are in contact, the former shows minor chilling effects, and is thought to be the younger rock. In the hanging wall of the Joker fault, an east-trending dike of dacite porphyry extends from the Christmas stock into the volcanic pile where it crosscuts hornblende andesite porphyry dikes.

Except for the absence of veining and the dull and occasionally bleached appearance, granodiorite porphyry strongly resembles Light Phase. Dacite porphyry, however, is distinctive (Figure 13). Phenocrysts make up only 15-20 percent of the rock, and, in decreasing order of abundance, are plagioclase, hornblende, biotite, and quartz, the latter in small rounded clots constituting less than one percent of the rock volume. The groundmass is a subpanidiomorphic-granular framework of tabular to equant plagioclase, prismatic pale-green amphibole, and sparse sulfide grains. Interstices between the larger grains are filled with plagioclase, quartz, biotite, and magnetite-ilemenite.

Granodiorite porphyry and dacite porphyry are characterized by propylitic alteration and weak, disseminated chalcopyrite-bornite mineralization. Mafic minerals in both phases are typically pseudomorphed by compact tufted masses of chlorite accompanied by small amounts of epidote, sphene, and calcite. Plagioclase is partially altered to sericite and/or albite.

The younger porphyry phases lack stockwork mineralization and secondary K-silicate minerals. In addition, K-silicate veins cutting
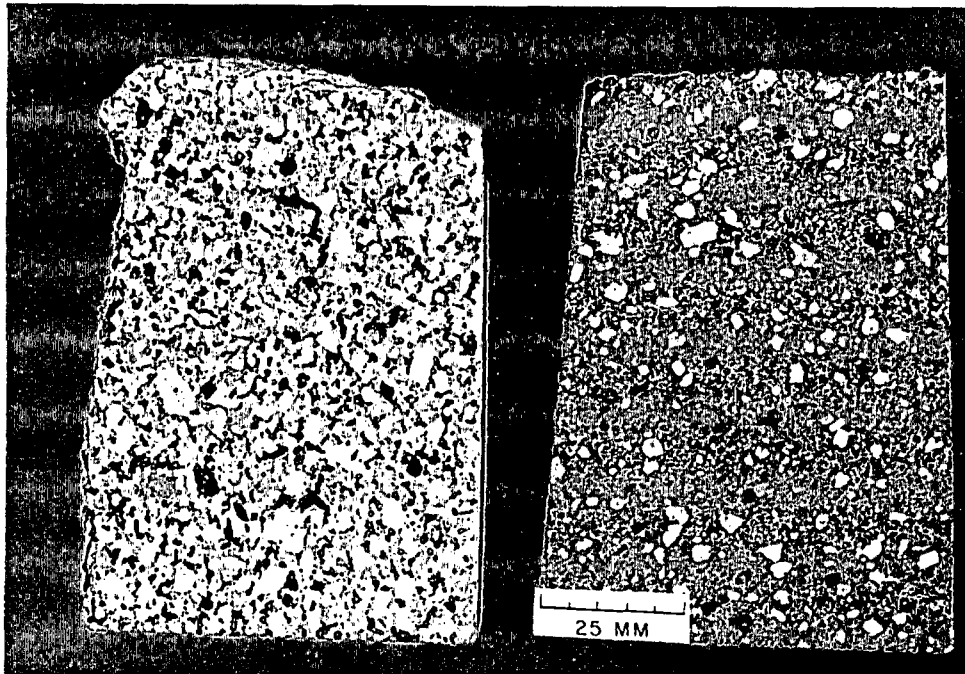
Figure 13. Hand samples of granodiorite porphyry (left) and dacite
porphyry.

quartz diorite and biotite granodiorite porphyry are truncated by the unveined porphyries. Although fracture-bound sulfides are absent, the unveined porphyries do host weakly disseminated bornite and chalcopyrite. These observations indicate that granodiorite porphyry and dacite porphyry were emplaced following stockwork veining and K-silicate alteration in the stock. The age of these phases relative to quartz-sericite alteration and associated pyritization is unknown.

Minor intrusive rocks

Other Laramide-age intrusive rocks in the mine area include quartz latite porphyry, plagioclase porphyry, and aplite. Discontinuous dikes, 3-15 m wide, of buff to light-gray quartz latite porphyry intrude the Williamson Canyon Volcanics in the northern part of the map area (Plate I). The dikes appear to have intruded along the same east-west structural zone inhabited by dikes of hornblende rhyodacite porphyry, and, in places, appear to embay and truncate the latter. However, the relative ages of hornblende rhyodacite porphyry and quartz latite porphyry are still uncertain. Some of the quartz latite porphyry dike segments are terminated against faults, but others appear to simply diminish in thickness and "pinch out" at one place only to reappear in another, producing an en echelon pattern. A characteristic feature of the dikes is a well-developed platiness and sheeting parallel to steep contacts with country rocks.

Quartz latite porphyry is invariably altered. Sparsely distributed phenocrysts of saussuritized plagioclase, chloritized biotite,

and blebby quartz total 15-25 percent of the rock volume, and are set into a felted anhedral-granular groundmass of alkali feldspar, quartz, and chlorite. A small amount of epidotized amphibole is present, and apatite is a common accessory mineral. Irregular elongate cavities are filled with quartz and epidote, and calcite is abundant in the ground-mass of some samples. Sparsely disseminated, oxidized pyrite is the only identifiable sulfide mineral.

Although not mineralized near Christmas, quartz latite porphyry dikes are associated with Pb-Zn-Cu mineralization at the Seventy Nine mine 6 km west of Christmas (Kiersch, 1949), and are reported to be cut by sulfide veinlets near other centers of mineralization in the Hayden quadrangle (Banks and Krieger, 1977).

An irregular plug of altered gray-green plagioclase porphyry intrudes the Williamson Canyon Volcanics 1.2 km east of the Christmas open pit (Plate I). Dikes radiating from this plug crosscut dikes of hornblende andesite porphyry. The rock generally has a seriate-porphyritic texture with the following mineral proportions: plagio-clase, 60-70 percent; quartz, 12-20 percent; biotite and hornblende (both altered), 10-15 percent; and K-feldspar and opaque minerals, 2-5 percent. Locally, the texture is more strongly porphyritic and the groundmass (about 40 percent quartz and 60 percent K-feldspar) accounts for up to 60 percent of the rock volume. Textural variations within the plagioclase porphyry mass suggest that the plug is a composite of two or more phases.

Plagioclase porphyry is, for the most part, propylitically

altered, but secondary biotite and K-feldspar veinlets were observed in a few places. A zone of brecciation, 5 m in width, in which the rock is totally converted to a bleached aggregate of quartz and sericite, extends from near the central portion of the plug southeastward into basaltic volcanic rocks. Limonite staining and scattered boxworks in the shattered zone are remnants of local mineralization. A short tunnel and shaft remain from what Ross (1925) referred to as part of the unproductive "Mellor prospect."

Aplite forms a resistent east- to east-northeast-trending dike, 3-5 m in width, intruding volcanic rocks east of the mine, and numerous stringers west of the open pit (Plate I). Crosscutting relationships indicate that the aplite is younger than hornblende andesite porphyry, but predates biotite rhyodacite porphyry and biotite granodiorite porphyry.

A probable continuation of the main dike is exposed in the open pit intruding altered Naco Limestone 100-120 m south of the central stock. Although the aplite itself is barren, the tenor of skarn ore increases sharply adjacent to the dike (David S. Cook, personal communication, 1976). This feature suggests that the dike, or possibly, a preexisting fracture zone, acted as a structural control during skarn mineralization.

The aplite is massive and aphanitic in hand specimen, and least altered samples consist of an aggregate of quartz, K-feldspar, and plagioclase with sparsely disseminated specks of pyrite or its oxidation products. Grain size averages 0.05 mm. Crisscrossing fractures

are coated with sericite, quartz, clay, and iron oxides. East of the mine, the aplite dike is subject to varying degrees of pervasive sericitization.

This type of aplite apparently predates emplacement of the Christmas stock and is not directly associated with mainstage mineralization. Thus, it is distinct in origin from aplitic K-feldspar-quartz veins which are a component of K-silicate alteration in the stock.

Narrow 0.5-1-m-dikes of andesite and basalt porphyry (not shown in Plate I) exposed in the western portion of the open pit represent the youngest igneous activity at Christmas. These dikes strike northwest to northeast and intrude, in part, along steeply dipping faults which offset the contact between the Christmas stock and Paleozoic sedimentary rocks. The dikes also transect intrusive rocks and quartz-sericite veins in the western apex of the Christmas stock, and clearly postdate Laramide alteration-mineralization.

Andesite porphyry is a medium-gray rock with porphyritic texture. Slender, prismatic hornblende needles up to 3 mm long, occasional hornblende clusters, and equant subhedral plagioclase grains are set in a felty to pilotaxitic groundmass of plagioclase microlites and opaque granules. A flow lineation, expressed by the subparallel arrangement of hornblende prisms, is present in some samples. In the few samples examined in thin section, plagioclase is partially or totally replaced by calcite and sericite, and hornblende is altered to calcite and chlorite.

Olive-gray basalt porphyry consists of subhedral phenocrysts

and cumulophyric clusters of augite and olivine, and lathlike micro-
phenocrysts of labradorite enclosed by an insertal aggregate of
plagioclase, clinopyroxene, interstitial brown glass, and pods of
yellowish-green montmorillonite. Magnetite octahedra are scattered
through the groundmass. Olivine in some samples is totally pseudo-
morphed by compact fibrous aggregates of pale- to bright-green clay
(nontronite?) occasionally accompanied by calcite. Intrusion of ande-
site and basalt porphyry dikes has had little noticeable effect on
igneous or carbonate wall rocks; the decomposition of phenocryst
minerals within the dikes is considered to be the result of deuteric
processes.

Breccia

Intrusion breccia

A steep-walled pipelike body (30 m by 20 m in plan) of poorly
sorted, heterogeneous breccia is emplaced between granodiorite porphyry
and quartz diorite near the southern edge of the stock in the central
pit area (Plate I). Closely packed angular fragments up to 10 cm in
diameter include quartzite, marble, garnetized limestone, hornfels, and
porphyry containing K-feldspar veinlets. Copper mineralization is con-
fined to calc-silicate fragments.

The matrix material appears to be igneous porphyry similar in
appearance to granodiorite porphyry, but modified locally by protoclastic

deformation. The deformational texture resembles magmatic-induced foliation described in border rocks of the Colville batholith by Waters and Krauskopf (1941). It consists of ragged rectangular strips of quartz, feldspar, and biotite drawn into a subparallel alignment. Where a flow fabric is not apparent, the distinction between igneous matrix and igneous fragments is somewhat arbitrary, but the matrix generally represents less than 50 percent of the rock.

This fragmental unit appears to be a pipe of intrusion breccia consisting largely of the remnants of a shattered block of altered limestone and early, veined porphyry which was engulfed in and carried upward by a late surge of magma. This late batch of magma may have been guided by a fracture or fault zone, or by an intersection of such structures. The body does not appear to represent a mineralized breccia pipe of the type described by Perry (1961) in the Cananea district, Mexico, or referred to as intrusive breccia by Bryant (1968) at Bisbee, Arizona.

Breccia dikes

A series of narrow (0.1-2 m) discontinuous dikelike bodies charged with heterogeneous, rounded to subangular fragmental debris (Figure 14) are termed breccia dikes. Dike segments are 20-50 m in length and generally have strikes within 10-20 degrees of east-west. They are most abundant in Cretaceous volcanic rocks between the Christmas stock-dike complex and the hornblende rhyodacite porphyry stocks and dikes 1 km to the north (Plate I).
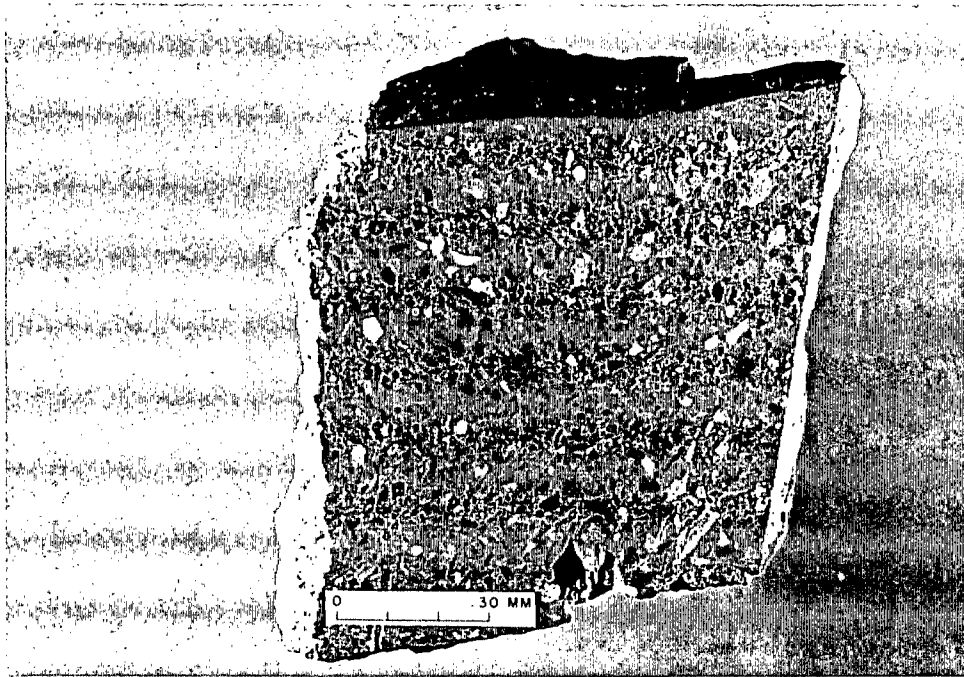
Figure 14. Sample of breccia dike with abundant siliceous and carbonate rock fragments in fine-grained epidotized matrix.

The poorly-sorted fragment load commonly includes abrasion-resistent and inert materials such as quartzite, sandstone, chert, and Precambrian granite, with lesser amounts of diabase, hornblende andesite porphyry, limestone, and calc-silicate hornfels(?). The fragment load varies, even within a single dike, from a coarse breccia (fragments 1-10 cm) to a coarse gritty sand.

Thin section examination of breccia dikes reveals that larger fragments are tightly fitted within a clastic matrix consisting of abundant, rather angular quartz chips, and sparse biotite, feldspar, and sphene grains, 0.1 to 0.5 mm across; these fragments are, in turn, enclosed by a fine rock flour. Where large fragments are broken, but remain essentially intact, a fine siliceous breccia has been injected along cracks. Strong undulatory extinction of quartz grains and bent mica flakes suggest considerable deformation during emplacement.

The fine fraction, plagioclase feldspar grains, and some rock fragments are partially to totally replaced by fine-grained epidote or an aggregate of epidote and quartz. Coarse epidote, quartz, and calcite occur as open-space fillings. A few dikes contain elongate vesicles lined with coarse euhedral pyrite crystals pseudomorphed by goethite. A minor amount of copper oxide was observed within a cavity of one specimen.

Breccia dikes or pipes have not been noted in the Christmas intrusive complex, and their time of emplacement into volcanic rocks is enigmatic. However, their general occurrence along east-west trends, fragment load, and the presence of pyrite suggest that emplacement

occurred after intrusion of hornblende andesite porphyry and before cessation of mineralization in the district.

The mixture of fragments by size, shape, and composition, and their somewhat deformed appearance, are evidence for a turbulent, perhaps explosive origin. To allow movement of pebble-size fragments, the controlling structures must have been a series of open fissures, possibly subsidiary extensional fractures strung out along east-west fault zones in a manner described by Micham (1974). The presence of abundant Precambrian rock fragments requires that the bulk of material was transported upward. The epidotized matrix material may be finely comminuted limestone and volcanic rock altered by fluids ascending or descending through the dikes.

GEOCHRONOLOGY AND CHEMICAL TRENDS

K-Ar Ages of Igneous Rocks and Vein Minerals

Eight new K-Ar age determinations for igneous rocks and vein minerals at Christmas and another from the literature (Creasey and Kistler, 1962) are summarized in Table 6 and presented graphically in Figure 15. Supporting analytical data and sample locations are given in Appendix II. Also included in Figure 15 is the period of intrusive activity in the nearby Ray district taken from K-Ar and fission track studies by Banks and others (1972) and Banks and Stuckless (1973), respectively.

The combined data show that Laramide magmatism in the Dripping

Table 6. K-Ar age dates from the Christmas mine area.

Sample number	Rock type/material dated	Apparent[1] age (m.y.)
74AB75	Lithic lapilli tuff from Williamson Canyon Volcanics/hornblende	76.2±2.6
54AB75	Hornblende andesite porphyry (fine-grained variety)/hornblende	81.7±1.8
72AB74	Hornblende andesite porphyry (coarse-grained variety/hornblende	76.2±1.3
GB-1	Hornblende rhyodacite porphyry (Granite Basin pluton)/hornblende	72.3±1.6
83AB75	Hornblende rhyodacite porphyry (McDonald stock)/hornblende	69.3±0.9
CS-1-75	Pegmatitic biotite vein in biotite granodiorite porphyry/ biotite (chloritized)	62.8±1.1
D148-337	Quartz-K-feldspar-sericite-chlorite vein in biotite granodiorite porphyry/sericite	62.5±1.0
AB49-73	Basalt porphyry/whole rock	25.5±0.2
KA9*	Biotite granodiorite porphyry/biotite	62

1. The ± value is the estimated analytical uncertainty at 1 standard deviation.

* Data from Creasey and Kistler (1962), error is estimated at ±4 percent.

Supporting analytical data and sample locations are presented in Appendix II.

Intrusive periods I-V,
Ray district (Banks
and others, 1972; Banks
and Stuckless, 1973)

S

Early vein, Christmas stock

B

Early vein, Christmas stock

B

Biotite granodiorite porphyry, Christmas
stock (Creasey and Kistler, 1962)

H   H

Hornblende rhyodacite porphyry

H=Hornblende
B=Biotite
S=Sericite

H   H

Hornblende andesite porphyry

H

Lithic lapilli tuff,
Williamson Canyon Volcanics

85   80   75   70   65   60   55

K-Ar age (X10^6 years before present)

Figure 15. K-Ar ages of hornblende, biotite, and sericite from
igneous rocks and veins at Christmas. Also included is the period
of intrusive activity for the Ray district. Horizontal bars
represent the analytical uncertainty in each determination.

Spring Mountains evolved over an extended period from within the Late Cretaceous ($\sim$75-80 m.y. ago) to the Early Tertiary ($\sim$60 m.y. ago). Ore deposits were formed at Christmas ($\sim$63-61 m.y. ago) and at Ray ($\sim$61-60 m.y. ago) as magmatic activity waned in early Paleocene time.

The single K-Ar age for hornblende from volcanic breccia of the Williamson Canyon Volcanics conflicts with ages for hornblende andesite porphyry dikes cutting the volcanic pile. This conflict may be the result of the volcanic hornblende age being too young (possibly reset by loss of radiogenic argon during a thermal event or alteration) and/or the porphyry dike hornblende ages being too old (because of excess argon, leaching of potassium, or contamination).

Although evidence is insufficient for an unequivocal explanation, the first option is preferred. Hornblende separated from lapilli tuff appears minimally altered, but rounded and embayed crystal margins indicate significant resorption effects. The sample also contains uralitized clinopyroxene, which probably formed during widespread propylitic alteration of the volcanic pile. Furthermore, the sample was collected less than 150 m from the western tip of the Christmas stock, a heat source, and rock fragments and matrix (although not the hornblende) are peppered locally with fine-grained secondary biotite, signifying the passage of a hydrothermal fluid phase. Despite evidence indicating that hornblende is more argon-retentive than other K-silicates during thermal events (Hart, 1964; Dalyrymple and Lamphere, 1969), the cumulative effects of partial recrystallization and hydrothermal alteration may have released enough argon to reset the potassium-argon "clock."

Alternatively, hornblendes from andesite porphyry dikes may
have yielded anomalously older ages. Since analyzed potassium contents
appear to be reasonable for igneous hornblendes (Deer and others, 1963)
and sources of contamination, such as mafic inclusions, were removed
before mineral separation, excess argon would seem the most likely
source of error. In the Ray district, anomalously old K-Ar ages
determined from hornblendes and chloritized biotites are believed
(Banks and others, 1972; Banks and Stuckless, 1973) to result from
incorporation of Ar from enriched (by leaching of Precambrian basement
rocks?) late-stage magmatic fluids. Discordant hornblende ages may re-
sult from local variability in partial pressure of argon in the parent
magmas. Such a mechanism cannot be ruled out at Christmas, and could
also suggest an explanation for the age variance between the two horn-
blende andesite porphyries.

The writer knows of no published age dates for the Williamson
Canyon Volcanics, but S. B. Keith (personal communication, 1976) of the
University of Arizona reports that K-Ar age determinations on hornblendes
from three andesite porphyry-type dikes from the nearby Saddle Mountain
mining district yielded an average age of 81 m.y. Thus, from Keith's
results and mine, five hornblende ages from andesite porphyry intruding
the Williamson Canyon Volcanics exceed 76 m.y. and four exceed 80 m.y.

If the age of hornblende from volcanic breccia is anomalous,
the eruption of the Williamson Canyon Volcanics and emplacement of some
hornblende andesite porphyry dikes occurred about, or prior to, 80 m.y.
before present. This point in time is consistent temporally with the

Late Cretaceous (approximately 80 m.y. ago) tectonic transition from "thin skinned" Sevier orogeny to classic Laramide orogeny in the North American Cordillera (Coney, 1972, 1976).

The K-Ar ages (69.8, 72.3 m.y.) of hornblendes from hornblende rhyodacite porphyry plutons near Christmas correlate closely with dates for preore Tortilla Quartz Diorite and Rattler Granodiorite (70±1 m.y.) belonging to Intrusive Period I in the Ray district (Banks and Stuckless, 1973). Consanguinuity of the petrographically similar Granite Basin laccolith (Willden, 1964) and McDonald stock is also indicated. The presence of east-west-trending hornblende rhyodacite porphyry dikes north of the Christmas mine and equivalent dikes with trends N65-70°E in the Hayden quadrangle (Banks and Krieger, 1977) suggests that extension fractures generated by northeast-directed compression (Banks and Krieger, 1977; Rehrig and Heidrick, 1972, 1976) may have developed in the Dripping Spring Mountains by approximately 70 m.y. ago.

Two K-Ar ages for vein minerals and a biotite age for their biotite granodiorite porphyry host in the Christmas stock (from Creasey and Kistler, 1962) support the viewpoint derived from field and petrographic observations that emplacement of biotite granodiorite porphyry and early hydrothermal alteration-mineralization (Stage I) are essentially synchronous events. However, the minerals dated, a chloritic biotite and coarse sericite, are less common constituents of early K-silicate veins. No time-limiting brackets can yet be placed on the total episode of intrusion and ore deposition at Christmas, or on specific events during the evolution of the deposit. These early Paleocene

ages at Christmas are roughly concordant with the age of Granite Mountain Porphyry (Intrusive Period III) and the apparent age of the Ray deposit (61-60 m.y.) reported by Banks and others (1972) and Banks and Stuckless (1973).

Laramide ages for igneous rocks from the Dripping Spring Mountains younger than approximately 60 m.y. have not yet been published. One of several basalt dikes emplaced along northeast- to northwest-trending fractures and faults in the Christmas open pit yielded a whole rock K-Ar age (Table 6) near the Oligocene-Miocene boundary (25.5 m.y.). The pattern of the host structures is diagnostic of Basin and Range tectonism, and the 25.5 m.y. date is characteristic of the mid-Tertiary magmatic pulse in Arizona (Damon and Mauger, 1966).

The Calc-Alkaline Trend

Chemical data for igneous rocks at Christmas (from Table 1), plotted in the normative quartz-orthoclase-plagioclase and AFM triangles of Figure 16 and the percent oxide vs. D.I. variation diagrams of Figure 17, illustrate a calc-alkaline differentiation trend. It should be noted here that representative samples chosen for analysis were free from obvious contamination (pervasive alteration, veins and fracture coatings, inclusions, and so forth). Most of the samples, however, when studied carefully in thin section, show evidence of "low grade" or deuteric alteration. For example, biotite in plutonic rocks may be weakly chloritized, and clinopyroxene in basalt converted to uralite
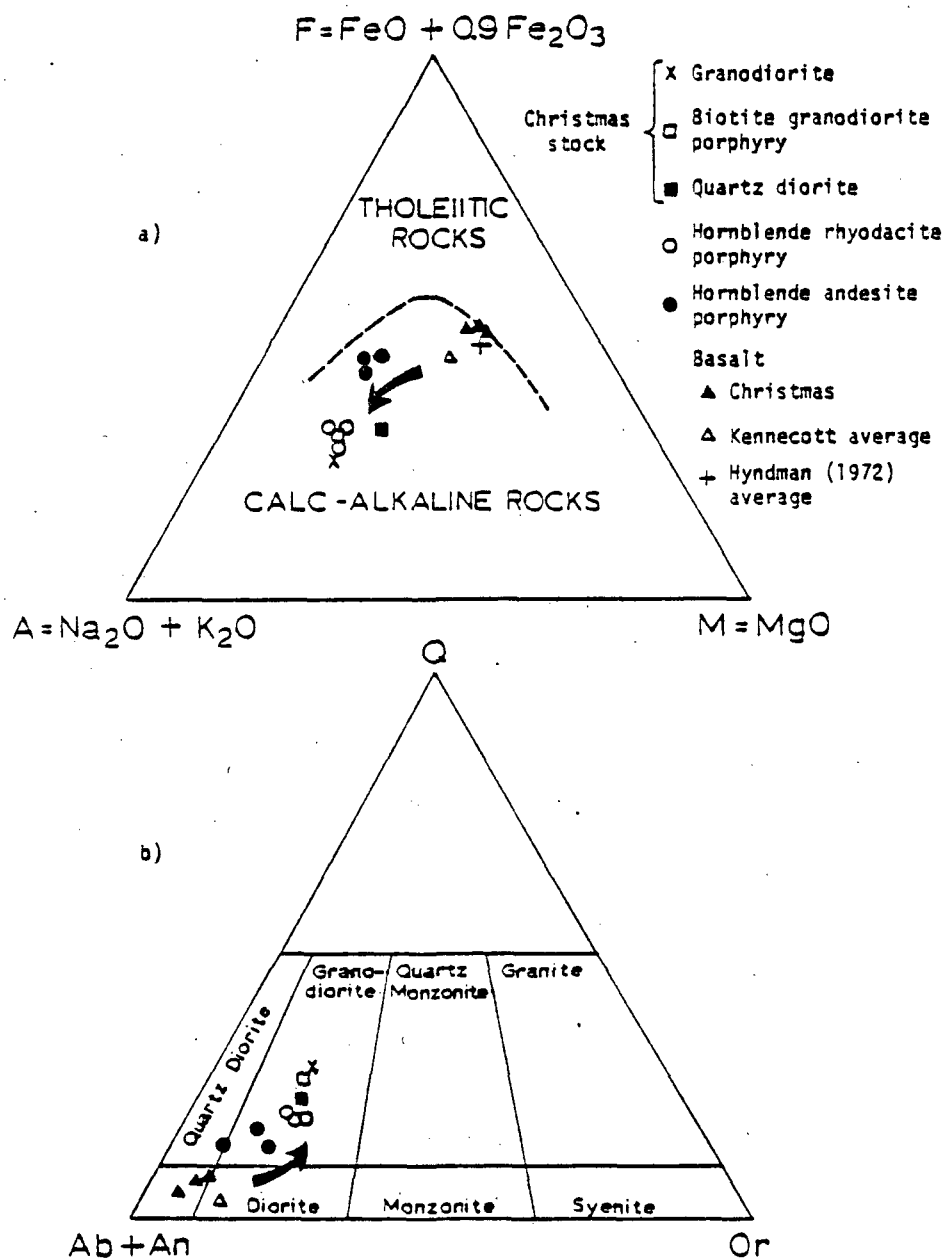
Figure 16. Chemical variation diagrams for Christmas igneous rocks:
(a) AFM diagram with separation of fields from Irvine and Baragar
(1971); (b) normative quartz, orthoclase, and plagioclase. Arrows
represent trend from older to younger rocks.
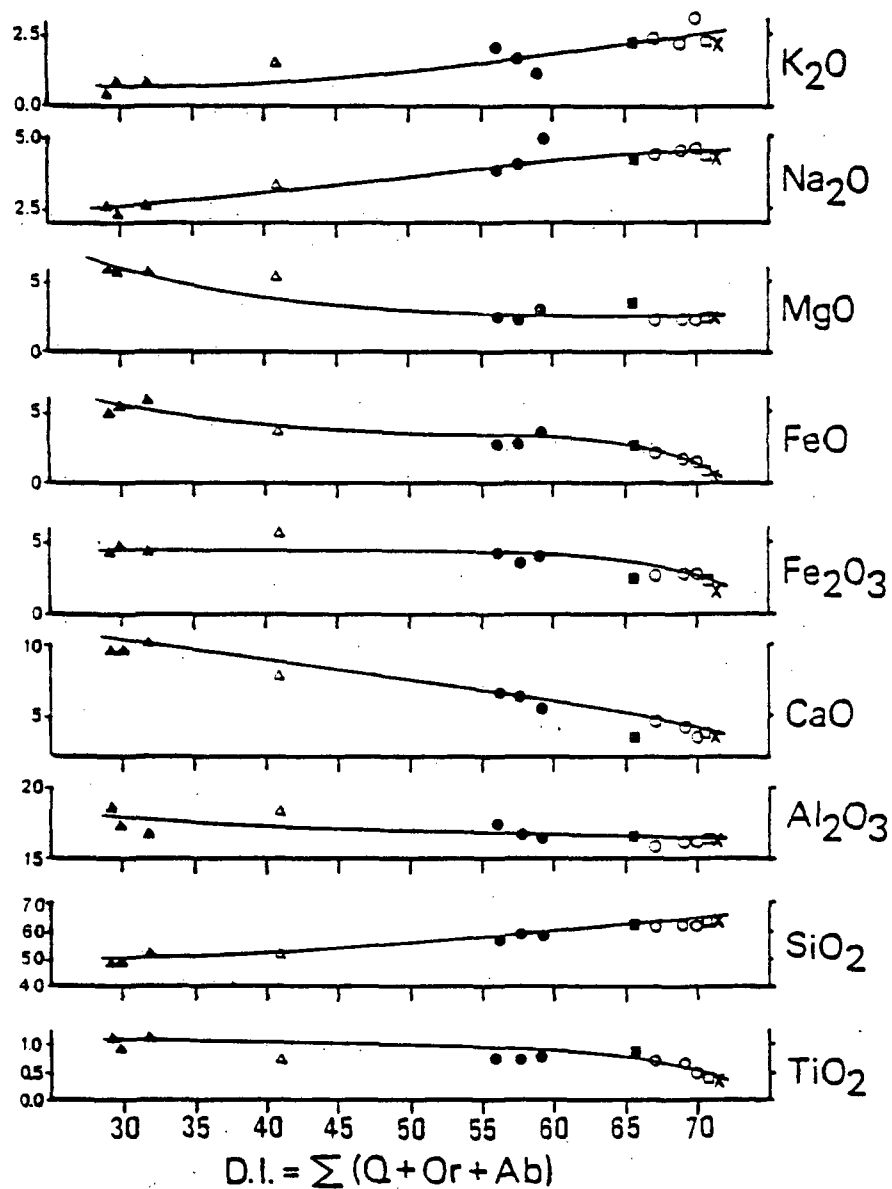
Figure 17. Oxide vs. D.I. variation diagram for igneous rocks at Christmas. The differentiation index (D.I.) of Thornton and Tuttle (1960), plotted along the abscissa, is the sum of normative quartz plus orthoclase plus albite. Weight percent oxides from rapid rock analyses (Table 1) are plotted along the ordinate. Symbols for igneous rocks are given in Figure 16.

(see sample descriptions presented in Appendix I). The effects of this weak pervasive type of alteration on whole rock chemistry is believed to be negligible for most samples, but there are two exceptions. One sample of hornblende andesite porphyry (highest D.I.) was collected from the weakly propylitized sill emplaced between Naco Limestone and Williamson Canyon Volcanics, and appears to be enriched in sodium and depleted in potassium. A second sample, quartz diorite from the Christmas stock, has abundant secondary biotite replacing hornblende; the analysis shows relatively high magnesium and low calcium.

Figure 16 and 17 also display chemical data provided by Kennecott Exploration, Inc. (Table 1, no. 4) which represent 21 analyses of the Williamson Canyon Volcanics collected from a section of flows and volcanic breccia 3 km southeast of Christmas. The higher values for normative Or and Ab in the average for these basalts may reflect the effects of alteration in some samples.

Volcanic rocks are high-alumina basalts with compositions that plot, for the most part, within the calc-alkaline field of the AFM diagram as defined by Irvine and Baragar (1971). The basaltic rocks analyzed in this study are also subalkaline; their normative compositions cluster near the average value (Figure 16a) for 141 analyses of circum-Pacific calc-alkaline basalts compiled by Hyndman (1972, p. 122).

Rocks within the Cretaceous volcanic pile at Christmas do not show the basalt-andesite-rhyolite association characteristic of the calc-alkali series. However, this absence of a calc-alkaline lineage

may be a matter of a restricted local perspective at Christmas. In the type section of Williamson Canyon Volcanics, Simons (1964) has described potassium feldspar-bearing "hornblende latite" and "hornblende andesite or dacite." More felsic volcanic rocks in the present area of study may have been removed by erosion. Furthermore, megascopic differences between basaltic and andesitic rocks may be subtle enough to prevent recognition of the latter in the field.

On a broader regional scale, Upper Cretaceous volcanic rocks of andesitic to rhyolitic composition are widespread (Hayes, 1970). For instance, in the Santa Rita Mountains, 125 km south of Christmas, dacitic to rhyodacitic flows and welded tuffs in the 1500-m-thick Salero Formation have been dated at approximately 72 m.y. (Drewes, 1970). Elsewhere, in the Tucson Mountains 80 km southwest of Christmas, a welded tuff unit of the Cat Mountain Rhyolite has yielded K-Ar dates of 65.6 and 70.3 m.y. (Bikerman and Damon, 1966). Therefore, the Williamson Canyon Volcanics may represent the early mafic endmember of a calc-alkaline volcanic suite of regional extent.

When volcanic and hypabyssal intrusive rocks at Christmas are considered together, the calc-alkaline or "Bowen trend," marked by enrichment of SiO_2, K_2O, and Na_2O, is well established in the basalt → granodiorite sequence (Figures 16 and 17). Conversely, FeO, Fe_2O_3, CaO, and TiO_2 are impoverished with increasing differentiation index.

Only the Christmas intrusive complex is strongly mineralized in the Christmas area, and these rocks are the most highly differentiated. Quartz diorite, however, has a lower D.I. than hornblende

rhyodacite porphyry. The ultimate product of calc-alkaline differen-
tiation, which Bowen (1928) referred to as "petrogeny's residua system,"
is present in the Christmas stock as quenched quartz-K-feldspar-
plagioclase groundmasses in biotite granodiorite porphyry, and stock-
work aplite and K-feldspar-quartz veins; their compositions would plot
along the calc-alkaline trend near the Q-Or sideline of Figure 16b.

The igneous geochronology and chemical trends at Christmas
suggest, but do not prove, that basalts of the Williamson Canyon Vol-
canics and granodioritic plutons that intrude them are products of
a common parent magma. Kuno (1960, 1968) has stressed that high-
alumina basalt is a primary magma type generated by partial melting
of mantle material in orogenic belts. According to Best (1969), high-
alumina basaltic magma can evolve, by fractionation of calcic plagio-
clase and, perhaps, aluminous hornblende, toward more alkaline and
silicic members of the calc-alkali series.

On the basis of his spatial model for Andean deposits (1973),
Sillitoe (1975, p. 1474) has suggested that Late Cretaceous calc-
alkaline volcanic rocks in southwestern North America represent "the
erosional remnants of volcanic piles surmounted by stratovolcanoes"
which were intruded and mineralized by comagmatic porphyritic stocks.
Magmatism is thought to have resulted from the shallow eastward or
northeastward subduction of oceanic crust beneath the westward-driving
North American plate during the period 80-40 m.y. ago (see Coney,
1976). The resulting column of mineralization in the Sillitoe model
extends from depth in the granodioritic to quartz monzonitic intrusive

complex upward through the volcanic pile. Although the mineralized volcanic rocks and stock-dike complex at Christmas appear to be part of a calc-alkaline sequence, and a geometry similar to that depicted by Sillitoe is indicated, more evidence (perhaps from strontium isotopes or trace element geochemistry) is needed to prove consanguinuity.

to 5 mm in width may exceed 90 percent chalcopyrite. The age relationship in the zone of overlap between early Stage I quartz-sulfide veins and later Stage II quartz-chlorite-pyrite-chalcopyrite veins is shown in Figure 19. Volcanic rocks cut by both Stage I and Stage II veins have upgraded copper values (0.4-1.0 percent Cu). Progressively younger Stage II veins and veins increasingly distant from the Christmas stock contain decreasing chalcopyrite/pyrite ratios resulting in the low-grade pyritic fringe zone (Figure 18). The approximate outer limit of 0.2-0.4 percent copper in igneous rocks east of the Christmas fault, derived from drill hole assay data, is also shown in Figure 18.

The general sequence of mainstage sulfide and magnetite mineralization in igneous rocks is summarized in the paragenetic diagram of Figure 20. Textural evidence (isolated anhedral sulfide grains and sulfide-secondary biotite intergrowths) suggests that some disseminated chalcopyrite and pyrite formed during the latter stages of normal magmatic crystallization or during deuteric recrystallization of the main igneous phases. Early-formed veins in the Christmas stock are barren or contain minor amounts of chalcopyrite and/or pyrite. Chalcopyrite appears to have been deposited through most of the mineralization episode from conditions approximating late magmatic to late hydrothermal. Some bornite may have formed contemporaneously with secondary biotite in the stock, but most appears to have been deposited in through-going quartz veins during later Stage I. The precipitation of bornite ceased before development of Stage II veins. Pyrite is sparse in early vein assemblages, but is abundant in all late veins.
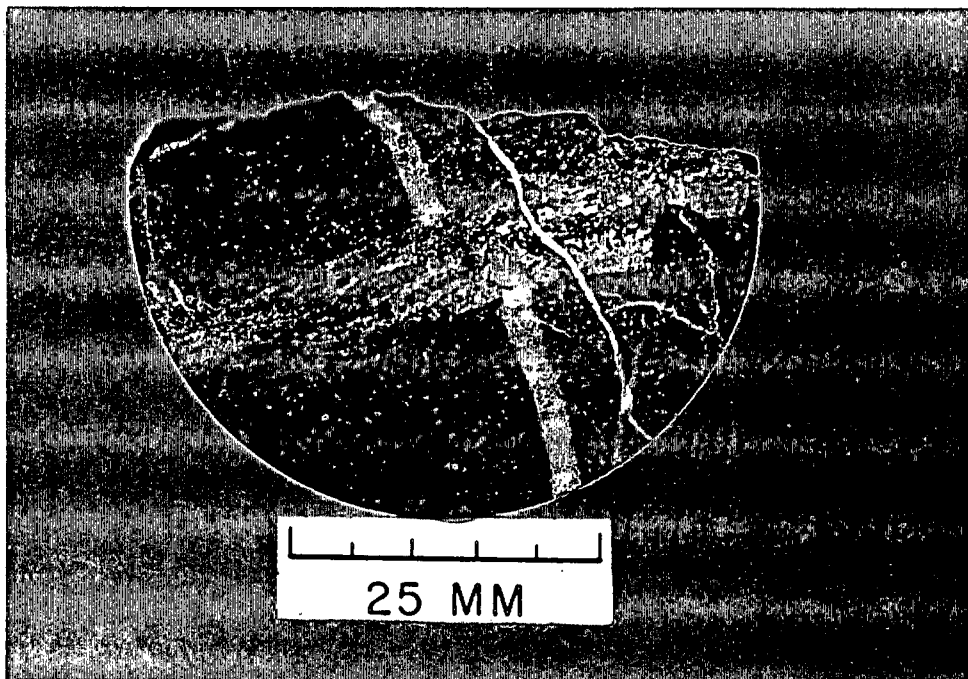
Figure 19. Sample of drill core showing Stage II quartz-chlorite-pyrite-chalcopyrite vein cutting Stage I quartz-sulfide vein.

		Stage I K-silicate Alteration	Stage II Quartz-Sericite-Chlorite Alteration
Intrusive Rocks	Pyrite		
	Chalco- pyrite		
	Bornite		
	Molyb- denite		
	Magnetite	?	
Volcanic Rocks	Pyrite		
	Chalco- pyrite	?	
	Bornite	?	
	Molyb- denite		
	Magnetite		

Figure 20. Sequence of hypogene sulfide and magnetite deposition in igneous rocks.

In the stock some magnetite formed during pervasive recrystallization of original mafic minerals to secondary biotite. It is also a constituent of Stage I veins in higher level intrusive and volcanic rocks. Secondary magnetite is most abundant in Stage II quartz-chlorite-sulfide veins in the Williamson Canyon Volcanics. Molybdenite deposition accompanied the formation of Stage I quartz-rich veins, particularly in the stock, but small amounts continued to precipitate in Stage II veins in the quartz-sericite zone.

Stage I: K-silicate Alteration

The early period of wall rock alteration and veining in the stock and adjacent volcanic rocks, referred to as Stage I, was chiefly an episode of K-metasomatism. This episode was, in large part, time equivalent with emplacement and consolidation of early intrusive phases, but preceded intrusion of granodiorite porphyry and dacite porphyry. The principal manifestations of Stage I alteration are: (1) variable pervasive secondary biotite in the stock; (2) biotitization of basaltic volcanic wall rocks; and (3) stockwork veins consisting of relatively early K-feldspar-rich veinlets in the stock, and later quartz-rich veins in the stock and volcanic rocks. Biotite and K-feldspar are diagnostic minerals of the K-silicate alteration type of Meyer and Hemley (1967), and this nomenclature is adopted for the occurrences listed above. The term potassic alteration (Creasey, 1966) is also widely established in the literature, and is equally applicable at Christmas.

Biotitization in the Christmas stock

Pervasive K-silicate alteration in early phases of the
Christmas stock is characterized by the partial to total replacement
of primary hornblende and biotite phenocrysts by compact pseudomorphous
clusters of fine-grained leafy biotite, and by the presence of small
anhedral flakes of biotite in aplitic groundmass. Although biotite
of this type may alternatively be described as secondary, replacement,
or hydrothermal, the environment of formation is probably late mag-
matic to early hydrothermal, the conditions broadly referred to as
deuteric.

Hornblende is more susceptible to replacement than biotite,
and rocks initially containing a higher percentage of hornblende gener-
ally contain more secondary biotite. I estimate from rough modes of
"least altered" samples that prealteration quartz diorite had 20-22
percent hornblende and 3-5 percent primary biotite. Biotite granodio-
rite porphyry modes (Table 5), by comparison, average approximately 5
percent hornblende and 4 percent biotite. The generally observed
greater amount of secondary biotite in quartz diorite (Dark Phase)
reflects, in large part, this original difference in hornblende content.

Hornblende-destructive biotitization appears to be most complete
in that part of the stock east of the Joker fault, and in peripheral
dikes and sills north and south of the central intrusive mass. In
these rocks, primary book biotite, as well as hornblende, is converted
to aggregates of fine, shreddy biotite. In contrast, quartz diorite
recovered from diamond drill holes along the south margin of the stock

west of the Christmas fault and granodiorite from the core of the intrusion contain fresh hornblende.

Textural characteristics of secondary biotite in quartz diorite and biotite granodiorite porphyry are shown in Figure 21. Secondary biotite is optically rather similar to primary biotite and occurs as 0.1-0.5-mm anhedral to subhedral plates, either randomly oriented or gathered into subparallel alignment along the prismatic cleavage of original amphibole crystals. A common arrangement in quartz diorite (Figure 21a) is a loosely connected network of biotite flakes entrapping anhedral pockets of quartz, calcite, apatite, opaque minerals, and clay(?). In this situation secondary biotite may extend beyond the limits of the original grain, and the form of the host is poorly preserved. Observations of less altered quartz diorite (e.g., Figure 9b) suggest that this "network" texture is partly inherited from the original magmatic configuration of hornblende grains.

Secondary biotite after hornblende in biotite granodiorite porphyry (Figure 21b) typically forms well-defined pseudomorphs. Recrystallization of book biotite in both quartz diorite and biotite granodiorite porphyry is generally incomplete, and appears to begin with the reconstitution of grain margins.

Secondary biotite in the central stock, whether generated from hornblende or biotite, has a golden-brown (X) to dark reddish-brown (Y = Z) pleochroism similar to primary biotite. The composition of this dark-brown "deuteric" mica from quartz diorite, determined by electron microprobe, is Mg-biotite (Foster, 1960) very similar in
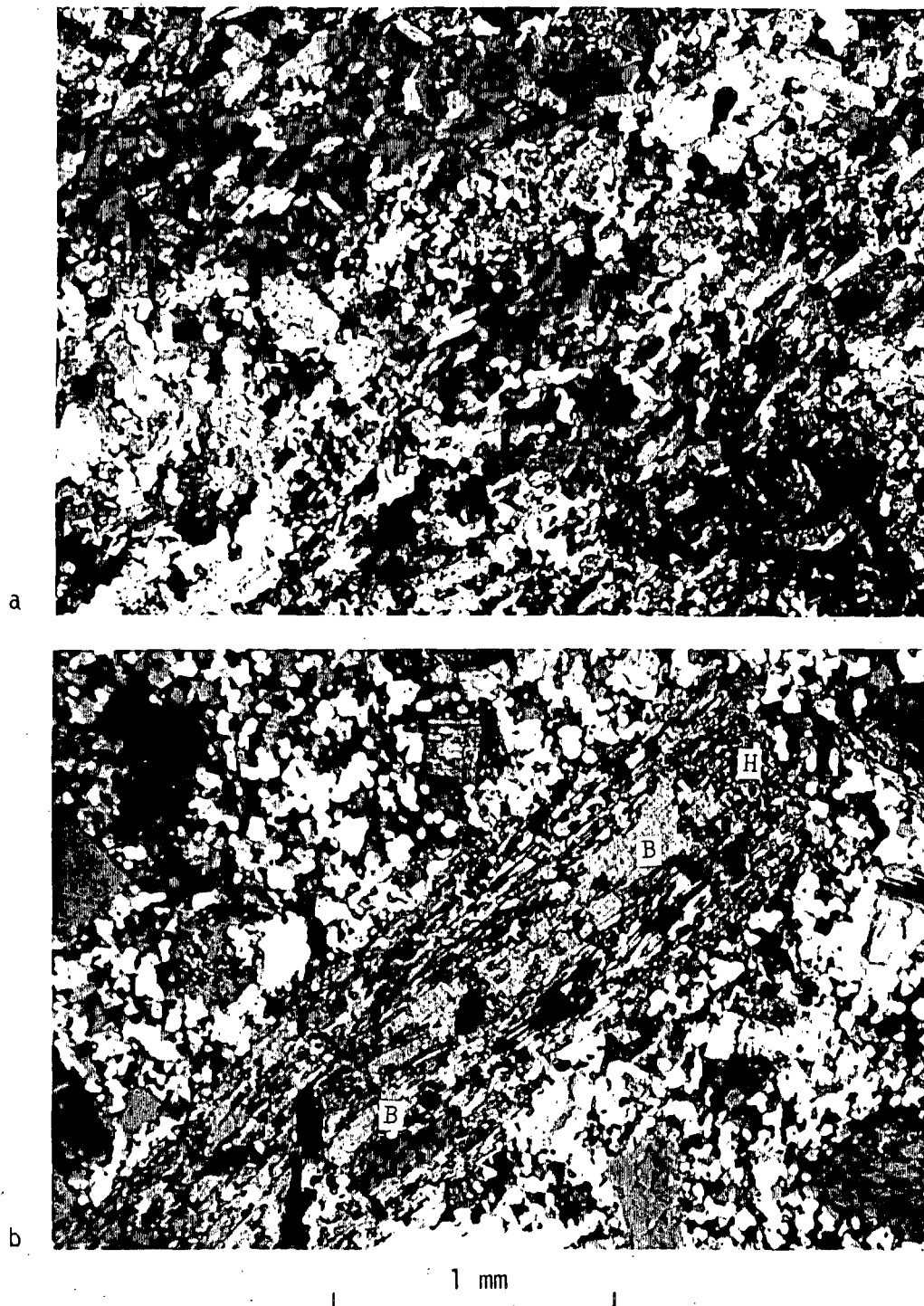
Figure 21. Texture of secondary biotite in the Christmas stock (crossed polarizers). (a) Loosely connected biotite aggregates pseudomorphing hornblende in quartz diorite. (b) Partial replacement of hornblende (H) by biotite (B) in biotite granodiorite porphyry.

composition to phenocrystic biotite from granodiorite and biotite granodiorite porphyry (see Appendix III). In peripheral dikes and sills, secondary biotite may be pale brown to reddish brown in color, and this variety has a phlogopitic composition. Plagioclase in some samples of Dark Phase is replaced by fine-grained aggregates of yellow-green to apple-green mica.

Chlorite is a common companion of secondary biotite. Where chlorite includes tiny grains of sagenitic rutile and anhedral sphene, it appears to be the encroaching phase. However, where secondary biotite and inclusion-free chlorite are intimately intergrown without bleached grain boundaries, they may have formed simultaneously. The amount of chlorite coexisting with biotite in this fashion is proportionately greater in biotite granodiorite porphyry than in quartz diorite. In general, it appears that younger mainstage intrusive phases have somewhat higher chlorite/secondary biotite ratios; postmainstage unveined phases (dacite porphyry and granodiorite porphyry) are characterized by chloritic alteration, and lack secondary biotite.

The stoichiometric conversion of hornblende to biotite liberates calcium, and small grains of epidote, apatite, and calcite are distributed throughout secondary biotite aggregates. Magnetite commonly forms clots and disseminations within clusters of fine-grained biotite. Chalcopyrite, bornite, and pyrite also occur occasionally in this manner. It appears that some magnetite and minor amounts of sulfide formed during early biotitization.

Biotitization of the Williamson Canyon Volcanics

Secondary biotite in mineralized mafic volcanic rocks, first noted by Eastlick (1968), occurs within a broad horseshoe-shaped zone, open to the west, enclosing the Christmas stock (Figure 22). The intensity of biotitization and grade of copper mineralization are strongly dependent on the density of fractures and veins, and reach maximum values adjacent to the Christmas stock east of the Christmas fault.

The biotitization halo can be subdivided (Figure 22) on the basis of rock texture, physical characteristics of the biotite, and associated alteration products into the outer zone of weak biotitization (fringe zone), the zone of moderate biotitization (intermediate zone), and the inner zone of strong biotitization (contact zone). A large portion of the area surrounding the mine east of the Christmas fault is covered by mine waste and alluvium, and the distribution pattern in that area is partly based on diamond drill core samples (see drill hole and surface sample locations in Plate III). Boundaries between subzones are quite gradational and irregular in detail, and their placement in Figure 22 was determined by interpolation between sample locations. The outer limit of biotitization is least clearly defined, but generally extends between 300 and 750 m north and south of the stock at the present level of exposure. The zone of secondary biotite grades outward into rocks with background actinolite-chlorite-epidote alteration.

The biotite zonation map of Figure 22 is generalized from Plate V. Samples plotted on Plate V were assigned a biotitization

Figure 22. Distribution of hydrothermal biotite in volcanic rocks.

Christmas
stock

20,000 E

10,000 N

	WEAK
	MODERATE	BIOTITIZATION OF VOLCANIC ROCKS
	STRONG

| 0 | 1000 | 2000 ft |
| 0 | 250 | 500 m |

86
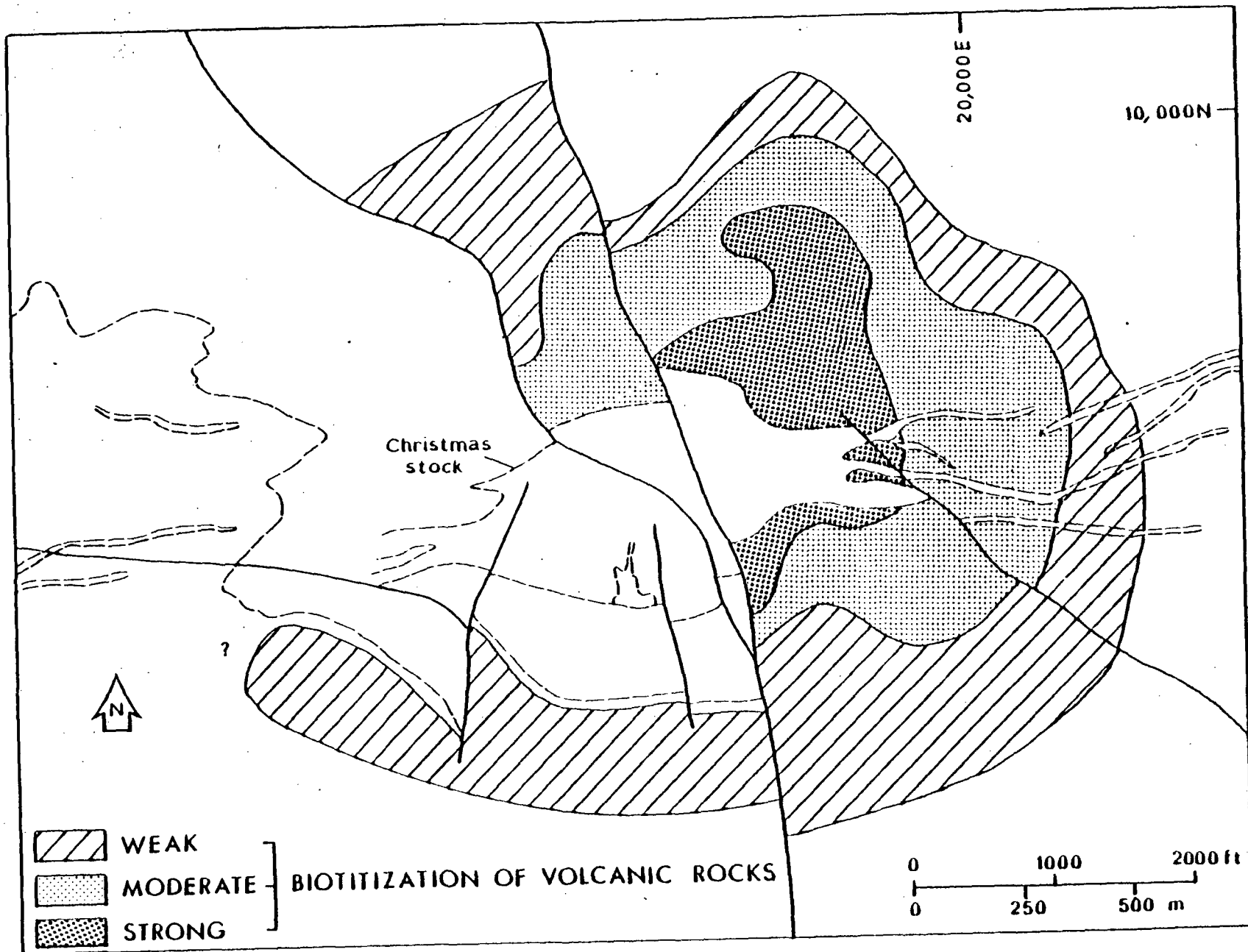
index (B.I.) of 0, 1, 2, or 3 corresponding to unaltered, weakly altered, moderately altered, or strongly altered, respectively. The method of ranking samples was qualitative because of the large number of samples examined and the local variability in alteration intensity, and based primarily on megascopic observations augmented by thin section identification and X-ray diffraction of whole-rock powders.

Prior to megascopic examination with an ordinary binocular microscope, most samples were slabbed and polished. One of the slabs was then etched in hydrofluoric acid and stained with sodium cobaltinitrite to check for K-feldspar and to highlight textural features.

Samples of volcanic rock which contain no visible biotite, or in which biotite identification was uncertain, were analyzed by X-ray diffraction. Slurries made from grinding whole-rock powders under water were poured onto glass slide mounts and X-rayed employing identical instrument settings for all samples. Rocks producing diffraction patterns with the diagnostic 10Å line for biotite were given a B.I. of 1; those with no mica peak were assigned a B.I. value of 0. Thin sections prepared from some samples verified that the reflection at 8.9 degrees 2θ was indicative of biotite rather than muscovite or another phyllosilicate. Furthermore, the X-ray method was sensitive enough to indicate the presence of less than 5 percent biotite.

Samples with visible biotite in envelopes along fractures or veins were assigned a B.I. of 2. Where the fracture density is high enough, fine-grained pale-brown biotite permeates the rock matrix. The original texture of the rock is largely preserved. Volcanic rocks

containing residual vitreous plagioclase phenocrysts (occasionally flecked with biotite) in a recrystallized matrix of relatively coarse-grained dark-brown biotite, often accompanied by visible quartz, were given a B.I. of 3. The original texture in strongly altered volcanic rocks is largely obliterated and the abundant secondary biotite imparts a distinctive dark-gray color to the rock.

Multiple samples were collected from drill holes to examine vertical variation in biotitization. Where biotitization indexes of different rank are present in a single drill hole, the dominant index is plotted in Plate V.

Zone of weak biotitization. The distribution of rocks with a B.I. of 1 (Plate V) defines the outermost zone of weak biotitization (Figure 22). Secondary biotite in the fringe zone is pervasive, but its presence is difficult to detect megascopically. In thin section, individual biotite grains are minute and exhibit a platy morphology. Grain size ranges between 5 and 20 microns, although a few grains may exceed 75 microns in maximum dimension. The color is generally pale brown to greenish brown, becoming less green and more brown as grain size increases toward the stock.

This incipient biotitization has two principal occurrences. Firstly, anhedral-granular biotite aggregates appear to occupy sites of original phenocrysts of olivine and pyroxene(?), and vesicles formerly filled with amygdaloidal minerals (Figure 23a). To a lesser extent biotite replaces plagioclase and uralitic amphibole. Since no

Figure 23. Photomicrographs (crossed polarizers) showing secondary biotite in mafic volcanic rocks. (a) Zone of weak biotitization: aggregates of very fine-grained pale-brown biotite (B) occupying sites of original mafic minerals. (b) Zone of moderate biotitization: biotite concentrated in the rock matrix. (c) Zone of strong biotitization: rock is largely recrystallized to biotite (B) + sodic plagioclase (P) + quartz (Q).

a
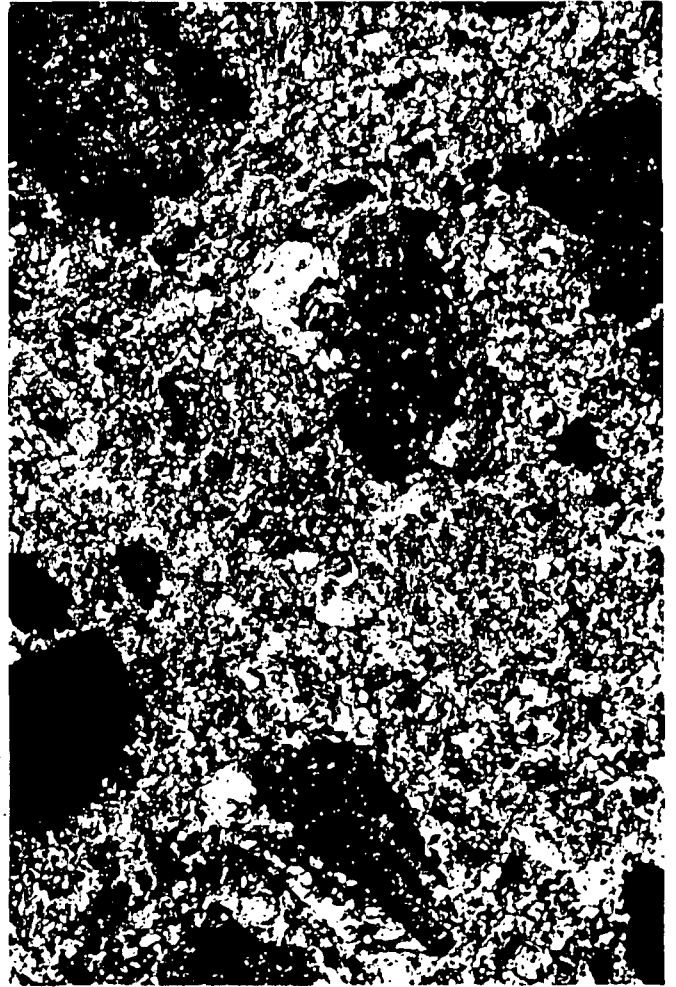
b

1 mm
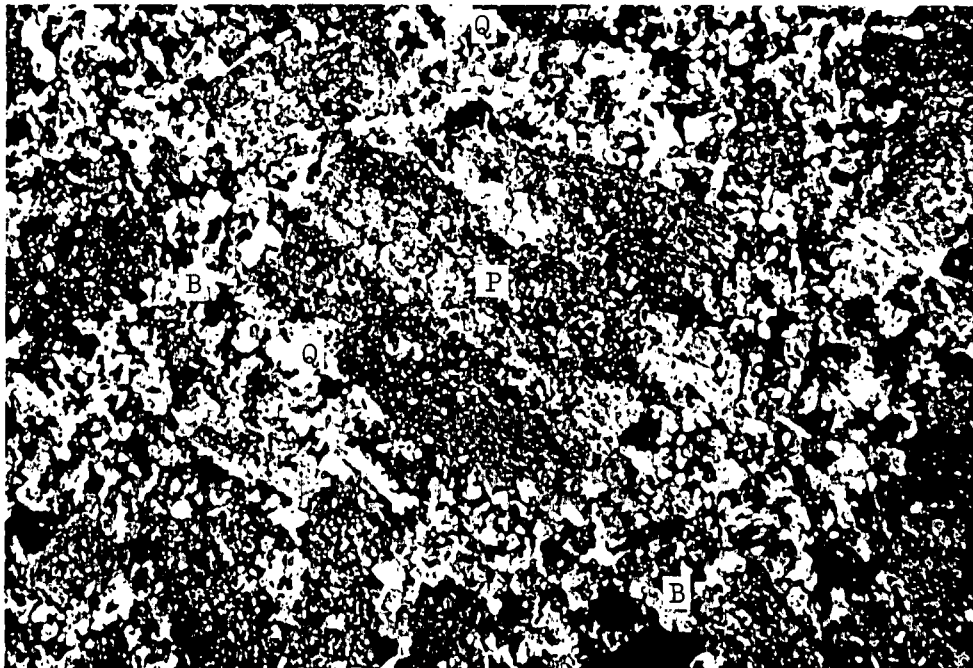
c

unaltered olivine has been observed in volcanic rocks beyond the secondary biotite zone, it is likely that biotite formed at the expense of minerals originally derived from the decomposition of olivine, such as montmorillonite and chlorite. Likewise, irregular areas with sharp boundaries, probably voids or amygdules in the original rock, are filled with biotite or with mixtures of biotite, chlorite, calcite, and actinolite. The general paucity of chlorite in the fringe zone suggests that it has been largely converted to biotite. Secondly, biotite preferentially replaces matrix materials of accessory volcanic and diabasic rock fragments in volcanic breccia, often flooding the interstices between intergranular plagioclase laths. In total, compact masses and disseminated flakes of biotite constitute up to 15 percent of the rock volume; modification of original volcanic textures is minimal.

Fracture and vein density is low in the peripheral biotite zone; mineralization consists mainly of pyrite coating fracture surfaces. Consequently, rocks in the zone of weak biotitization average less than 0.1 percent Cu.

Zone of moderate biotitization. An intermediate zone of moderate biotitization, determined by the distribution of samples with a B.I. of 2, separates the fringe zone from strongly altered volcanic wall rocks adjacent to the stock (Figure 22). Located entirely within the hanging wall of the Christmas fault, moderate biotitization extends 300 to 400 m north and south of the stock, and several hundred meters along the rhyodacite porphyry dikes east of the stock.

The outer edge of the zone of moderate biotitization is marked by the appearance of megascopically visible biotite envelopes along mineralized fractures. Typically, the fractures also host Stage II quartz-chlorite-sulfide veins. Areas between fractures have the alteration intensity equivalent to the zone of weak biotitization. As fracture and vein density increases approaching the stock-dike complex, the biotite-rich envelopes widen and coalesce until a continuous network of fine-grained biotite pervades the intervein portions of the wall rock.

The increased biotite content (15-55 percent of pervasively altered rock) is concentrated in the rock matrix, having formed at the expense of mafic minerals and opaque dust (Figure 23b). Only coarse-grained actinolite and plagioclase escape complete destruction. Pale-brown to pale greenish-brown flakes measure 10-60 microns in long dimension, and plumose clusters of somewhat coarser tabular crystals are approximately 0.1 mm in length. Although hand specimens show little textural modification, the whole-rock color is rendered a dull gray.

Zone of strong biotitization. The occurrence of samples with a B.I. of 3 mark the zone of strong biotitization (Figure 22), or the contact zone, developed in volcanic wall rocks adjacent to the Christmas stock. Volcanic rock in the contact zone is highly altered and, in places, reconstituted to such a degree that a distinction between intrusive (particularly quartz diorite) rock and Williamson Canyon Volcanics basalt is difficult.

The distribution of the inner zone of strong biotitization is

spatially related to the location of the Christmas intrusive complex and the distribution of Stage I quartz-sulfide veins. For example, the lobe of biotitic alteration extending northeastward from the stock (Figure 22) reflects the subsurface distribution of dikes or apophyses of K-silicate-altered biotite granodiorite porphyry in the "northeast salient." The wedge block between the Christmas and Joker faults and volcanic rocks along the steeply dipping south contact have very narrow zones of intense biotitization.

Basaltic wall rocks in the contact zone adjacent to the Christmas stock are completely recrystallized to an interpenetrating assemblage of biotite + quartz + magnetite + sodic plagioclase ± hornblende(?) ± apatite ± anhydrite ± chalcopyrite ± bornite. All of these minerals except plagioclase also occur in Stage I veins near the stock. In thin section the rock is flooded with anhedral to subhedral flakes of strongly pleochroic brown mica, 0.05-0.35 mm across, constituting between 20 and 55 percent of the rock volume (Figure 23c). An analysis of biotite from the contact zone is only slightly more magnesian than compositions of "deuteric" biotites from quartz diorite (see Appendix III). It is apparent that, within the biotite halo in volcanic rocks, the increase in grain size, coloration, and content of biotite toward the Christmas stock correlates with stronger copper mineralization.

The presence of disseminated quartz suggests addition of silica during biotitization. Pale, nonfibrous hornblende(?) associated with clusters of biotite probably represents altered actinolite. Plagioclase is partially to completely replaced by: (1) tiny crystals of one or

more of biotite, quartz, anhydrite, apatite, epidote, and pale-green hornblende(?); and (2) patchy areas of albite, quartz, K-feldspar (rare), and clay minerals. Although fine detail of original growth zoning and twinning is blurred by these alteration effects, crude measurements of extinction angles on relict albite twin lamellae indicate a composition of sodic to intermediate andesine. Thus, plagioclase (originally labradorite) may have been enriched in the albite molecule during alteration, a process believed to have occurred concomitantly with biotitization of mafic volcanic rocks in some Andean deposits (Gustafson and Hunt, 1975; Camus, 1975).

Anhydrite occurs as granular disseminations in the most thoroughly recrystallized volcanic rocks adjacent to the Christmas stock east of the Joker fault.

Stockwork veining

A complex stockwork of Stage I veins, centered on the Christmas stock, consists principally of K-feldspar veinlets and quartz-K-feldspar veins in the intrusive complex, and quartz-sulfide veins in volcanic wall rocks east of the Christmas fault. Less common vein types in the core of the stock are composed of pegmatitic biotite, aplite, and the coarse-grained vuggy assemblage K-feldspar-sericite-chlorite-quartz.

The distribution of Stage I veins shown in Figure 24 is derived from the results of surface mapping and detailed sampling presented in Plate VI. It is evident that the outer limit of Stage I veining coincides rather closely with the outer limits of strong biotitization (Figure 22) and chalcopyrite-bornite mineralization (Figure 18).

Figure 24. Distribution of Stage I (K-silicate) and Stage II (quartz-sericite-chlorite) veins in the Christmas intrusive complex and the Williamson Canyon Volcanics.

Christmas stock

Outer limit of biotitization in volcanic rocks

20,000 E

10,000 N

Stage I (K-silicate) veins
-K-feldspar-quartz veins in intrusive rocks
-quartz-sulfide veins in volcanic rocks

Stage II (quartz-sericite-chlorite) veins
-quartz-sericite veins in intrusive rocks and feldspathic sandstone
-quartz-chlorite veins in volcanic rocks

N

| 0 | 1000 | 2000 ft |

| 0 | 250 | 500m |

108
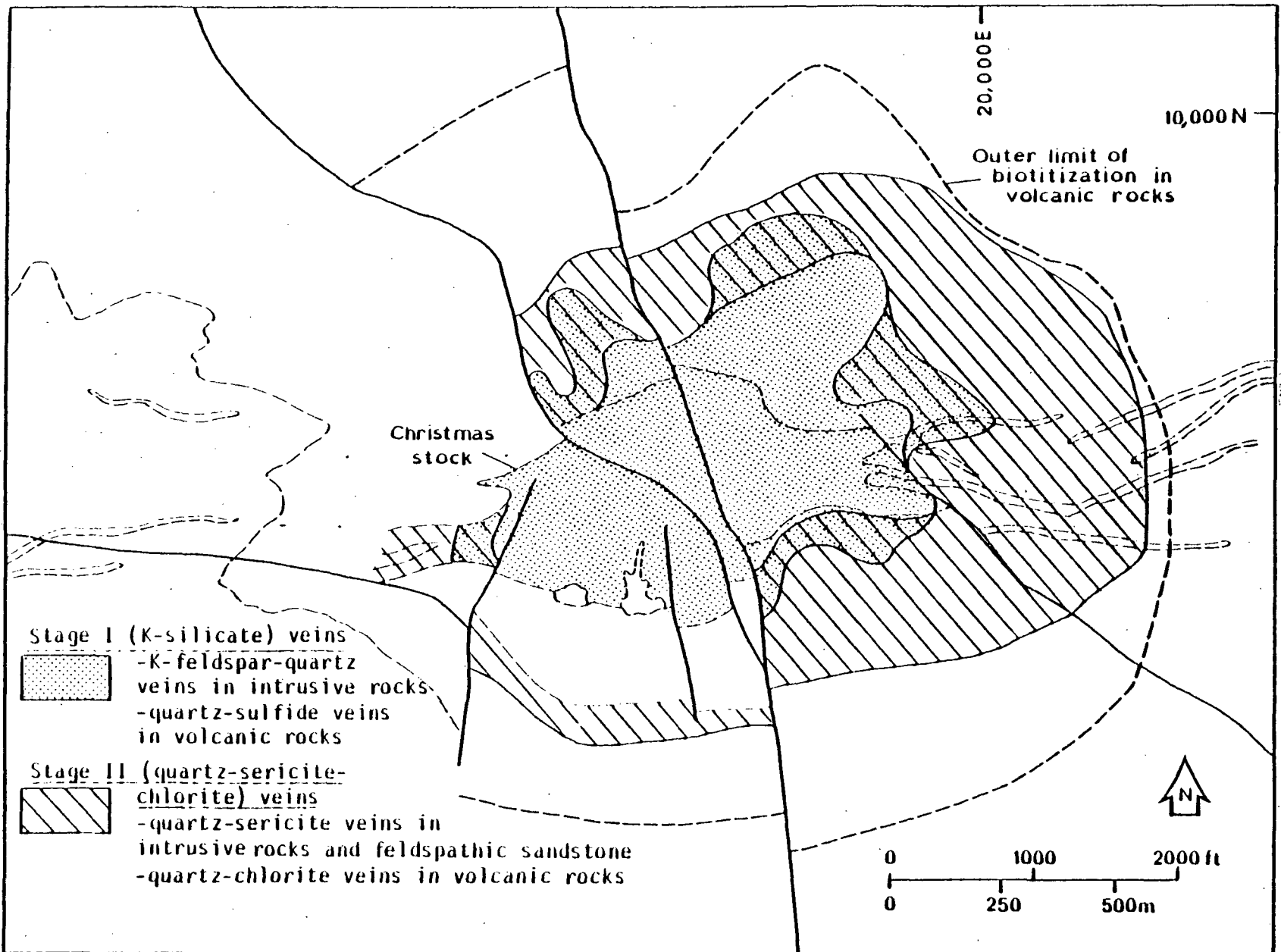
Christmas stock. Within the stock, Stage I veins penetrate quartz diorite, biotite granodiorite porphyry, and granodiorite, but are absent in and truncated by dacite and granodiorite porphyries. Early, disoriented 0.5-2-mm-veinlets of pale-pink K-feldspar, generally a somewhat turbid and weakly perthitic orthoclase, are consistently cut by well-defined, steeply dipping quartz-rich veins up to 5 cm in width (Figure 25). The reverse relationship may occur, in which quartz veins are cut by K-feldspar veinlets, but is more difficult to document because quartz is not easily replaced by K-feldspar.

Precipitation of K-feldspar within veinlets was composite, that is, K-feldspar formed from deposition in open channelways as well as from orthoclazation of phenocrystic and groundmass plagioclase. A typical veinlet in biotite granodiorite porphyry has a variable appearance: smooth and continuous when traversing plagioclase grains, diffuse in aplitic groundmass, and absent or intermittent where the host fracture cuts grains of quartz and biotite. Since K-feldspar veinlets penetrate phenocrysts and locally maintain straight or slightly curvilinear forms, they must have formed, for the most part, after consolidation of the main intrusive phases. A minor amount of K-feldspar, however, particularly in quartz diorite, occurs in irregular swirly masses associated with lenses of granular quartz, and apparently crystallized while the magma was still mobile.

The more through-going quartz-rich veins typically have sharp contacts against intrusive wall rocks, and contain narrow borders and discontinuous medians of K-feldspar. Many, if not all, zoned quartz-
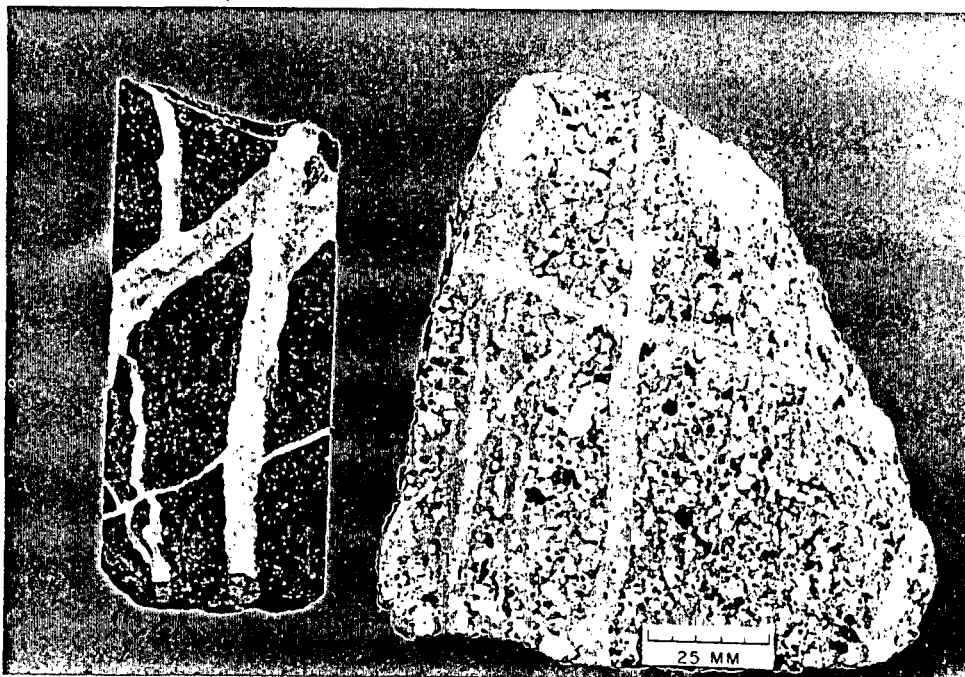
Figure 25. Examples of Stage I stockwork veins. In the sample of biotite granodiorite porphyry on the right, K-feldspar veinlets (stained yellow) are cut by through-going quartz-rich veins. The sample of basalt on the left is cut by vitreous quartz-sulfide veins.

rich veins may have formed along reopened fractures initially healed by K-feldspar. The widest quartz veins have near vertical attitudes, very minor K-feldspar, and cut all other K-feldspar-bearing veins. Therefore, disoriented K-feldspar veinlets and steep quartz veins represent the early and late endmembers, respectively, of a system of veins probably formed during a continuous episode of fracturing. Stage I veins offset at junctions with other Stage I veins suggest that structural adjustments continued in the pluton during the period of early veining.

In addition to quartz and K-feldspar, Stage I veins in the stock contain small amounts of calcite, biotite, chlorite, epidote, apatite, stilbite, pyrite, chalcopyrite, bornite, molybdenite, and rarely, anhydrite.

The genetic relationship between Stage I veining and pervasive biotitization in the stock is not entirely understood. In biotite granodiorite porphyry, all hornblende within K-feldspar envelopes is converted to biotite, but relatively fresh or partially biotitized hornblende may occur in wall rock just beyond the K-feldspar-rich selvage. Some samples of quartz diorite with pervasive secondary biotite, however, contain little or no vein-related K-feldspar. Furthermore, stained thin sections of quartz diorite and biotite granodiorite porphyry indicate that little or no secondary K-feldspar coexists with secondary biotite between vein envelopes. These observations suggest that the bulk of pervasive secondary biotite formed independently of, and probably prior to, the deposition of fracture-controlled K-feldspar.

Williamson Canyon Volcanics. Stage I stockwork veins in volcanic rocks are simple aggregates of vitreous quartz and small but significant amounts of chalcopyrite and bornite. The sulfides typically occur along marginal zones and crosscutting fractures. Anhydrite, an otherwise uncommon mineral in igneous rocks of the Christmas deposit, is abundant in quartz veins near the stock. Other minerals present in sparse amounts are magnetite, molybdenite, chlorite, calcite, biotite, hornblende, and late-forming zeolite. K-feldspar is not a constituent of Stage I veins in volcanic rocks.

The contacts between Stage I quartz-sulfide veins and strongly biotitized volcanic wall rock are generally sharp (Figure 25). The vein system consists of steeply dipping, mutually crosscutting veins up to 3 cm in width anastomosing into numerous subparallel 1-mm-veinlets. Typically, veins are offset where intersected by another of the same type. In a few places, the veins are coarse vuggy aggregates of sugary quartz and sulfide grains which appear to grade outward into silicified host rock. The vein mineralogy and general style of fracturing and veining suggest that quartz-sulfide veins represent genetically equivalent continuations of Stage I quartz-K-feldspar veins in the stock.

Observations made during early stages of mapping in the open pit suggested a possible radial pattern for through-going Stage I veins in the stock. Strike measurements of more than 230 steeply dipping quartz-rich veins (David S. Cook, personal communication, 1976) cutting Light Phase, Dark Phase, and volcanic rocks within the K-silicate zone, plotted in the form of rose diagrams in Figure 26, serve to amplify

Figure 26.   Rose diagrams showing strike orientations for Stage I
veins cutting biotite granodiorite porphyry, quartz diorite, and the
Williamson Canyon Volcanics.   Structural data from David S. Cook
(personal communication, 1976).
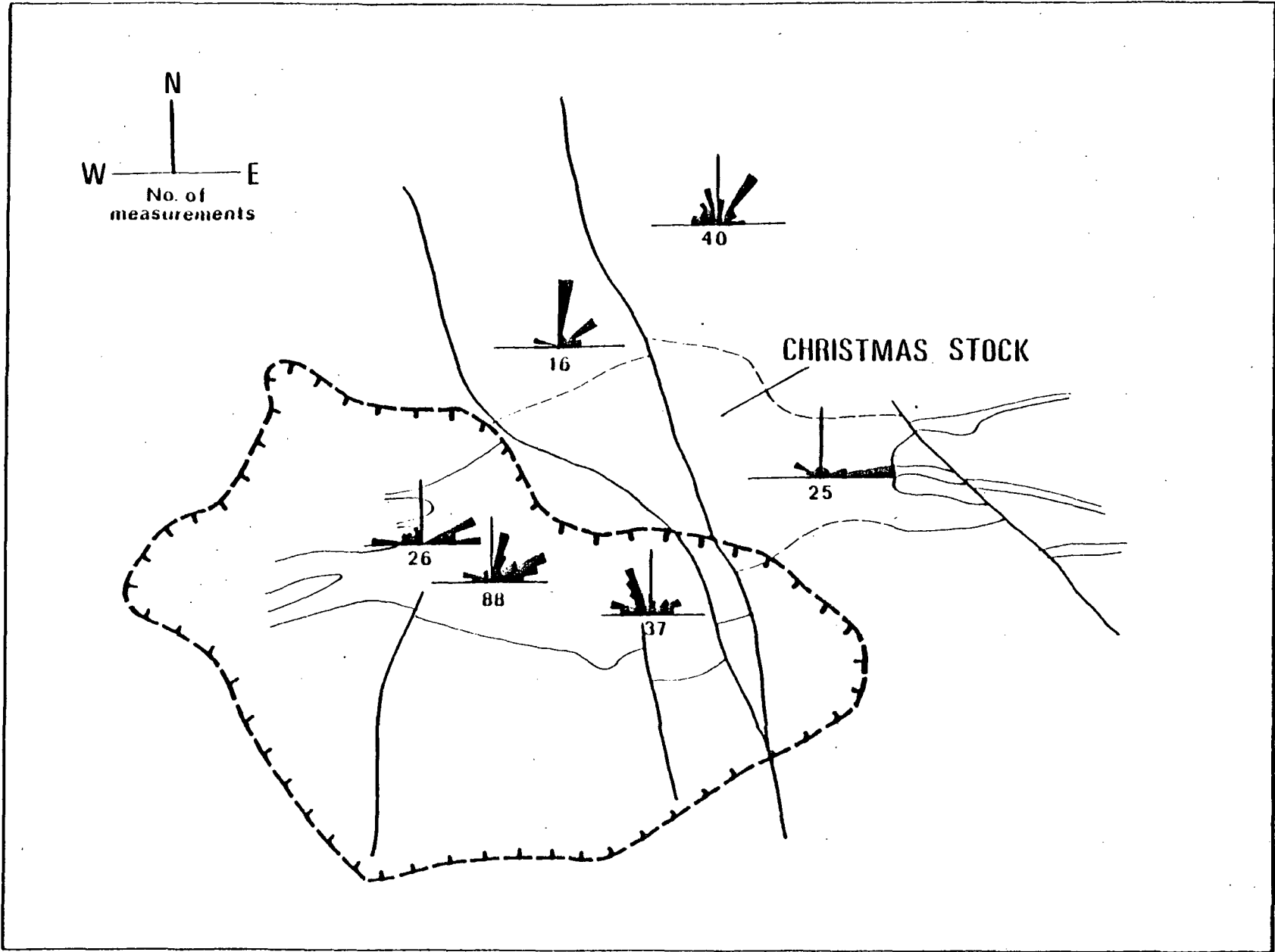
this pattern. Each rose diagram summarizes total measurements re-
corded within the several subareas, and the results are therefore some-
what generalized. However, the elements of a radial fracture (and vein)
pattern emerge with the geometric center near the north-central edge of
the intrusive mass. Increased exposure will permit more detailed anal-
ysis and interpretation, but the development of radial extension frac-
tures may be the result of excess pressure produced by late surges of
upward-wedging magma, possibly including the granitoid-textured phase
exposed at depth.

Stage II: Quartz-Sericite-Chlorite Alteration

The second major episode of alteration, Stage II, is character-
ized by sericite and/or chlorite plus quartz, pyrite, and chalcopyrite
in composite veins, that is, veins consisting of a central fracture
filling and a wider, more diffuse wall rock envelope. Chlorite is the
dominant phyllosilicate in Stage II veins in basaltic volcanic rocks,
sericite in intrusive and clastic sedimentary rocks. Stage II alter-
ation assemblages represent an episode of retrograde hydrogen metaso-
matism during the evolution of the Christmas deposit.

The distribution of quartz-sericite-chlorite alteration, shown
in Figure 24, is generalized from Plate VI. In both intrusive and
volcanic rocks, the zone of Stage II quartz-sericite-chlorite altera-
tion overlaps with but is largely peripheral to the zone of Stage I
stockwork veining.

Quartz-sericite alteration in intrusive rocks

K-silicate-altered rocks in the main body of the stock are flanked east and west by structurally-controlled quartz-sericite alteration (Figure 24). In the west end of the stock, quartz, sericite, pyrite, and chalcopyrite are concentrated in closely spaced, steeply dipping sheet fractures (Figure 27). Chlorite is less common, and apatite is a rare constituent. If K-feldspar was originally present along these fractures, it is now entirely altered.

In bleached vein envelopes enclosing the fractures, plagioclase phenocrysts and groundmass feldspar are replaced by fine-grained sericite, and mafic minerals (both phenocrystic and secondary biotite) by pale chlorite and sericite. Where fracture density is high, alteration envelopes overlap, and sericitization becomes pervasive (Figure 27). Relict outlines of biotite and plagioclase remain, but only quartz, apatite, and zircon of the original rock appear unaltered. Plagioclase between encroaching vein envelopes is altered to montmorillonite.

Where alteration is pervasive the combined fracture-bound and disseminated sulfide may total up to 10 percent of the rock volume with a high (>10:1) pyrite/chalcopyrite ratio. Wall rock between bleached vein envelopes contains much less sulfide (<1 percent), usually as isolated blebs.

Mineralized fractures in the western apex of the stock have orientations parallel to the margins of the intrusive, that is, nearly east-west with near-vertical dips. The intensity of alteration decreases eastward toward the interior of the stock and the quartz-sericite zone
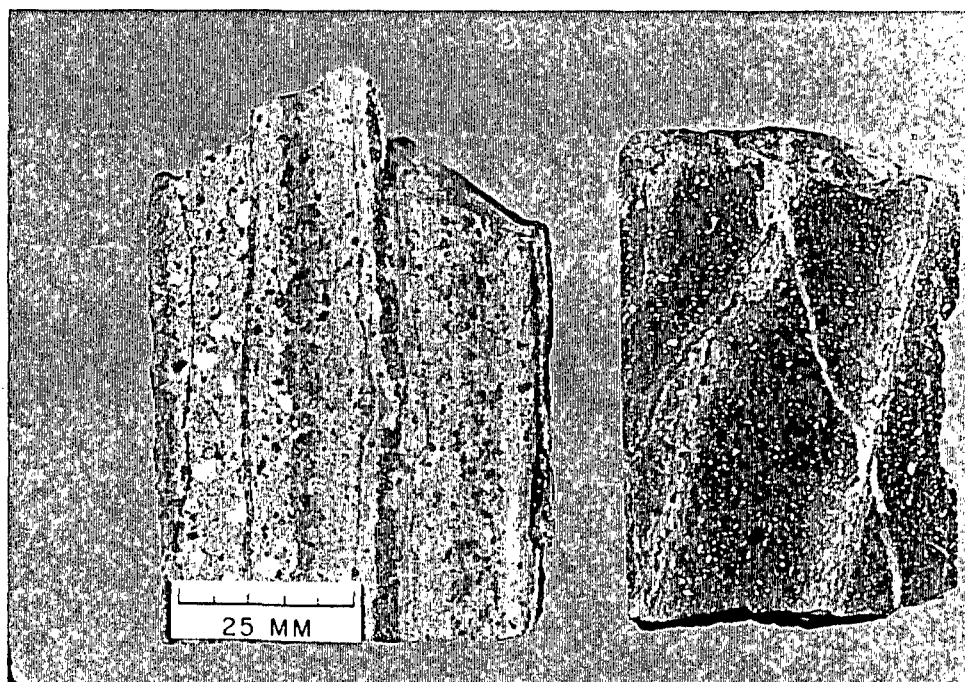
Figure 27. Examples of Stage II alteration. In the sample of quartz diorite on the left, closely-spaced quartz-sericite-pyrite veins have overlapping alteration envelopes resulting in pervasive sericitization. The sample of basalt on the right is cut by quartz-chlorite-pyrite-chalcopyrite veins.

merges gradationally with the central K-silicate zone over a distance of 50-100 m. Thus, the transition outward from K-silicate to quartz-sericite alteration in the stock corresponds with a structural transition from stockwork fractures to closely spaced vertical sheet fractures conformable with the intrusive-metasedimentary rock contact.

The eastern quartz-sericite zone centers on rhyodacite porphyry dikes, but extends laterally into porous beds of feldspathic sandstone and siltstone in the Williamson Canyon Volcanics. Like the western zone, the transition from K-silicate alteration to quartz-sericite alteration corresponds with the change from stockwork fractures in the stock to vertical parallel fracturing in the porphyry dikes. The development of vertical sheeting and related alteration reaches a maximum intensity approximately 125-175 m east of the stock. With increasing distance away from the stock, fracturing in the dikes diminishes and quartz-sericite alteration yields to alteration of the propylitic type.

The strong vertical deformation is largely internal to the dikes. Parallel fractures are typically 1-5 cm apart, and the intervein portions of rhyodacite porphyry are converted to thoroughly bleached light gray to buff "quartz porphyry." Large blebby quartz "eyes" and compact felted masses of sericite (after plagioclase) and sericite intergrown with colorless to pale-green chlorite (after mafic minerals) are set in a field of fine-grained sericite and quartz. Sites of original book biotite are also marked by rods, needles, and anhedral grains of rutile which are often aligned along relict mica cleavages.

At the surface the fractures are vuggy and, where originally

filled with sulfides, now contain quartz and yellow to reddish-brown oxidation products, principally colloform jarosite and geothite. The resulting gossan is characteristic of rhyodacite porphyry dikes east of the Christmas stock.

Coarser-grained feldspathic sedimentary rocks in the volcanic pile, cropping out east of the Christmas stock, are flooded by veins and podlike masses of granular quartz. Detrital plagioclase and lithic grains are converted to sericite along fractures. Loose aggregates of tiny rutile granules may mark the original sites of Fe-Ti-oxide grains. Secondary quartz in clastic sedimentary rocks is abnormally rich in halite-bearing fluid inclusions.

Quartz-chlorite-sulfide veins in volcanic rocks

Stage II quartz-chlorite-pyrite-chalcopyrite veins (Figure 27) in volcanic rocks contribute to ore-grade mineralization east of the Christmas fault in a zone overlapping with, but largely peripheral to, the zone of Stage I quartz-sulfide veins (Figure 24). Where overlap occurs, Stage II quartz-chlorite-sulfide veins crosscut Stage I quartz-sulfide veins (Figure 19).

Unlike sheeted Stage II veins in intrusive rocks, Stage II veins in volcanic rocks form an intricate stockwork. Quartz-chlorite-sulfide veins are superimposed on earlier biotitization. Where earlier biotite alteration is not pervasive (that is, biotite occurs along fractures), the periphery of Stage II veins is separated from "fresh" volcanic wall rock by a relict fringe of biotitization. Bleached light-gray to

grayish-green envelopes enclosing the central fracture mark the outwardly encroaching zone of biotite-destructive chloritization. Chlorite within the vein envelope does not generally extend beyond the limit of biotitization, although patchy chloritization between veins may be a contemporaneous product of Stage II alteration. Disseminated quartz, sericite, calcite, and sulfides also occur with chlorite in the vein envelope, and plagioclase is converted to albite. The bulk of Stage II sulfides appears to be confined to veins.

The central fracture filling varies in width between 1 mm and 3 cm, and is commonly zoned with chlorite and occasionally sericite at the margins and sulfides, magnetite, quartz, calcite, and calcium zeolites at the center. The in-filling material often occurs in separated bands of sulfide, magnetite, chlorite, and quartz implying successive periods of fracturing, deposition, and refracturing. The pyrite/chalcopyrite ratio is variable, but increases outward toward the limits of the zone where Stage II veins are simple aggregates of chlorite and pyrite coating fractures.

The calcium zeolites chabazite, laumontite, heulandite, and stilbite occur as late constituents of Stage II veins in mafic volcanic rocks. Chabazite, in particular, is commonly intergrown with pyrite and chalcopyrite along vein centers suggesting that zeolitization occurred during the waning stages of sulfide deposition.

Propylitic Alteration

Pervasive alteration of biotite rhyodacite porphyry dikes

East and west of the pyritic quartz-sericite zones, grayish-green biotite rhyodacite porphyry dikes host the development of the propylitic assemblage epidote-chlorite-albite-sphene. The transition outward from quartz-sericite to propylitic alteration is gradational and coincides with the diminution of steep parallel sheet fractures.

Propylitic alteration in dikes is pervasive and mafic-destructive as biotite and hornblende are altered to aggregates of chlorite, epidote, sphene, and rutile. Hornblende is more readily altered than biotite, and both are more susceptible than plagioclase. The destruction of biotite is particularly distinctive. Where alteration is complete, barrel-shaped book biotite is pseudomorphed by leafy chlorite enclosing lenses of granular epidote, anhedral sphene, and minute rod-shaped clusters of rutile (Figure 28a). Epidote and secondary Ti-minerals are aligned along basal mica cleavages. Subhedral apatite prisms are probably original magmatic inclusions. Where epidote is less abundant or absent, chloritized biotite may contain small amounts of interleaved prehnite.

Where propylitization is intense, nodular aggregates of coarse, bladed epidote appear to have developed randomly at sites in plagioclase phenocrysts (Figure 28b). Epidote apparently originates as small kernels near the grain perimeter and expands (as alteration proceeds) to consume the entire phenocryst and adjacent portions of the groundmass. This expansion of epidote beyond phenocryst boundaries does not occur
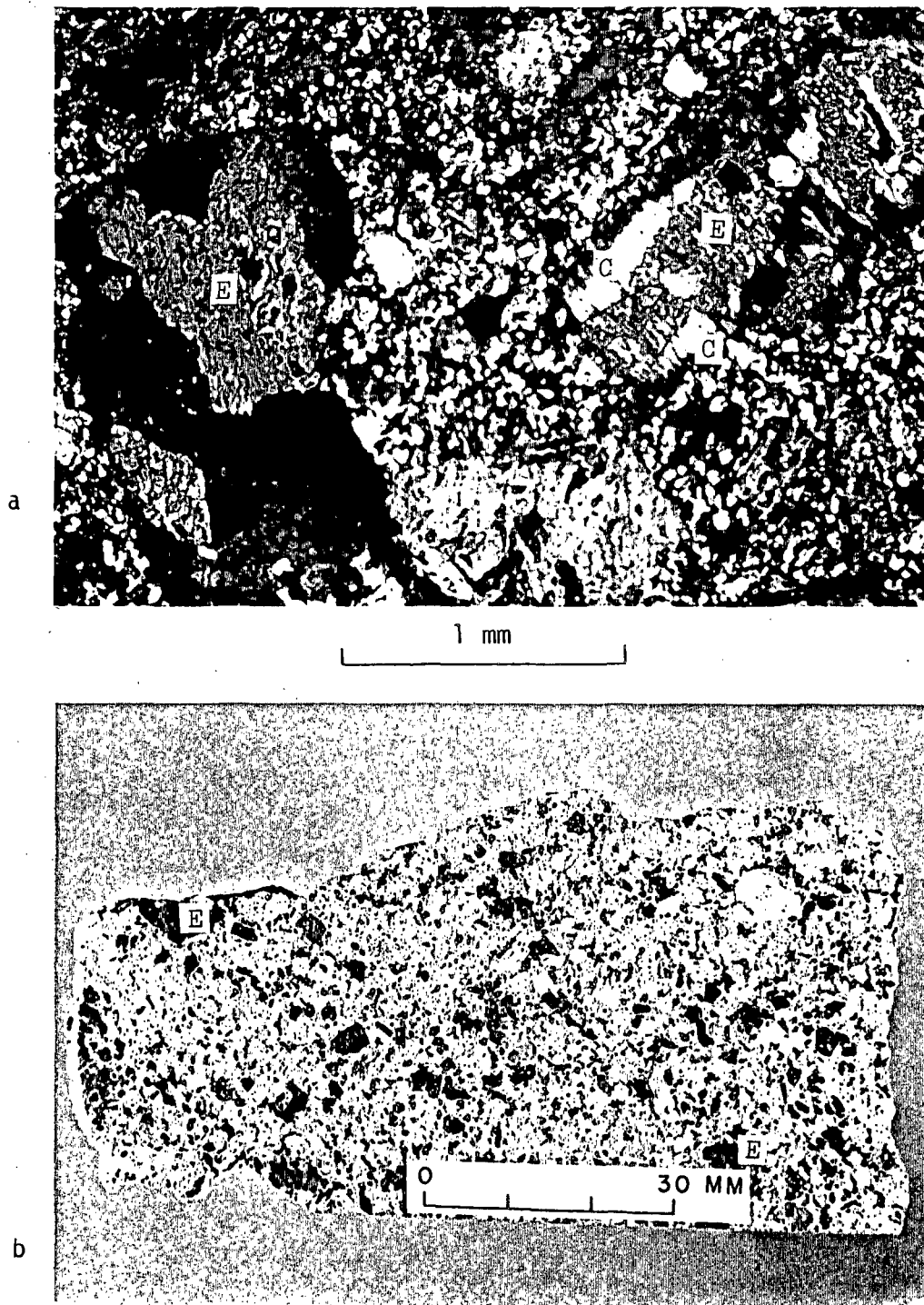
Figure 28. Strong propylitic alteration of biotite rhyodacite porphyry dike. (a) Photomicrograph (crossed polarizers) showing book biotite pseudomorphed by chlorite (C) enclosing coarse, granular epidote (E). (b) Coarse nodules of epidote (E) replacing plagioclase and groundmass.

in deuterically altered dacite and granodiorite porphyry of the
Christmas stock.

Plagioclase not converted to epidote is susceptible to patchy
or wormy replacement by albite which obscures twinning and zoning
features. Epidote within a plagioclase host may be mantled by albite.
Other fine-grained secondary minerals dispersed within plagioclase
grains include calcite, sericite, quartz, clinozoisite, and, less
commonly, anhydrite and prehnite.

In contrast to its disappearance in the quartz-sericite zone,
groundmass K-feldspar in propylitically altered dike rocks is generally
preserved. Primary magnetite-ilmenite appears to be unstable during
this type of propylitic alteration, and is, in part, replaced by sphene.
Unlike the K-silicate alteration zone, sphene rather than rutile appears
to be the dominant titaniferous alteration product.

Pyrite may occur as scattered blebs (replacing magnetite-
ilmenite?) or coatings on microfractures, and is much more abundant than
chalcopyrite. However, the amount of total sulfide is low, generally
less than 1 percent of the rock volume. Cu values approach trace levels.

Propylitization of dike rocks may also be a deuteric type of
alteration, although a chemical analysis (Table 7) suggests that signi-
ficant gains in Ca and Na, and losses of K may have occurred during
intense epidotization. The alteration is pervasive, internal to the
dikes, unrelated to fractures, and extends east and west beyond the
limits of the map area. Pervasive propylitization does not appear to
overlap pervasive biotitization in the Christmas intrusive complex, and

these mafic-destructive alteration types may be, at least to some extent, contemporaneous early alteration phenomena. Both types of pervasive alteration appear to be earlier than superimposed Stage II quartz-sericite-sulfide veins.

Epidote-quartz veins

In volcanic rocks near the deposit, but largely peripheral to the zone of Stage II quartz-chlorite-sulfide veins, epidote-quartz veins are narrow (<1 cm) with diffuse epidotized reaction selvages in adjacent wall rock. Pyrite and traces of chalcopyrite occur within the veins and along fractures in nearby host rock.

At greater distances from the deposit, weakly banded vuggy veins of coarse epidote and milky quartz occupy fractures and shear zones (Plate I). Calcite and zeolite (laumontite) are commonly present as cavity linings and interstitial fillings between prismatic epidote crystals. Single veins are discontinuous and generally less than 10 cm in width; in aggregate they may constitute zones one meter across. Scattered blebs and veinlets of oxidized sulfide, probably pyrite originally, are common, and copper oxide staining is present at a few localities. Semi-quantitative spectrographic analyses of samples from two epidote-quartz veins reveal the presence of small amounts of Mn, Cu, Pb, and Zn.

Supergene Alteration

The principal consequence of supergene alteration in igneous
rocks at Christmas is the near-surface oxidation and total leaching of
sulfides in the highly fractured, pyritic quartz-sericite alteration
zones. Steeply dipping sheet fractures originally occupied by pyrite
and chalcopyrite now contain crusty yellow-brown (jarositic) to reddish-
brown (goethitic) seams of indigenous limonite accompanied by quartz
and gypsum. Sericite between fractures is variably altered to
kaolinite or, less commonly, montmorillonite; the ultimate product
of intense leaching of wall rock is a compact massive aggregate of
kaolinite and quartz.

Fractures with jarosite and goethite are often crudely zoned:
jarosite along the contact with host rock enclosing vuggy goethite at
the center. Irregular masses of exotic jarosite also occur with seri-
cite and clay in sites of original mafic and plagioclase phenocrysts.
Along fractures and in phenocryst pseudomorphs, jarosite appears to
be replacing sericite.

The abundance of jarosite relative to goethite in the oxidized
capping may be explained in terms of the chemical environment of the
quartz-sericite zone. Jarosite and goethite commonly occur together
in gossans overlying mineralized rocks, but jarosite is less stable and
often converts to goethite or hematite in mature gossans (Blanchard,
1968). According to Kelly and Goddard (1969) and Brown (1971), the
formation of jarosite should be favored over goethite in wall rocks with

low pH, moderately high Eh, and high aK^+. Thus the interaction of oxygenated ground water with pyrite in sericitically altered porphyry is a nearly ideal mechanism for formation of jarosite. As pyrite is completely oxidized and leached, the solution pH increases (through dilution) and the activities of Fe^{3+} and SO_4^{2-} decrease, and goethite becomes the stable Fe-bearing phase. Much of the goethite near the center of the fracture may be replacing earlier-formed jarosite. The persistence of jarosite in leached gossan is probably due to the arid climate but may also be caused by a sluggish jarosite $\rightarrow$ goethite reaction rate (Brown, 1971).

Although data from the dikes east of the mine are lacking, the development of gossan in intrusive rocks is apparently a very shallow phenomenon. Limonite-rich fractures exposed near the western rim of the Christmas open pit are transitional downward to pyritized fractures over a vertical distance of 20-50 m. Pyrite and chalcopyrite immediately below that level are commonly covered with a thin film of chalcocite, but copper enrichment is minimal.

Oxidation is more widespread in mineralized Paleozoic sedimentary rocks where chrysocolla, cuprite, and copper carbonates are concentrated along faults, fractures, and old mine workings. Supergene alteration along the Christmas and Joker faults extends to depths of 430 m (Eastlick, 1968).

Supergene alteration in basaltic volcanic rocks east of the Christmas fault has an erratic distribution. Fresh pyrite and chalcopyrite are abundant in veins and fractures in many samples of drill

core within a few meters of the surface, but assays of drill core show significant copper oxide values in some drill holes to depths of 330 m. The highest oxide values occur in strongly shattered and mineralized wall rocks hosting Stage II veins north and east of the Christmas stock. Sulfide minerals are altered to iron oxides and small amounts of cuprite, malachite, and native copper. Chrysocolla forms as a fracture coating in intrusive rocks. Concentration of copper by supergene processes in volcanic rocks also appears to be insignificant.

Discussion of Zonation

Zoning of hypogene silicate-sulfide assemblages had been described at several porphyry-type deposits (e.g., Gilluly, 1946; Sales and Meyer, 1948; Metz and Rose, 1966; and Nielsen, 1968) before Lowell (1968) and Lowell and Guilbert (1970) developed their concentric zonation model based on studies at the San Manuel and Kalamazoo deposits in Arizona. This model has been employed with considerable success as a prospecting tool, and as a framework for topical studies of porphyry copper and molybdenum deposits, during the 1970's. Briefly, the model depicts a series of concentric nonoverlapping zones, each with characteristic alteration-mineralization assemblages and textural properties, which are centered on, but not necessarily confined to, a calc-alkaline porphyry intrusion (Figure 29a). In sequence outward (and upward?) from the core, the zones of alteration and characteristic mineral assemblages described by Lowell and Guilbert are: potassic or K-silicate (biotite-orthoclase), phyllic or sericitic (quartz-sericite-
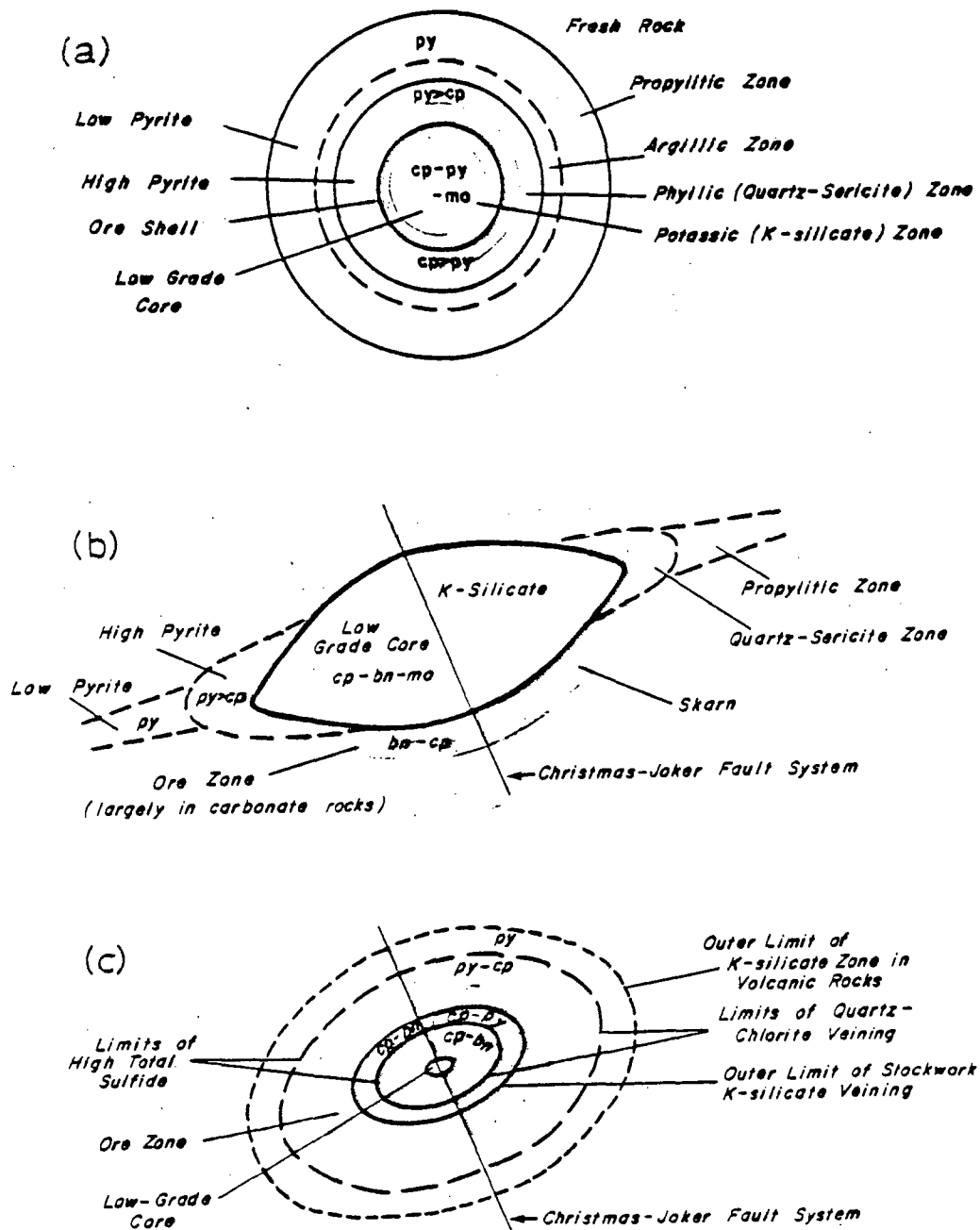
Figure 29. Variations in porphyry copper zonation. (a) The Lowell-Guilbert model of alteration-mineralization zonation. (b) Zonation at the lower level (reconstructed) intrusive-carbonate rock environment at Christmas. (c) Zonation at the upper level (reconstructed) intrusive-volcanic rock environment at Christmas.

pyrite), argillic (quartz-kaolinite-montmorillonite), and propylitic. (epidote-calcite-chlorite). The copper ore "shell" with high chalco-pyrite:pyrite ratios straddles the interface between the sulfide-poor K-silicate core and the pyrite-rich sericitic zone.

The alteration-mineralization pattern at Christmas is a composite of two distinct levels within the porphyry copper system. The relatively high, intrusive-mafic volcanic rock environment, and the deeper, intrusive-carbonate rock environment are juxtaposed by approximately 1 km of near-vertical displacement along the Christmas-Joker fault system.

The lateral zonation pattern at the lower, subvolcanic level, exposed west of the Christmas fault, is shown schematically in Figure 29b. Although somewhat speculative, the eastern half of the pattern is reconstructed as the mirror image of the western half.

Zonation at this level resembles the Lowell-Guilbert model along an east-northeast axis through the Christmas intrusive complex. Relatively low-grade (0.05-0.1 percent Cu), low total sulfide (less than one percent by volume) chalcopyrite-bornite-molybdenite mineralization in the K-silicate-altered core yields outward (east and west) to high total sulfide (1-10 percent) pyrite-chalcopyrite mineralization in the zones of quartz-sericite alteration. Total sulfide, chalcopyrite/pyrite ratios, and copper contents decrease rapidly toward background values in propylitically altered dike rocks beyond the quartz-sericite zones. Ore-grade copper mineralization (bornite-chalcopyrite) at this level occurs almost entirely in the carbonate rock environment.

Within the Christmas stock-dike complex, quartz-sericite alteration is superimposed on earlier K-silicate and propylitic alteration. The intermediate position of the quartz-sericite-pyrite zone reflects the distribution of through-going vertical sheet fractures. The absence of steeply dipping fractures may have been a major factor inhibiting the development of Stage II alteration-mineralization along the north and south margins of the stock.

A zone of hypogene argillic alteration, which occurs marginally to the phyllic zone in the Lowell-Guilbert model, is lacking at Christmas. Intense argillic alteration of quartz diorite in the western apex of the Christmas stock is believed to be related to supergene processes.

West of the Christmas fault, K-silicate and quartz-sericite alteration zones terminate abruptly at contacts with carbonate wall rocks. The formation of calc-silicate mineral assemblages in limestone and dolomite -- referred to as the "pyrometasomatic type" of alteration by Titley (1973) -- may be temporally equivalent to higher temperature (K-silicate) alteration in igneous rocks. Although correlations between silicate alteration assemblages in igneous and carbonate rocks have been recognized at the Ely, Nevada porphyry copper deposit (James, 1976), the genetic counterparts of K-silicate and sericitic alteration have not been identified in metasedimentary rocks at Christmas. Retrograde actinolite veinlets cutting diopsidic hornfels in the Naco Limestone may, however, be contemporaneous with K-metasomatism in intrusive rocks (M. T. Einaudi, personal communication, 1977).

The reconstructed higher-level zonation pattern in the Christmas porphyry copper system, shown schematically in Figure 29c, is developed across silicate wall rocks of contrasting compositions. The broad K-silicate zone encompasses pervasive biotitization and K-feldspar-bearing stockwork veins in the stock, and quartz-sulfide veins and widely dispersed biotitization in the mafic volcanic environment. The widespread distribution of biotite in basalt is an expression of the fundamental control of wall rock composition. The Fe-Mg-rich basaltic rocks were a sensitive environment for crystallization of biotite during Stage I potassium metasomatism.

Both fracture density and the intensity of biotitization decrease outward from the stock. The occurrence of dispersed secondary biotite beyond the zone of high fracture density might indicate that additional structural controls, such as vesicular zones or porous horizons in poorly-sorted volcanic breccia, may have been effective in transmitting hydrothermal fluids.

East of the Christmas fault quartz-sericite-chlorite alteration occurs in an essentially continuous zone across three separate wall rock environments. Again, the controlling influence of wall rock composition is evident. Whereas sericite is the principal phyllosilicate of Stage II veins in rhyodacite porphyry dikes and feldspathic sandstones, chlorite is dominant in basalt.

In basaltic rocks the zone of quartz-chlorite-sulfide veins overlaps the zone of strong biotitization (and Stage I quartz-sulfide veins), but does not appear to extend to the outer limit of the fringe

zone of biotitization. Thus, unlike relations predicted by the Lowell-Guilbert model, K-silicate alteration at Christmas (although weak) reaches beyond the outer limit of the quartz-chlorite or "phyllic" zone. Furthermore, the presence of an argillic zone has not been identified in volcanic rocks and the inner limit of vein-related epidotization may coincide generally with the outer limit of the quartz-chlorite zone. No outer limit of porphyry-related propylitic alteration can be established because of the widespread regional epidotization of the Williamson Canyon Volcanics.

The present level of exposure east of the Christmas-Joker fault system intersects a high level, possibly the roof zone of the stock, and the domed top of the ore zone which spans the somewhat irregular contact between intrusive and volcanic rocks. Early, low total sulfide chalcopyrite-bornite, and later, high total sulfide pyrite-chalcopyrite mineralization are telescoped in the chemically reactive basaltic wall rocks. The sulfide zonation derived from these superimposed mineralization episodes, moving away from the Christmas stock, is chalcopyrite-bornite, chalcopyrite-bornite plus chalcopyrite-pyrite, pyrite-chalcopyrite, and pyrite. The presence of Pb, Zn, and Cu in outlying epidote-quartz veins may signify a larger-scale base metal zonation.

At Christmas, lateral overlapping of alteration-mineralization zones and crosscutting vein relations are manifestations of discrete and successive hydrothermal episodes. The concentric zonation model of Lowell and Guilbert does not embrace the concept of multistage alter-

ation and mineralization in porphyry copper systems. Instead, Lowell and Guilbert (1970, p. 403-404) stress that "alteration-mineralization zonal boundary interfaces appear to have been established as standing forms rather than as upward and outward advancing mega envelopes." The superposition of sericite-chlorite alteration and pyritic mineralization on earlier K-silicate alteration has also been described by Gustafson and Hunt (1975) at the El Salvador, Chile porphyry copper deposit.

Vertical zonation of sulfide mineralization is also evident in the Christmas porphyry copper system. In contrast to the nearly sulfide-barren deep core of the intrusion west of the Christmas fault, the upper level east of the Joker fault contains ore-grade copper mineralization. Adjacent country rocks at both levels are heavily mineralized, but the limit of ore is well within the outer limit of hydrothermal alteration. The reconstructed, prefault form of the ore body (ignoring, for purposes of this discussion, irregularities relating to dikes and apophyses of the stock) might then approximate a dome or inverted cup, similar to the geometric model for mineralization zonation in porphyry copper deposits suggested by James (1971). These observations underline the importance of considering depth of erosion when evaluating zonation in porphyry-type deposits.

Chemical Gains and Losses in Altered Igneous Rocks

Whole rock chemical analyses of several altered igneous rocks at Christmas are presented in Table 7. The chemical gains and losses, calculated in gram equivalents/1000 cubic cm and reported in Table 8, were determined by comparing analyses of rocks in Table 7 with compositions of their "unaltered" equivalents from Table 1. Cu and S contents are also compared in Table 8. The specific alteration sequences represented include the biotitization of biotite granodiorite porphyry and Williamson Canyon Volcanics basalt, the quartz-sericite alteration of quartz diorite, and the propylitic alteration of biotite rhyodacite porphyry dike rock. In addition, variations along a north-south trend in volcanic rocks enclosing the Christmas stock are illustrated by the chemical profiles in Figure 30. The data are meant to portray chemical changes during pervasive wall rock alteration and all samples were trimmed to remove obvious veins and mineralized fractures before analysis.

The chemical data for biotite granodiorite porphyry in Table 8 suggest that, with the exception of moderate increases in the Fe^{2+}/Fe^{3+} ratio and hydrogen ion content, early pervasive biotitization was essentially an isochemical process with respect to the major elements. It is significant that the total replacement of primary biotite and hornblende by secondary biotite required no apparent addition of potassium. The sample of porphyry with strong secondary biotite has higher Cu and S values which reflect the presence of a small amount of disseminated chalcopyrite and pyrite.

Table 7. Chemical analyses* of representative altered igneous rocks at Christmas. Oxides and S in weight percent; Cu in ppm.

Description number	14	15	16	17
Sample number	D237-700	D248-320	P-30-74	61AB74B
SiO_2	64.7	55.0	61.9	63.9
Al_2O_3	16.1	16.8	16.6	16.2
Fe_2O_3	1.2	2.4	4.3	3.0
FeO	2.5	4.2	1.6	1.2
MgO	2.1	6.5	4.4	2.4
CaO	3.5	4.6	.68	5.7
Na_2O	4.0	2.2	.26	5.2
K_2O	2.2	2.6	3.3	.45
H_2O^+	1.4	3.7	3.8	1.2
H_2O^-	.53	1.7	.81	.21
TiO_2	.71	.99	.62	.50
P_2O_5	.18	.21	.28	.21
MnO	.05	.07	.00	.00
CO_2	.02	.02	.08	.04
Total	100	101	99	100
S	0.15	0.095	2.30	0.0025
Cu	1000	5000	1500	1.5

* Analysts and analytical methods listed under Table 1.
14. Biotite granodiorite porphyry, strong biotitization.
15. Basalt from Williamson Canyon Volcanics, strong biotitization.
16. Quartz diorite, strong quartz-sericite alteration.
17. Biotite rhyodacite porphyry, strong propylitic alteration.
Sample locations and descriptions are given in Appendix I.

Table 8. Chemical gains and losses (in gram equivalents/1000 cubic centimeters). Calculations made assuming constant total volume during alteration. S.G. = specific gravity.

	AB77F-73 Biotite granodiorite porphyry (S.G. = 2.65)	D237-700 Biotite granodiorite porphyry, strong secondary biotite (S.G. = 2.65)	Change
Si	117.7	114.4	-3.3
Al	25.0	25.0	0.0
Fe^{3+}	2.1	1.2	-0.9
Fe^{2+}	1.4	1.8	+0.4
Mg	3.0	2.7	-0.3
Ca	3.4	3.3	-0.1
Na	3.5	3.5	0.0
K	1.2	1.2	0.0
H	2.8	4.1	+1.3
S (wt. percent)	0.0025	0.15	
Cu (ppm)	50	1000	

	39AB74 Unaltered basalt (S.G. = 2.81)	D248-320 Basalt, strong biotitization (S.G. = 2.66)	Change
Si	92.7	97.7	+5.0
Al	57.6	52.7	-4.9
Fe^{3+}	9.7	4.8	-4.9
Fe^{2+}	4.0	3.2	-0.8
Mg	8.0	8.5	+0.5
Ca	9.6	4.4	-5.2
Na	2.0	1.9	-0.1
K	0.5	1.5	+1.0
H	6.6	10.9	+4.3
S (wt. percent)	0.0025	0.095	
Cu (ppm)	20	5000	

Table 8 (continued).

	D99-430 Quartz diorite (S.G. = 2.63)	P-30-74 Quartz diorite, quartz-sericite alteration (S.G. = 2.66)	Change
Si	110.9	109.9	-1.0
Al	50.9	52.0	+1.1
Fe^{3+}	4.2	8.6	+4.4
Fe^{2+}	3.1	1.1	-2.0
Mg	4.8	5.7	+0.9
Ca	3.2	0.6	-2.6
Na	3.4	0.2	-3.2
K	1.2	1.8	+0.6
H	4.7	11.2	+6.5
S (wt. percent)	0.014	2.3	
Cu (ppm)	1500	1500	

	AB77F-73 Biotite granodiorite porphyry (S.G. = 2.65)	61AB74B Biotite rhyodacite porphyry, propylitic alteration (S.G. = 2.60)	Change
Si	117.7	110.6	-7.1
Al	50.0	49.8	-0.2
Fe^{3+}	4.3	5.9	+1.6
Fe^{2+}	1.4	0.8	-0.6
Mg	3.0	3.0	0.0
Ca	3.4	5.4	+2.0
Na	3.5	4.4	+0.9
K	1.2	0.3	-0.9
H	2.8	3.4	+0.6
S (wt. percent)	0.0025	0.0025	
Cu (ppm)	50	1.5	

Figure 30. Chemical profiles (north-south) for basaltic volcanic rocks along 19,200E at Christmas. Na_2O and K_2O analyzed by flame photometer (G. Ambats, analyst); other elements by emission spectroscopy (L. Mei, analyst). F = basalt without secondary biotite; W = weak biotitization; M = moderate biotitization; S = strong biotitization; C = Christmas stock. Sample locations shown on Plate I.
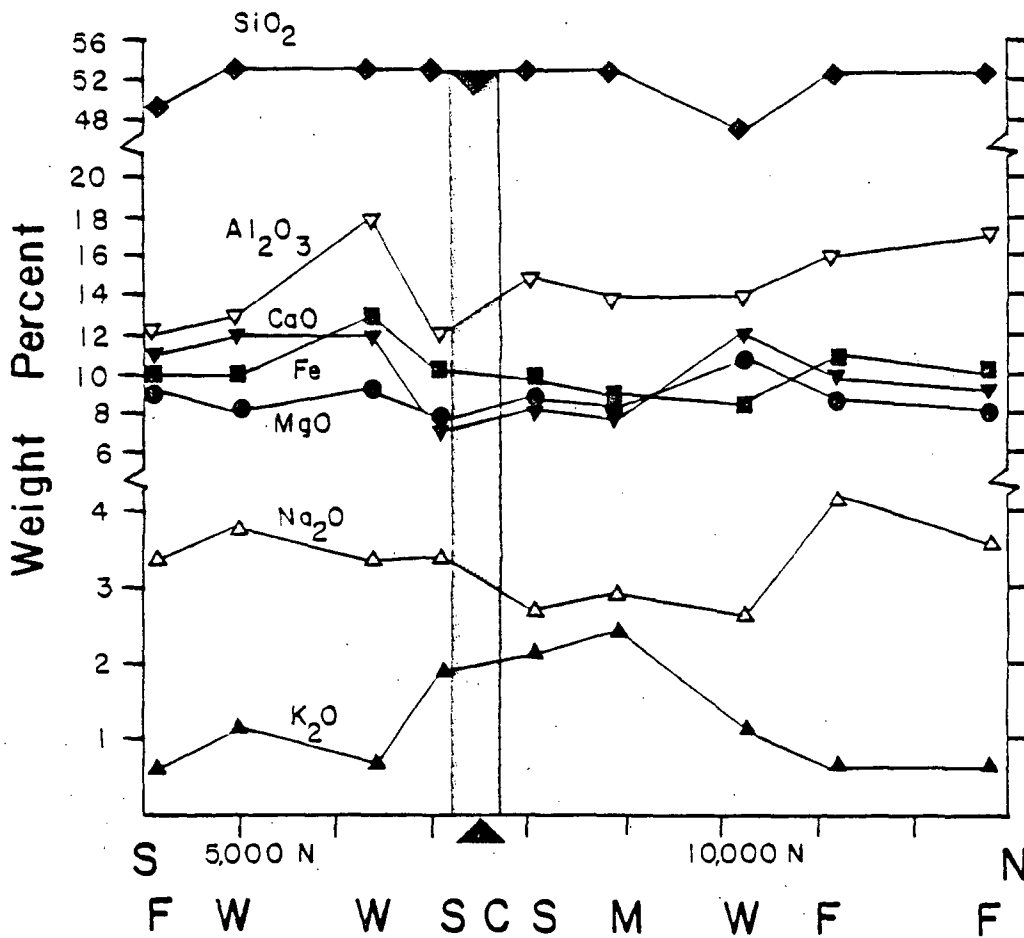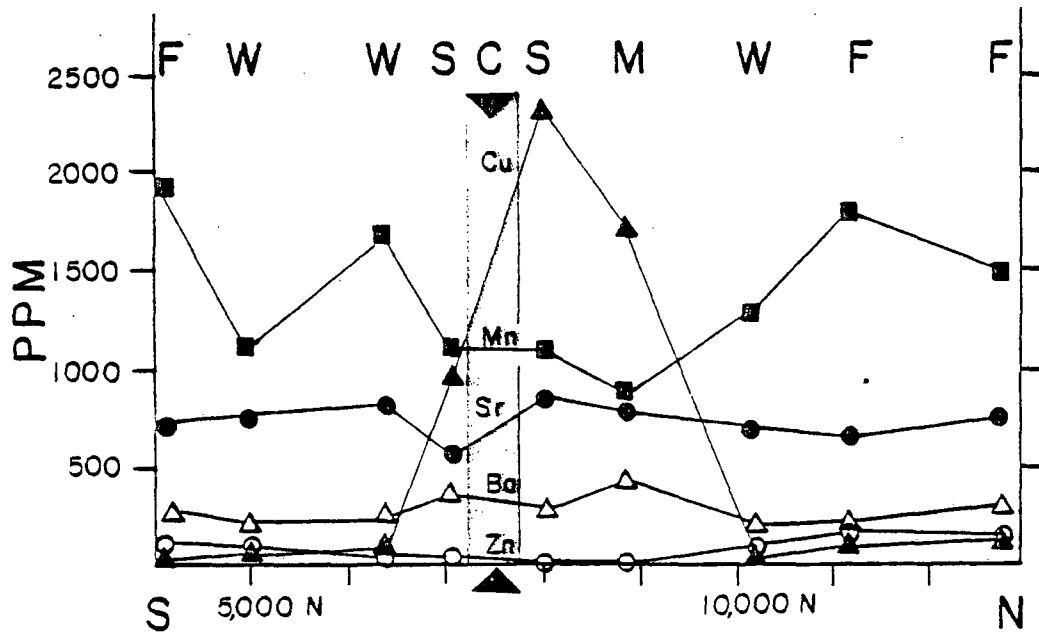
Table 8 indicates that during the development of intense biotitic alteration, basaltic country rocks gained Si, K, H, S, and Cu which is consistent with the addition of quartz, biotite, and copper sulfides. It is interesting to note that during K-metasomatism, significant quantities of H (in terms of gram-equivalents) also have been added. Losses in Fe and Ca are related to the breakdown of clinopyroxene (or uralite) and calcic plagioclase. The alteration of uralite and, perhaps, chlorite could have released Mg (which shows little change in Table 8) utilized in the formation of secondary biotite.

The significant loss of Fe^{3+} may correspond to the destruction of abundant opaque (magnetite-ilmenite?) dust, although some ferric and ferrous iron are retained in coarse magnetite, a part of which may be secondary. The net loss in total iron during alteration suggests that some Fe was actually removed from the wall rock, possibly to be fixed in vein sulfide minerals, rather than reduced from Fe^{3+} to Fe^{2+}.

An apparent loss in Al is somewhat puzzling because much of the aluminum released by destruction of plagioclase should be utilized by the formation of biotite, and aluminum is generally the least mobile of cations during hydrothermal alteration (Meyer and Hemley, 1967). Part of the "apparent" loss in aluminum may be due to original compositional differences in the two samples.

Quartz diorite initially containing secondary biotite from the west quartz-sericite zone has been converted to the assemblage quartz-sericite-chlorite-pyrite. Data in Table 8 show that the principal

chemical changes among major elements involve leaching of Na and Ca, conversion of Fe^{2+} to Fe^{3+}, and strong hydrogen metasomatism. The gain in hydrogen ion exceeds the total loss in base cations. K, Mg, and Al have been retained, or may have been added in small amounts during formation of sericite and chlorite.

Although the sericitic sample appears to be free of iron oxide, some Fe^{3+} may be present in finely dispersed hematite; additional ferric iron is probably contained in pale-green chlorite. The minor change in Si suggests that much of the fine-grained disseminated quartz in wall rock from the quartz-sericite zone is inherited from the original groundmass or formed during breakdown of primary feldspar. The increase in S content is expected from the presence of abundant pyrite (5 percent of the total rock volume), and the latter may also contribute to the slight increase in specific gravity.

The interpretation of chemical changes during propylitic alteration of porphyritic rocks is complicated by possible differences in original compositions of the two rocks analyzed. For instance, the apparent loss of Si probably reflects an initial modal difference of five percent quartz phenocrysts as determined in thin section. Nevertheless, the apparent increases in Ca, Na, and Fe^{3+}/Fe^{2+}, and the depletion of K are compatible with the observed replacement of hornblende, biotite, and plagioclase phenocrysts, and groundmass by the secondary assemblage epidote-chlorite-albite (the mode for sample 61AB74B is: 50.8 percent groundmass, 28.3 percent albitized plagioclase, 1.4 percent quartz, 15.1 percent epidote, and 4.4 percent chlorite).

Chemical profiles for selected elements in basaltic volcanic rocks along a north-south trend near 19,200E at Christmas are depicted in Figure 30. Surface and drill hole samples (locations are shown on Plate I) were collected north and south of the Christmas stock and east of the Christmas-Joker fault system. Na_2O and K_2O were analyzed by flame photometer, and the other elements by emission spectrograph. Despite imprecision in some of the spectrographic analyses, the profiles indicate that with increasing biotitization approaching the Christmas stock (C in Figure 30), the volcanic rocks are enriched in K, Cu, and, possibly, Ba. Na, Ca, Mn, and Zn appear to be depleted. Variations in K, Mn, and, perhaps, H (not plotted) may be the most sensitive chemical indicators of pervasive K-silicate alteration in the mafic volcanic environment at Christmas.

Fluid-Inclusion Petrography

A reconnaissance study of fluid inclusions was undertaken in an attempt to compare the variety and distribution of fluid inclusions with alteration and mineralization zonation. In conjunction, information was sought to semi-quantitatively characterize hydrothermal fluids through space and time. Petrographic techniques recently outlined by Nash (1976) were applied to standard thin sections at room temperature, and his classification scheme is adopted here. Using an X100 oil immersion objective (total magnification = 1250X), inclusions in quartz

veins, pervasive secondary quartz, and quartz phenocrysts were characterized according to type, population density (sparse, moderate, abundant), size, form, proportion of fluid phases, daughter minerals, and mode of occurrence (isolated or along microfractures). The determination of internal characteristics (daughter minerals, phase proportions, and so forth) was hindered by the small size (5-20 microns) of inclusions in most samples.

Three types of inclusions were identified (Figure 31), and they are reported to be typical of other porphyry copper deposits (Nash and Theodore, 1971; Roedder, 1971; and Moore and Nash, 1974). Nash (1976, Table 1) lists fluid-inclusion data for 36 porphyry copper deposits including the occurrence of types I and III at Christmas (written communication from D. P. Wheeler to Nash, 1973).

At the Christmas deposit, type I or moderate-salinity inclusions contain a liquid water phase and a relatively small vapor bubble occupying between 5 and 40 percent of the inclusion volume. Halite is absent, but one or more tiny daughter minerals may be present including orange-red hematite; other solid phases are colorless and weakly birefringent. Fluid-inclusion shapes range from spherical to irregular, but ellipsoidal or teardrop forms are most common. Moderate-salinity inclusions are found in all vein types at Christmas, but are most abundant in Stage I veins. Perry (1969) also notes the presence of liquid-rich (type I?) fluid inclusions in diopside of Ca skarn and endoskarn, and cites them as evidence in favor of a subcritical hydrothermal fluid phase during skarn formation.
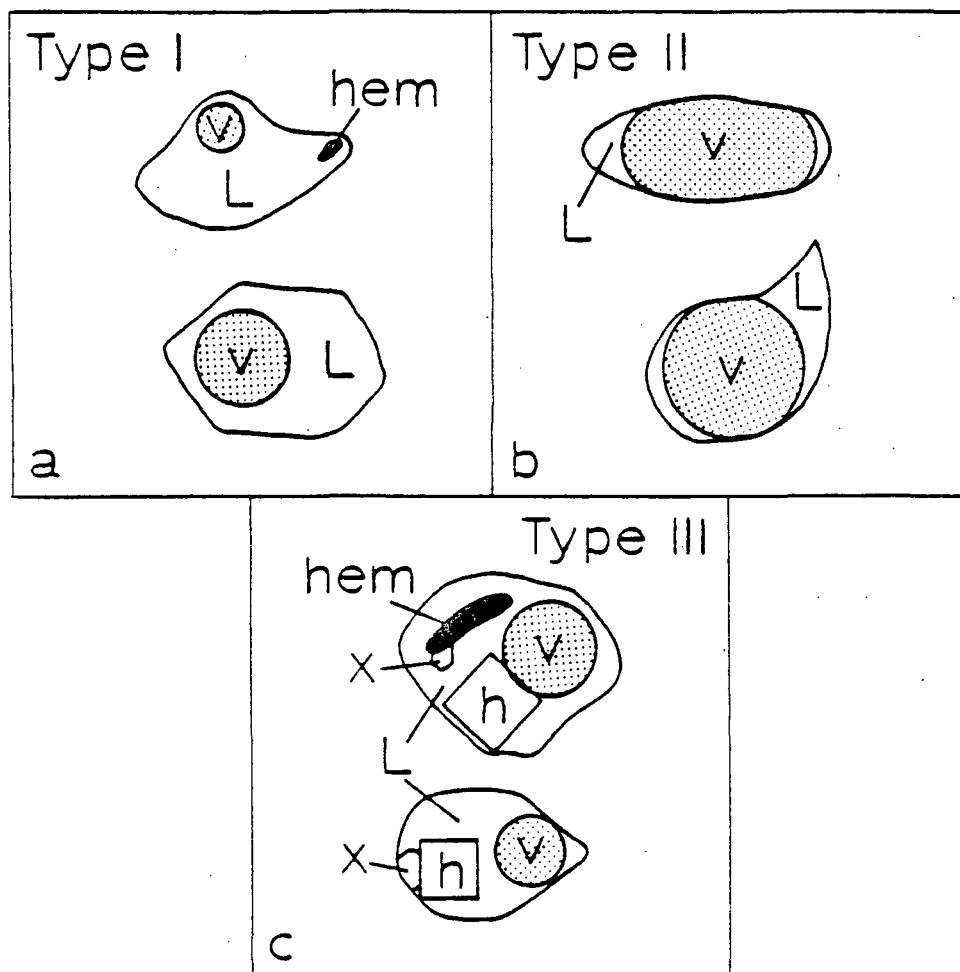
Figure 31. Fluid-inclusion types in the Christmas deposit. (a) Moderate salinity, type I. (b) Gas-rich, type II. (c) Halite-bearing, type III. L = liquid, v = vapor, h = halite, hem = hematite, and x = unknown solid phase.

Type II or gas-rich inclusions contain low- or moderate-salinity liquid and greater than 50 percent vapor phase; this variety is generally believed to represent entrapment of dense steam (Roedder, 1971; Nash, 1976). Opaque daughter minerals (hematite?) are observed when the bubble is significantly smaller than the inclusion volume, that is, about 50-60 volume percent. Gas-rich inclusions are most common as isolated, negatively faceted forms, but assume irregular shapes when strung out along wispy "trails," an occurrence which is no doubt secondary. All gradations appear to exist between type I and type II fluid inclusions and they commonly occur together within the same host crystal.

Type III or halite-bearing inclusions contain a liquid phase, 5-20 percent gas phase, and a cube of halite. Other daughter minerals are invariably present, but only hematite can be identified with confidence. The number of solid phases usually ranges between three and five, but as many as nine have been observed crowded into one inclusion. The halite cube generally has dimensions equal to, or greater than, that of the vapor bubble, and may have crystallized during cooling from a dense fluid containing more than 50 weight percent NaCl, a fluid analagous to the "hydrosaline melt" of Roedder (1971). Type III inclusions are, with a few exceptions, much less abundant than type I and type II in Stage I and II veins, and are rather sparse in igneous rocks of the deposit as a whole.

The distribution of fluid-inclusion types in mainstage veins is summarized in Table 9. Although many exceptions occur locally, some systematic variations can be detected for the deposit as a whole. Stage

Table 9. Distribution of fluid-inclusion types in mainstage veins.

Vein type	Host rock	Number of samples	Relative abundance of fluid-inclusion types	Comment
Stage I:				
Quartz-K-feldspar	Christmas stock	21	type I>type II>type III or type II=type I>type III	sparse-moderate moderate-abundant
Quartz-sulfide	Williamson Canyon Volcanics-basalt	6	type II>type I>type III	moderate
	Williamson Canyon Volcanics-sandstone	3	type II>type III>type I	moderate-abundant
Stage II:				
Quartz-sericite-pyrite (west zone)	Christmas stock	9	type I>type II>type III	sparse
Quartz-sericite-pyrite (east zone)	Biotite rhyodacite porphyry dikes	4	type I	sparse
Quartz-chlorite sulfide	Williamson Canyon Volcanics	3	type II>type I	sparse-moderate (zeolite absent)
		2	type I=type II	sparse (zeolite present)

I veins, for example, are characterized by low to moderate fluid-inclusion populations with various combinations of primary and secondary type I and type II inclusions. No significant differences in proportions or abundances of fluid-inclusion types were discerned among K-feldspar veinlets and quartz-K-feldspar veins. The gas-rich/moderate-salinity fluid-inclusion ratio in stockwork veins in the stock is generally less than or near unity, but the gas-rich variety is dominant in quartz-sulfide veins in volcanic rocks. Secondary quartz disseminated in strongly biotitized volcanic rocks cut by Stage I veins contains a very low fluid-inclusion population consisting mainly of the moderate-salinity type.

Narrow Stage II veins (quartz-sericite-sulfide in intrusive rocks and quartz-chlorite-sulfide-zeolite in volcanic rocks) with low quartz contents typically contain very sparse populations of small (<10 micron) moderate-salinity and/or gas-rich inclusions. Zeolite-free late veins with an appreciable amount of quartz may contain moderate fluid-inclusion populations and a higher type II/type I ratio.

Halite-bearing inclusions are invariably present (although less than about 10 percent of the total population) in Stage I veins, but are most abundant (10-25 percent of the population) in granular quartz veins cutting silicified clastic sedimentary rocks, volcanic rocks, and porphyry dikes near the east end of the Christmas stock. These veins also contain the highest fluid-inclusion population densities observed in the study. The area marked by abundant type III inclusions represents the transition zone between K-silicate alteration (and Stage I

veins) and quartz-sericite-chlorite alteration (Stage II veins). Type III inclusions are rare in all peripheral Stage II veins.

In summary, early stockwork veins are characterized by low to moderate populations of moderate-salinity and gas-rich fluid inclusions, and minor (with the exception noted above) but ubiquitous halite-bearing inclusions. Type I and type II inclusions become less abundant in younger (Stage II) veins and type III inclusions are not present. At this point it should be stressed that although some variations according to vein type have been recognized, the age relationships between the three fluid-inclusion types remain problematical.

The greater abundance of type II fluid inclusions in Stage I veins in the hanging wall of the Christmas fault may be indicative of vertical fluid-inclusion zonation. Rocks east of the Christmas fault are at a relatively high level within the porphyry system, an environment (high temperature-lower pressure) favorable for boiling of hydrothermal fluids. In contrast, rocks collected from deep drill holes and underground mine workings west of the Christmas fault are approximately 1.5 km lower in the system, and have granitoid textures and few quartz veins; magmatic quartz from these rocks contains very sparse type I and type II fluid inclusions. At an intermediate level, Stage I veins collected from the open pit have moderate fluid-inclusion populations and approximately subequal numbers of type I and type II inclusions when all samples are considered.

According to Burnham (1967), boiling is likely to occur when magmas with initial water contents of two percent or more are emplaced

at shallow levels (3 km or less) within the crust. The attenuated fluid phase produced tends to migrate into high levels within the intrusion and into openings present in overlying country rock. Thus the vertical increase in abundance and proportion of gas-rich inclusions may reflect increasing boiling in response to a decreasing pressure gradient at progressively higher elevations in and above the epizonal Christmas stock. Boiling is believed to have been an important process in the evolution of fluids in many porphyry copper deposits (Roedder, 1971; Nash and Theodore, 1971; and Moore and Nash, 1974).

Blebby quartz phenocrysts in biotite granodiorite porphyry as well as in highly altered rhyodacite porphyry dikes of the quartz-sericite and propylitic alteration zones are typically charged with gas-rich inclusions. Moderate-salinity and halite-bearing inclusions are invariably present in minor numbers. The inclusions tend to "streak" across the host grains in parallel rows. The long axes of elongate inclusions within each row have subparallel orientations. These inclusions appear to be largely of secondary origin, and may represent gas streaming during a postconsolidation episode of boiling in the intrusive complex. However, their age and relationship with respect to fluid inclusions in stockwork veins is unknown.

A TWO-STAGE MODEL FOR ALTERATION AND MINERALIZATION
OF THE IGNEOUS ROCKS

The evolution of porphyry-type alteration and mineralization in igneous rocks at Christmas will be discussed within the framework of a sequential two-stage model. The model is constructed largely on the basis of mineral zonation and paragenesis as observed in the field and in thin sections. Additional supporting data were derived from chemical analyses and from fluid-inclusion petrography. Although Stages I and II are distinguished by contrasting secondary mineral assemblages, they are believed to be events in a continuous ore-forming episode.

Stage I: Intrusion and Early Alteration

Following deposition and actinolite-chlorite-epidote alteration of the Late Cretaceous Williamson Canyon Volcanics, the volcanic pile was intruded by a sequence of calc-alkaline stocks, dikes, and small pluglike bodies. In early Paleocene time ($\sim$62 m.y. ago), the granodioritic magma which crystallized to form the Christmas intrusive complex traversed the underlying Paleozoic section and penetrated a minimum of 450-600 m upward into the Williamson Canyon Volcanics. The principal structural control during emplacement was provided by the pronounced system of east-northeast to east-west-trending fractures which formed in response to Laramide northeast-directed regional compression and differential uplift in southeastern Arizona (Banks and Krieger, 1977; Rehrig and Heidrick, 1972, 1976). The occurrence of the Christmas

stock at the intersection of the east-northeast fracture zone and the Christmas-Joker fault system may be more than a fortuitous circumstance, but no evidence has been obtained that the northwest-trending faults have a premineralization ancestry.

The actual depth of emplacement of the Christmas stock cannot be determined by geologic reconstruction because of uncertainty regarding the thickness of the Williamson Canyon Volcanics and any overlying formations at the time of intrusion. It is known that the uppermost portion of the stock, downdropped by the Christmas-Joker fault system, has been removed by erosion, and that the stock has cut through a vertical section of Williamson Canyon Volcanics (approximately 450-600 m) nearly equivalent to the thickest section (750-900 m) preserved and documented elsewhere (Simons, 1964).

Thus, unless the volcanic pile was much more extensive and much thicker than is indicated from present exposures, the depth of emplacement of the Christmas stock was probably shallow. A tentative estimate of 1-2 km may be reasonable. This figure is not inconsistent with estimates of 1.5-3 km made by Sillitoe (1973) for minimum depths of emplacement of porphyry copper stocks intruding penecontemporaneous volcanic piles or stratovolcanoes, and is within the range of depth estimates for porphyry copper mineralization formulated by other means, such as 0.5 km at Santa Rita, New Mexico (Nielsen, 1968, by stratigraphic reconstruction), 1.5-2 km at Copper Canyon, Nevada (Nash and Theodore, 1971, from both stratigraphic reconstruction and fluid-inclusion data), and 2.5 km at Bingham, Utah (Moore and Nash, 1974, from fluid-inclusion

data). Gas-rich fluid inclusions suggestive of boiling conditions during mineralization, particularly in upper portions of the porphyry system, also support the view of shallow intrusion. Lithostatic pressure on the evolving intrusive complex at these shallow depths may have been within a few hundred bars (plus or minus) of 0.5 kb.

The spatial configuration of the reconstructed Christmas intrusive complex, viewed along a north-south cross section at approximately 18,000E, and the general sequence of emplacement of the major intrusive phases are shown schematically in Figure 32. Seriate-porphyritic quartz diorite was intruded first, either as a thick tabular mass or a series of narrower, closely spaced dikes. Although sills of quartz diorite penetrated the Naco Limestone to the south, the magma did not form dikes along the east-west fracture zone. Following at least partial consolidation, the quartz diorite was intruded and breached by numerous surges of biotite granodiorite porphyry, which in aggregate form the core of the complex. Emplacement of the Light and Dark Phases was largely passive, and large elongate blocks of sedimentary and volcanic rock were engulfed in upwelling magma.

One or more pulses of magma ultimately migrated outward along the fracture zone to form rhyodacite porphyry dikes, and apophyses invaded volcanic rocks to form the "northeast salient." Tongues of Light Phase magma pushed through quartz diorite to form dikes and sills in the Naco Limestone. Intrusive phases crystallizing at different rates produced groundmass textures ranging from hypidiomorphic-granular to aplitic. Strong oscillatory zoning in plagioclase indicates periods

Reconstructed Christmas Intrusive Complex
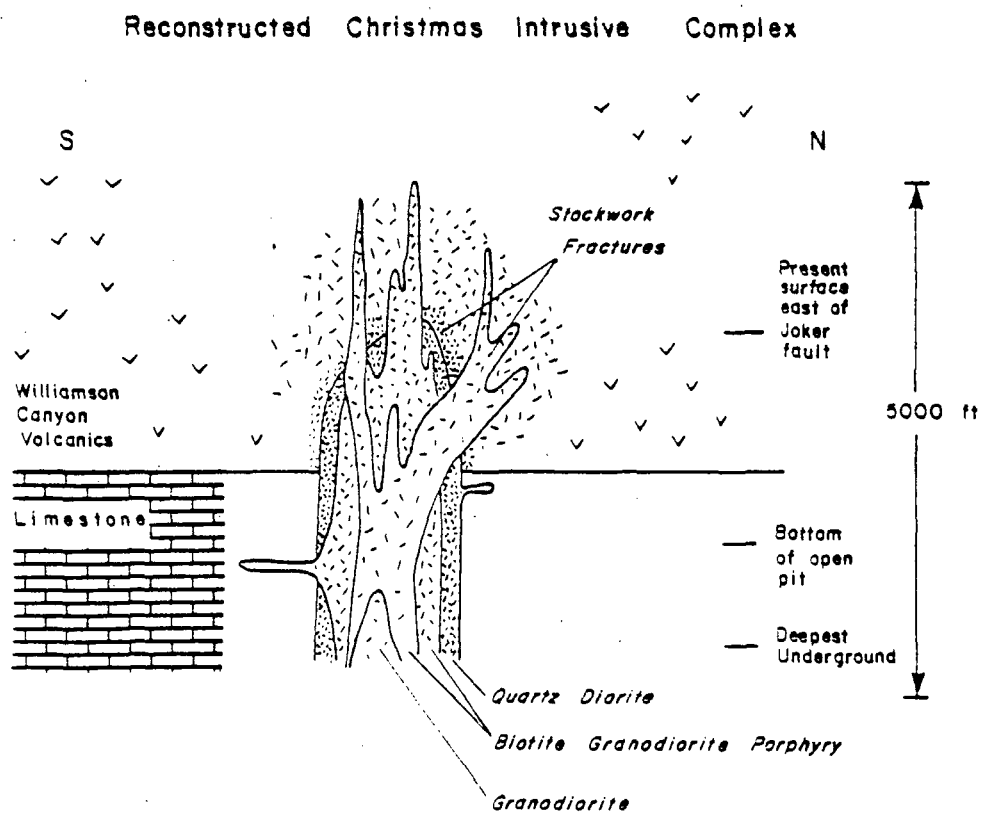
Figure 32. Diagrammatic configuration of the reconstructed Christmas intrusive complex, viewed along a north-south section at approximately 18,000E, showing the general sequence of emplacement of mainstage intrusive phases and the fracture distribution pattern.

of considerable disequilibrium between crystals and melt, perhaps a function of fluctuations in water pressure (Turner and Verhoogen, 1960). Magma crystallizing in the core of the complex developed a granitoid texture.

A system of disoriented microfractures was generated within each intrusive phase during or shortly after consolidation. Fractures migrating through phenocrysts rather than around them suggests that, in most cases, the host rocks were able to deform by brittle fracture, that is, the fractures were postconsolidational. An external tectonic propagation mechanism cannot easily be invoked to explain the random and fine-scale nature of the microfractures. An internal process, such as the escape of volatiles from the consolidating magma, is more likely. Burnham (1967) has proposed that granodioritic magmas, initially under-saturated with respect to water $(P_{H_2O} < P_{total})$, are capable of rising to relatively shallow levels in the crust. If such a magma becomes saturated $(P_{H_2O} = P_{total})$ during ascent, water may escape in response to further decrease in confining pressure and/or by second boiling. Entrapment of fluid beneath impermeable rock, such as the early-crystallized shell of an epizonal pluton, might lead to fluid over-pressure $(P_{H_2O} > P_{total})$ high enough to generate fractures in over-lying rock.

Phillips (1973) advances this argument somewhat further by proposing that 1 percent by weight of water, exsolved from a crystal-lizing magma at a depth of 2 km by retrograde boiling, would have a specific volume of 4, and could produce, by brecciation, an increase

in volume for the total mass of 10 percent. Furthermore, the differential stresses resulting from expansion could cause shear fracturing in the enclosing wall rocks.

The amount of energy necessary to accomplish this type of fracturing by internal means would be enormous, and experimental work by Burnham and Davis (1969) on the system albite-water may be applicable to this problem. They assume that the system $NaAlSi_3O_8-H_2O$ is a reasonable model for water in felsic magmas, and then calculate that retrograde boiling and the increase in total volume, at least in simple melts, could be accompanied by a release of mechanical energy equivalent to that released during major volcanic eruptions (approximately 10^{24} ergs km^{-3} of magma).

The lateral and vertical expansion during explosive release of volatiles is compatible with the disoriented fine-scale geometry of microfracturing at Christmas, and retrograde boiling is a plausible causative mechanism. Although a single discrete early-crystallized outer shell probably did not develop in the Christmas stock, individual phases may have had broadly consolidated roof and marginal zones which fractured as crystallization progressed inward and forced retrograde boiling. Several generations of fractures were superimposed on earlier intrusive phases.

Much of the shattering and ground preparation of enclosing volcanic wall rocks may have developed in response to brecciation and expansion of the intrusive mass. Other fractures in the heated volcanic host rocks may have been generated by differential thermal

expansion of pore fluids (Knapp and Knight, 1977). A generalized fracture distribution pattern is shown in Figure 32.

Intrusion of quartz diorite and biotite granodiorite porphyry, K-silicate alteration, and associated chalcopyrite-bornite minerali-zation are believed to be broadly contemporaneous features. K-Ar ages for Stage I vein minerals (Table 6) are within error limits of the age determined for primary biotite from Light Phase. Early alteration-mineralization, however, did not evolve in a static system, but rather during a period of repeated surges of magma, particularly within the core of the stock.

The sequence of alteration and mineralization along a declining pressure-temperature path in the Christmas porphyry copper system is summarized graphically in Figure 33. Initially, confining pressure was equal to the weight of the overlying rock, perhaps 0.5 kb for the top of the system at a proposed depth of about 2 km. Early K-silicate alteration may have begun with temperatures at or somewhat below the solidus for granodioritic magma, which probably ranges between 700°-800°C at pressures below 1 kb (see, for instance, Piwinskii and Wyllie, 1968). Fluid inclusions from early veins at Christmas indicate that alkali-rich, high-salinity fluids were present during Stage I alteration and mineralization. The initial K^+/H^+ ratio was high, but may have been decreasing steadily as K-silicate alteration proceeded.

The distribution and pervasiveness of secondary biotite in the stock, its similarity in composition to primary biotite (Appendix III), and the nearly isochemical nature of the alteration (Table 8) suggest

TEMPERATURE

700°C   600°C   500°C   400°C   300°C   200°C

PRESSURE — HYDROSTATIC / LITHOSTATIC

STAGE I   STAGE II

MAGMATIC   MAGMATIC-   METEORIC-
          HYDROTHERMAL   HYDROTHERMAL

Quartz-zeolite (pyrite)

Quartz-chlorite veins

Quartz-sericite veins
(pyrite-chalcopyrite)

Quartz-sulfide veins
(chalcopyrite-bornite-magnetite)

Quartz-K-feldspar veins
(chalcopyrite-bornite-molybdenite)

Biotitization of volcanic rocks

K-feldspar veinlets
(chalcopyrite, pyrite)

Secondary biotite (Christmas stock)
(chalcopyrite, pyrite)

Propylitic(?)

Figure 33. The sequence of alteration-mineralization along a
declining pressure-temperature path in the Christmas
porphyry copper system.

that hornblende-destructive biotitization was, at least in part, a late magmatic or "deuteric" process. Applying the biotite geothermometer of Beane (1974), based on the ratio of octahedrally coordinated. Mg^{2+}, Fe^{2+}, and Fe^{3+}, to compositions of this pervasive biotite results in an estimated temperature of formation of approximately 450°C. This temperature is within the temperature range (350°-550°C) of K-silicate alteration at several porphyry copper deposits calculated from secondary biotite compositions by Beane (1974). Fournier (1967), however, has calculated somewhat higher temperatures of formation of 600°-700°C for biotite replacing hornblende during the early alteration stage at Ely, Nevada. Beane's biotite geothermometer must be used with caution because of the requirement that biotite be part of an equilibrium assemblage with a K-feldspar phase and magnetite. At Christmas, secondary K-feldspar occurs along fractures, but is generally not intergrown with pervasive secondary biotite and disseminated magnetite.

The pervasive and apparent "deuteric" character of mafic-destructive propylitic alteration in peripheral biotite rhyodacite porphyry dikes suggests that it may have developed concurrently with secondary biotite in the stock during and following emplacement of the Christmas intrusive complex.

During Stage I the degree of hornblende-destructive biotitization was increasing in upper and marginal portions of the porphyry system. In addition to hornblende, biotite phenocrysts in dikes and sills marginal to the main intrusive mass were being converted to shreddy biotite pseudomorphs. This pattern of biotitization implies that early

fluids migrating upward and outward through the stock, either through the residual melt before consolidation, or through stockwork fractures after complete crystallization, were concentrating potassium due, at least in part, to a declining temperature gradient. Experimental work by Orville (1963) is relevant to this point. He demonstrated that the equilibrium K/K + Na ratio in an aqueous phase coexisting with two alkali feldspars will decrease with decreasing temperature. Similarly, the alkali-rich fluids rising in the intrusion were passing down the thermal gradient and releasing K, thereby increasing the stability of biotite relative to hornblende.

The distribution of secondary biotite has a second genetic implication. Progressively younger intrusive phases have a diminishing secondary biotite/hornblende ratio and a corresponding increase in the chlorite/secondary biotite ratio. It is apparent that K- and H-metasomatism were both operating during early alteration, and fluids were evolving with time through decrease in K^+/H^+ ratio, and possibly through increase in Mg (R. O. Fournier, personal communication, 1977).

K-feldspar did not form with secondary biotite during deuteric alteration, but began to replace plagioclase along newly generated fractures. The plagioclase-destructive alteration appears to have been triggered by a change in confining pressure. Recent experimental work on alkali exchange at high temperatures and low vapor pressure by Fournier (1976) indicates that alkali feldspar coexisting with Na-rich Na-K-Cl brine and vapor at subcritical pressures is relatively more enriched in K than at higher pressures. This enrichment is promoted

by K-Na exchange through the vapor phase. Both brine and gas phases are strongly enriched in K owing to precipitation of NaCl with decreasing pressure.

Such a mechanism could help explain the apparent time discordancy in hornblende and plagioclase alteration during early alteration. Aqueous fluids in the residual melt of each intruding phase may have been above the critical point and were relatively homogeneous, with high Na activity and lesser but significant K contents. In that environment hornblende was unstable relative to biotite, but plagioclase was still stable with respect to K-feldspar. Final consolidation followed by buildup of fluid pressure caused brecciation and a sudden drop in confining pressure from lithostatic to hydrostatic. The fluid became subcritical, separated into brine and vapor, and NaCl precipitated. The gas and liquid phases, strongly enriched in K, exchanged alkalies with plagioclase in immediately adjacent wall rock, forming K-feldspar-rich envelopes. Hornblende surviving earlier biotitization was converted to biotite in the alteration envelopes.

Only small amounts of sulfide were deposited in the Christmas stock during early K-silicate alteration. Bornite and chalcopyrite and, in places, chalcopyrite with small quantities of pyrite were disseminated in zones of intense biotitization. Some magnetite also formed with secondary biotite. Early K-feldspar veinlets were host to minor chalcopyrite and pyrite mineralization.

The formation of K-feldspar veinlets marked the beginning of magmatic-hydrothermal alteration (Figure 33). As fluid continued to

pass through the magma at depth, many fractures repeatedly healed and reopened. Confining pressure was fluctuating between lithostatic and hydrostatic. At that point, newly developing fractures, many with an apparent radial orientation, were becoming progressively more through-going and steeply dipping. This change in fracture style, whether caused by external tectonic stress, the pressure of upwelling magma on consolidated rock, hydraulic action of hydrothermal fluids, or some other mechanism, coincided with the formation of increasingly quartz-rich, K-feldspar-poor veins. Although veins were becoming wider, K-feldspar envelopes remained narrow, suggesting that fluid and wall rock were in near chemical equilibrium. Only minor amounts of chalco-pyrite and, locally, molybdenite were deposited in quartz-rich veins in the core of the complex, but increasing quantities of chalcopyrite with bornite were precipitating in upper levels of the Stage I vein system, perhaps in response to a steeper temperature gradient. The presence of both primary and secondary gas-rich fluid inclusions in Stage I quartz veins indicates that boiling was a recurring event. Nash (1976) estimates from filling temperatures of such inclusions that temperatures of formation of quartz-sulfide veins for many porphyry cop-per deposits were approximately 400°±100°C.

The direction of movement of Stage I fluids and the geometry of early alteration-mineralization are shown in Figure 34. As potassic fluids emanating from the stock encountered the steep chemical gradient provided by basaltic volcanic rocks, K, Si, H, Cu, and S were added during a nearly complete reconstitution to the assemblage biotite-
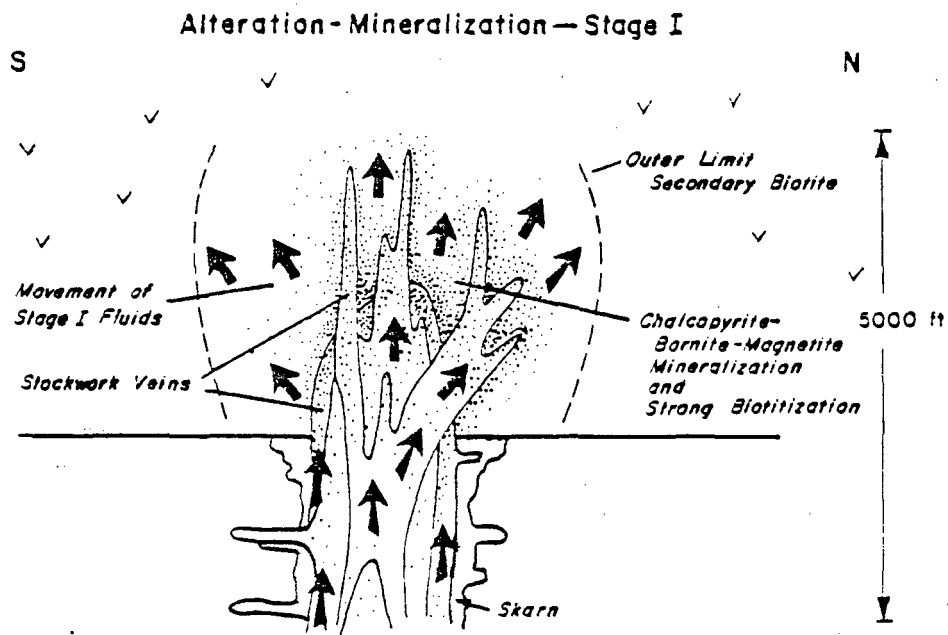
Figure 34. Diagrammatic representation of Stage I alteration and mineralization. Arrows indicate movement of magmatic-hydrothermal fluids.

quartz-sodic plagioclase-hornblende-chalcopyrite-bornite-magnetite. The biotitic alteration and ore-grade mineralization were centered on the network of quartz-rich veins building upward into the shattered volcanic pile. Biotitization, mineralization, and stockwork quartz veining in volcanic rocks were broadly contemporaneous Stage I events.

Fe- and Mg-rich basalts of the Williamson Canyon Volcanics were chemically receptive to the formation of secondary biotite during K-metasomatism resulting in a large biotite halo. Narrow biotite selvages along veins in the intermediate zone of biotitization suggest that alteration was initially fracture controlled. Toward the stock pervasive biotitization developed as vein envelopes widened and coalesced in response to stronger fluid-wall rock interaction and higher fracture density.

The distribution of strong biotitization was also controlled by the configuration of genetically related intrusive rocks. Whereas a narrow zone developed along the steep south contact of the Christmas stock, a broad lobe of intense biotitic alteration formed over shallow apophyses of K-silicate-altered porphyry in the "northeast salient" (see Figure 34). Like the contact between intrusive and carbonate rocks at depth, the contact between intrusive and volcanic rocks may also have served as a major conduit for ascending ore fluids.

Anhydrite formed in strongly biotitized volcanic wall rock and in Stage I quartz-sulfide veins near the intrusive contact. Although $CaSO_4$ has retrograde solubility in pure water, anhydrite will precipitate with decreasing temperature in $NaCl-H_2O$ solutions at temperatures

above the solubility minimum (Blount and Dickson, 1969). Saturation may have been achieved as SO_4^{2-}-bearing fluids entered cooler volcanic rocks from which Ca^{2+} was being liberated during biotitization. The limited occurrence away from the contact and the occasional vugginess of Stage I veins suggest that some anhydrite may have been dissolved by cooler ground water entering the system.

Stage II: Late Alteration and Mineralization

Following the formation of quartz-rich Stage I veins, a fundamental change occurred in the nature of fluid-wall rock interaction in igneous rocks peripheral to the central stock. K-metasomatism was declining in intensity, yielding to processes that were predominantly hydrolitic in character. Quartz-sericite-chlorite-pyrite-chalcopyrite became the stable silicate-sulfide assemblage in igneous host rocks. The transition from K- to H-metasomatism was largely a function of decrease of the K^+/H^+ ratio and/or cooling of the hydrothermal fluids (Hemley and Jones, 1964; Meyer and Hemley, 1967). The similarities in the distribution patterns of fracture-related chloritic alteration in mafic volcanic rocks and sericitic alteration in intermediate intrusive and clastic sedimentary rocks suggest that these types of alteration resulted from the same process acting in host rocks of contrasting composition.

The transition from Stage I to Stage II alteration-mineralization may have occurred with the first significant incursion of meteoric

water into the porphyry system. Evidence for this interpretation, in
lieu of stable isotopic data, includes (1) the configuration of the
zone of quartz-sericite-chlorite alteration and its overlapping but
largely marginal position with respect to Stage I stockwork veins; and
(2) the abundance of relatively dilute moderate-salinity fluid inclu-
sions and paucity of halite-bearing fluid inclusions in Stage II veins.
Furthermore, the thoroughly shattered pile of interlayered basaltic
flows and breccias could have contained the necessary supply of ground
water. It is significant to the above hypothesis that studies of hydro-
gen and oxygen isotope ratios of sericites and clays from Santa Rita,
New Mexico (Sheppard and others, 1971), El Salvador, Chile (Sheppard
and Gustafson, 1976), and several other porphyry copper deposits (Taylor,
1974), indicate that hydrothermal fluids from which these minerals
formed had a large meteoric water component.

Other mechanisms could have been a factor in changing the K^+/H^+
ratio of the fluids but processes such as prolonged wall rock interac-
tion, irreversible adiabatic expansion by throttling (Rose, 1970), or
the gradual cooling of the entire hydrothermal system cannot, in them-
selves, account for the sharp distinction and crosscutting relation-
ships between Stage I and Stage II veins, the overlapping zonal dis-
tribution, and the absence of Stage II veins in the central stock.

The simple cooling effect brought about by mixing of magmatic
and meteoric waters may have been sufficient to stabilize chlorite and
sericite without strongly affecting the K^+/H^+ ratio. However, hydrogen
metasomatism also could have been enhanced by the increased ionization

of contained acids at lower temperatures (Barnes and Ellis, 1967) and, if the ground waters were oxygenated, by oxidizing H_2S to H_2SO_4.

The general convection model shown in Figure 35 may reasonably account for the distribution of Stage II alteration-mineralization features at Christmas. The model is similar to that proposed by Taylor (1974) for porphyry copper deposits in general. The circulation of meteoric water was guided by the extensive system of fractures which were particularly abundant in volcanic rocks near the stock. The convection cell was generated, and then perpetuated, by the density differential between high-temperature fluids near the Christmas stock and cooler fluids in volcanic country rock more distant from the heat source.

Stage II alteration-mineralization, under conditions referred to as meteoric-hydrothermal in Figure 33, may have begun following the last major surge of biotite granodiorite porphyry and magmatic-hydrothermal fluid from the cooling intrusive center. As cool meteoric waters and fluids from the magma intermixed, sulfide solubilities decreased and large amounts of pyrite and chalcopyrite were dumped along fractures. Fluids near the stock and the source of copper were depositing more chalcopyrite relative to pyrite than fluids in distal portions of the convection cell. As the intrusive center continued to cool, the convection cell was drawn inward toward the stock resulting in overlap of Stage I and Stage II alteration and mineralization (Figure 35). Meteoric-hydrothermal fluids were able to penetrate the intrusive complex only along closely spaced vertical sheet fractures. Since the

Alteration-Mineralization—Stage II
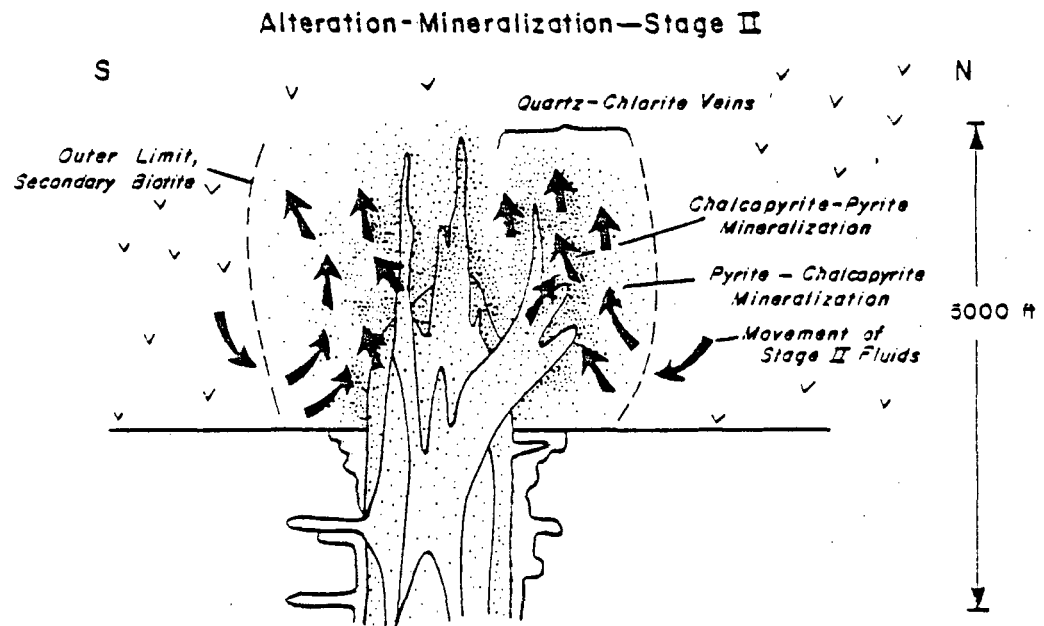
Figure 35. Convection model for Stage II alteration-mineralization. Arrows indicate movement of meteoric-hydrothermal fluids and waning magmatic-hydrothermal fluids.

outer limit of quartz-sericite alteration in porphyry dikes was also
fracture controlled, the zone of Stage II alteration developed in an
intermediate position between zones of K-silicate and propylitic
alteration.

Although uncommon, Stage I quartz-sulfide veins with the sulfide
assemblage chalcopyrite-pyrite may be a transitional type. These have
been observed cutting Stage II veins suggesting that more than one con-
vection cycle may have occurred, possibly as a response to fluctuations
between lithostatic and hydrostatic pressure in the intrusive complex.
Although lower pressures tend to retard hydrolysis reactions (Hemley
and Jones, 1964), quartz-sericite-chlorite alteration probably occurred
under hydrostatic conditions (Figure 33).

Wall rock alteration during Stage II was strongly fracture con-
trolled, and the strongly leached and bleached alteration envelopes
imply considerable chemical disequilibrium between wall rock and trans-
mitted fluids. In intrusive rocks the meteoric-hydrothermal fluids
traversed the well-developed system of sheet fractures leaching Ca
and Na from the adjacent wall rock in exchange for H. Under the stimu-
lus of low K^+/H^+, plagioclase was converted to sericite and biotite to
chlorite. K-feldspar, if originally present, was completely sericitized.
Since the rock probably had little K-feldspar, the fluids must have had
an appreciable supply of K^+ in order to stabilize sericite. Some potas-
sium may also have been provided by the chloritization of biotite. The
sheet fractures effectively channeled enough fluid to maintain a K^+/H^+

gradient low enough for expansion and ultimately, coalescence of sericitic vein envelopes. Sulfur and copper from the fluid combined with iron from the wall rocks to form pyrite and chalcopyrite in the vein envelopes as well as in fractures.

Hydrolyzing fluids (low K^+/H^+) traversing the more irregular fractures in mafic volcanic rocks reacted with earlier-formed secondary biotite to form chlorite. Chloritization along fractures was accompanied by albitization of plagioclase and silicification; development of sericite and clay was minimal. Iron leached from the enclosing wall rock probably contributed to the precipitation of sulfides and magnetite along fractures. The narrow vein envelopes and multiple vein fillings suggest that relatively small volumes of fluid were transmitted although fractures were repeatedly healed and reopened.

The last minerals to form in chloritic veins in volcanic rocks were pyrite, chalcopyrite, and the Ca-zeolites chabazite and laumontite. Experimental work by Liou (1971a, 1971b) suggests that at shallow depths and confining pressures of approximately 500 bars laumontite has a maximum thermal stability limit of 225°C. Contamination of the fluid phase by CO_2, S, and NaCl depresses the limit to lower temperatures. The high temperature stability limit for chabazite, although not yet established experimentally, would be somewhat lower (J. G. Liou, personal communication, 1977), and thus, the final deposition of sulfides may have occurred at temperatures near, or below, 200°C (Figure 33).

Following mainstage mineralization, granodiorite porphyry and

dacite porphyry intruded the south margin of the stock with sharp contacts. These phases postdate K-silicate alteration, but their temporal relationship with quartz-sericite-chlorite alteration is unknown. The chlorite-epidote alteration in these late phases is most reminiscent of the deuteric alteration prevalent in the McDonald stock northeast of the Christmas mine. However, disseminated bornite and chalcopyrite suggest that substantial concentrations of metals and sulfur were present in the late-forming magmas, or were introduced during late propylitic alteration in the Christmas stock.

IMPLICATIONS AND SUGGESTIONS FOR EXPLORATION IN THE REGION

Hydrothermal alteration patterns and copper mineralization in the Williamson Canyon Volcanics at Christmas are significant in regard to regional exploration. Two observations are emphasized here. Firstly, it is stressed that the volcanic rocks are basaltic in composition and a major host for copper ore. The chemical reactivity of thoroughly fractured basalt has induced telescoped Stage I and Stage II alteration and sulfide assemblages thereby upgrading copper values. It is suggested that Laramide-age mafic and intermediate volcanic sequences be given higher priority as favorable host rocks for ore.

Secondly, the increased stability of biotite in a mafic rock environment undergoing K-metasomatism considerably expanded the dimensions of the K-silicate zone. The zone of secondary biotite in basalt extends beyond the zone of well-defined quartz-sericite-chlorite

alteration, and well beyond the limits of ore-grade mineralization. Where propylitic alteration related to mineralization may be obscured by low-grade propylitic alteration of regional extent, biotitization may be the more reliable porphyry-related "fringe" alteration in mafic volcanic terranes. In addition, biotite halos may effectively increase the dimensions of reliable prospecting targets.

Biotitization of basalts and andesites has been recognized as porphyry-type alteration at Safford, Arizona (Robinson and Cook, 1966), El Salvador (Gustafson and Hunt, 1975) and El Teniente (Camus, 1975), Chile, and at the La Florida prospect in Sonora, Mexico (Theodore and Priego de Wit, 1977). Although the occurrence of secondary biotite in volcanic rocks is not in itself prima facie evidence that ore-grade mineralization exists nearby, its presence is a positive indication of porphyry-type hydrothermal alteration. It is equally important to note that no biotitization occurs in basaltic country rocks adjacent to barren granodioritic stocks near Christmas.

Although the presence of fine-grained disseminated biotite in basalts may escape detection, particularly during reconnaissance mapping programs, chip samples can be checked quickly in the field office with a binocular microscope. If identification is still uncertain, X-ray diffraction provides a rapid, accurate, and inexpensive method of analysis. The presence of biotite in altered basalts may also be indicated by anomalous potassium values in chemical analyses. Considering the number of Laramide volcanic fields in southeastern Arizona

hosting comagmatic or younger intrusive rocks, the recognition and interpretation of secondary biotite should be an important contribution to future exploration for porphyry copper deposits.

APPENDIX I. LOCATIONS AND DESCRIPTIONS OF ANALYZED SAMPLES (TABLES 1 AND 7).

Description number	Sample number	Location Latitude/Longitude Inspiration Company grid coordinates Northing/Easting	Sample description
1	39AB74	33°04'28"/110°43'34" 12,380N/22,840E	Medium-gray, moderately porphyritic, non-vesicular basalt with saussuritized plagioclase (labradorite) and augite phenocrysts in a felty matrix of plagioclase microlites. Coarse subhedral chlorite may represent altered orthopyroxene.
2	1AB75	33°03'34"/110°43'22" 6,980N/24,015E	Gray, fine-grained, porphyritic basalt with weakly saussuritized plagioclase and uralitized clinopyroxene phenocrysts set in an intergranular matrix of plagioclase laths, interstitial uralite, and opaque granules. Sparse disseminated pyrite.
3	74AB75	33°03'28"/110°45'04" 6,240N/15,480E	Dark-gray volcanic breccia with porphyritic, hornblende-bearing lithic and mafic volcanic lapilli, rounded hornblende crystal fragments, and rare chips of quartz in a tuffaceous matrix. Pyroxene in mafic lithic fragments is altered to uralite. Very fine-grained disseminated biotite in matrix of lithic fragments and in breccia matrix.
5	72AB74	33°03'02"/110°43'15" 3,670N/24,690E	From grayish-green hornblende andesite porphyry dike. Strongly porphyritic with 2-cm subhedral to euhedral hornblende, much smaller plagioclase, and sparse augite phenocrysts in aphanitic, locally pilotaxitic groundmass. Plagioclase saussuritized; augite partially altered to epidote; hornblende weakly chloritized. Moderate K-feldspar in groundmass.

6	54AB75	$33^{0}02'59"/110^{0}45'08"$ 3,360N/14,970E	From moderately porphyritic, medium-grained hornblende andesite porphyry dike. Similar in mineralogy and alteration to 72AB74. Hornblende very fresh in thin section. Moderate groundmass K-feldspar.
7	AB68-73	$33^{0}03'24"/110^{0}44'56"$ 5,810N/16,005E	From fine-grained, porphyritic hornblende andesite porphyry sill. Hornblende phenocrysts generally fresh, but locally replaced by chlorite and/or epidote; plagioclase is cloudy and saussuritized. Very fine-grained biotite scattered through groundmass, and locally replacing hornblende. Pyrite as disseminations and along fractures.
8	AB64-73A	$33^{0}04'30"/110^{0}43'17"$ 12,445N/24,395E	Hornblende rhyodacite porphyry from the McDonald stock. Massive and strongly porphyritic with well-formed plagioclase, hornblende, and biotite phenocrysts, and sparse rounded quartz blebs in turbid groundmass of interlocked quartz and feldspar. Moderate propylitic alteration with biotite pseudomorphed by chlorite enclosing lenses of epidote; hornblende partially replaced by chlorite, epidote, and calcite; plagioclase saussuritized. Moderate K-feldspar in groundmass.
9	83AB75	$33^{0}05'01"/110^{0}43'38"$ 15,675N/22,660E	Hornblende rhyodacite porphyry from the McDonald stock. Similar to AB64-73A, but less altered. Hornblende and plagioclase are fresh or show very weak propylitic alteration; biotite partially replaced by chlorite hosting lenses of prehnite.
10	GB-1	$33^{0}07'08"/110^{0}40'56"$	Hornblende rhyodacite porphyry from laccolith in Granite Basin. Less altered than AB64-73A and 83AB75. Very weak propylitic alteration, principally minor albitization of plagioclase.

11	D99-430	$33^0 03' 41''/110^0 44' 24''$ 7,568N/18,845E	Quartz diorite (Dark Phase) from the Christmas stock. Seriate-porphyritic with subhedral plagioclase and sparse, corroded biotite phenocrysts in interlocking matrix of quartz, plagioclase, and biotite. Ragged clusters of biotite pseudomorph original hornblende. Disseminated magnetite and chalcopyrite. Very sparse groundmass K-feldspar.
12	AB77F-73	$33^0 03' 33''/110^0 44' 35''$ 6,760N/17,828E	Biotite granodiorite porphyry (Light Phase) from the Christmas stock. Strongly porphyritic with plagioclase, biotite, hornblende, and quartz phenocrysts set in aplitic groundmass. Fresh in appearance away from veins, except for partial replacement of hornblende by fine-grained biotite. Weak groundmass K-feldspar.
13	D256-148	$33^0 03' 40''/110^0 44' 44''$ 7,570N/17,070E	Granodiorite from the Christmas stock. Hypidiomorphic-granular with interstial K-feldspar. Fresh in appearance except for variable chloritization of mafic minerals.
14	D237-700	$33^0 03' 46''/110^0 44' 44''$ 8,068N/16,984E	Biotite granodiorite porphyry from north margin or apophysis of the Christmas stock. Phenocrystic biotite and hornblende completely replaced by compact pseudomorphous aggregates of fine-grained biotite; plagioclase cloudy. Disseminated chalcopyrite and pyrite.
15	D248-320	$33^0 03' 42''/110^0 44' 42''$ 7,791N/17,211E	Basalt from zone of strong biotitization. Rock consists of intergrown fine-grained aggregate of cloudy, partly sericitized plagioclase, biotite, hornblende, and quartz. Texture of original volcanic rock is strongly modified. Loosely arranged clusters of hornblende may be replacement of original mafic phenocrysts. Disseminated bornite and chalcopyrite.

16	P-30-74	$33^\circ03'32''/110^\circ44'58''$ 6,824N/15,955E	Quartz diorite from the zone of quartz-sericite alteration at the west end of the Christmas stock. Plagioclase phenocrysts completely altered to sericite and subordinate clay; mafic minerals to chlorite and sericite. Groundmass is aggregate of quartz, sericite, chlorite, and pyrite.
17	61AB74B	$33^\circ03'33''/110^\circ45'28''$ 6,700N/13,235E	From strongly propylitized biotite rhyodacite porphyry dike west of the Christmas stock. Hornblende and biotite completely replaced by epidote and chlorite; plagioclase strongly saussuritized. Scattered 5-mm-nodules of epidote replace plagioclase, hornblende, and groundmass. Epidote and chlorite compose about 20 percent of the rock volume.

APPENDIX II.   K-Ar AGES: SAMPLE LOCATIONS AND ANALYTICAL DATA.

Sample number	Location Latitude/Longitude Inspiration Company grid coordinates Northing/Easting	Rock type/ material dated	K_2O (percent)	$Ar^{40}Rad$ (moles/gm)	$\dfrac{Ar^{40}Rad}{Ar^{40}Total}$ X100	Apparent age (m.y.)
74AB75	33°03'28"/110°45'04" 6,240N/15,480E	Lithic lapilli tuff from Williamson Canyon Volcanics/ hornblende	0.495	5.52154×10^{-11}	28.9	76.2±2.6
54AB75	33°02'59"/110°45'08" 3,360N/14,970E	Hornblende andesite porphyry (fine-grained variety)/ hornblende	0.494	5.93090×10^{-11}	33.03	81.7±1.8
72AB74	33°03'02"/110°43'15" 3,670N/24,690E	Hornblende andesite porphyry (coarse-grained variety)/ hornblende	0.548	6.12518×10^{-11}	40.7	76.2±1.3
GB-1	33°07'08"/110°40'56"	Hornblende rhyodacite porphyry (Granite Basin pluton)/ hornblende	0.528	5.59510×10^{-11}	29.2	72.3±1.6
83AB75	33°05'01"/110°43'38" 15,675N/22,660E	Hornblende rhyodacite porphyry (McDonald stock)/hornblende	0.516	5.27260×10^{-10}	22.1	69.8±0.9
CS-1-75	33°03'34"/110°44'41" 6,950N/17,250E	Pegmatitic biotite vein in biotite granodiorite porphyry/ biotite (chloritized)	3.74	3.44414×10^{-10}	64.1	62.8±1.1

D148-337	$33^0 03'40"/110^0 44"49"$ 7,600N/16,605E	Quartz-K-feldspar-sericite-chlorite vein in biotite granodiorite porphyry/ sericite	10.45	9.56757×10^{-10}	86.32	62.5 ± 1.0
AB49-73	$33^0 03'22"/110^0 44'44"$ 5,680N/16,995E	Basalt porphyry/ whole rock	1.78	6.58740×10^{-11}	77.11	25.5 ± 0.2

Mineral separates and whole rock sample prepared by R. A. Koski. Potassium analyses by flame photometer; analysts: S. Neil and J. Christie. Argon mass analyses using standard isotope-dilution techniques with a Nier-type mass spectrometer; analyst: E. H. McKee. Age calculations by E. H. McKee. All analyses in laboratories of the U.S. Geological Survey.

Constants used for the age calculations are $\lambda_\epsilon = 0.581 \times 10^{-10} yr^{-1}$, $\lambda_\beta = 4.962 \times 10^{-10} yr^{-1}$, and $K^{40}/K_{total} = 1.167 \times 10^{-4}$ mole/mole.

APPENDIX III: BIOTITE COMPOSITIONS

Several recent studies (e.g., Moore and Czamanske, 1973; Roberts, 1973; and Jacobs and Parry, 1976) have indicated that magmatic and hydrothermal biotites from the porphyry copper environment possess discrete compositional differences. Chemical compositions for nine primary and secondary biotites from igneous rocks at Christmas are listed in Table 10 along with structural formulas and the octahedral cation ratio Mg/Mg + Fe.

All analyses were performed with an ARL Model EMX electron microprobe on grains from purified biotite separates mounted on edge in epoxy, polished, and carbon coated. ADP, RAP, and LiF crystals were used to analyze eleven elements in the following combinations: Ca, K, Na; Fe, Mn, Mg; Si, Ti, Al; and Ba, F. During the analyses, the accelerating potential was 15 Kv, the sample current 0.02 microamps measured on brass, and the beam diameter approximately 2-3 microns. A procedure was followed whereby at least two points on 5-10 grains were analyzed for an interval (approximately 10 seconds) equal to a preset quantity of beam current.

The following standards were used during the biotite analyses: Biotite 56, a well-analyzed and homogeneous (with respect to K) mica for K, Mg, Si, Al, and Ba; B65DS, a high iron biotite for Fe and Ti; Carmichael's #3 biotite for F; Crystal Bay bytownite for Na and Ca;

Table 10. Compositions of primary and secondary biotites from igneous rocks at Christmas.

Description number	1	2	3	4	5	6	7	8	9
Sample number	D256-148	UG-16-7	AB77F-73	D99-430	P-34-74	AB781-73	CC-21-75	CC-42-75	D248-328
SiO_2	37.3	37.1	37.4	38.0	38.0	38.0	40.0	38.8	37.9
Al_2O_3	14.5	13.3	13.9	14.2	14.7	14.1	13.7	14.4	14.2
TiO_2	5.5	6.4	5.7	5.9	5.2	5.0	4.1	4.7	4.3
Total Fe as FeO	13.7	13.9	14.0	13.0	13.6	14.5	9.6	10.1	13.0
MgO	13.9	13.3	14.8	14.2	14.1	13.9	17.6	17.0	15.1
MnO	0.14	0.23	0.22	0.16	0.12	0.16	0.10	0.14	0.17
CaO	0.04	0.04	0.04	0.04	0.05	0.03	0.04	0.06	0.07
K_2O	9.0	8.7	8.8	9.1	9.0	8.1	10.2	9.7	8.8
Na_2O	0.19	0.15	0.17	0.19	0.16	0.13	0.23	0.21	0.17
BaO	0.47	0.33	0.43	0.17	0.21	0.35	0.10	0.05	0.12
F	0.43	0.36	0.45	0.35	0.45	0.45	1.7	0.77	0.35
Total	95.2	93.8	95.9	95.3	95.6	94.7	97.4	95.9	94.2

Table 10 (continued). Compositions of primary and secondary biotites from igneous rocks at Christmas.

Description number	1	2	3	4	5	6	7	8	9
Sample number	D256-148	UG-16-7	AB77F-73	D99-430	P-34-74	AB781-73	CC-21-75	CC-42-75	D248-328

Structural formulas

		1	2	3	4	5	6	7	8	9
Si $]$	Z	5.56	5.62	5.55	5.62	5.61	5.67	5.74	5.63	5.66
		8.00	7.99	7.98	8.00	8.00	8.00	8.00	8.00	8.00
$Al^{IV}]$		2.44	2.37	2.43	2.38	2.39	2.33	2.26	2.37	2.34
Al^{VI}		0.11	0.00	0.00	0.10	0.17	0.14	0.05	0.10	0.17
Ti		0.61	0.72	0.64	0.66	0.58	0.57	0.44	0.52	0.49
Fe	Y	1.71	1.76	1.74	1.61	1.68	1.80	1.15	1.23	1.62
		5.55	5.52	5.67	5.53	5.56	5.63	5.41	5.56	5.66
Mn		0.02	0.03	0.03	0.02	0.02	0.02	0.01	0.02	0.02
Mg		3.10	3.01	3.26	3.14	3.11	3.10	3.76	3.69	3.36
Ca		0.01	0.01	0.01	0.01	0.01	0.01	0.01	0.01	0.01
Na	X	0.06	0.04	0.05	0.06	0.04	0.04	0.06	0.06	0.05
		1.82	1.75	1.75	1.79	1.75	1.61	1.95	1.87	1.75
K		1.72	1.68	1.67	1.71	1.69	1.54	1.87	1.80	1.68
Ba		0.03	0.02	0.02	0.01	0.01	0.02	0.01	0.00	0.01
F		0.14	0.12	0.15	0.11	0.15	0.15	0.55	0.25	0.12
		4.00	4.00	4.00	4.00	4.00	4.00	4.00	4.00	4.00
(OH)*		(3.86)	(3.88)	(3.85)	(3.89)	(3.85)	(3.85)	(3.45)	(3.75)	(3.88)

100 Mg/Mg + Fe

	1	2	3	4	5	6	7	8	9
	64	63	65	66	65	63	77	75	67

* Includes Cl; calculated by difference assuming ideal occupancy.
Structural formulas calculated on the basis of 22 oxygens for the general formula $X_2Y_{4-6}Z_8O_{20}(OH,F)_4$ (Deer, Howie, and Zussman, 1962). 1 and 2. Phenocrystic biotite from granodiorite phase. 3. Phenocrystic biotite from biotite granodiorite porphyry. 4, 5, and 6. Secondary biotite from quartz diorite phase. 7. Secondary biotite from quartz diorite sill. 8. From pegmatitic biotite vein, biotite granodiorite porphyry. 9. Secondary biotite from basalt, zone of strong biotitization. Analyses by R. A. Koski.

and rhodonite for Mn. Raw X-ray data from electron microprobe anal-
yses were corrected on-line using a minicomputer and a revised version
of the FRAME program (Yakowitz and others, 1973). Mineral norms were
calculated on the basis of 22 oxygens per formula.

To augment the microprobe data, eight of the mica samples were
also analyzed by standard wet chemical methods for ferrous and total
iron (Table 11). The Fe^{3+}/total Fe calculated from the partial chemi-
cal analyses were then multiplied by the values for Fe in the structural
formulas of Table 10 to determine an approximate value for Fe^{3+} in octa-
hedral coordination (Table 11). With this additional data, the biotites
can be classified according to the relative proportion of octahedral
cations as shown in Figure 36, modified from Foster (1960). Six of the
biotites plot within a small area in the Mg biotite field of Foster,
and two plot in the phlogopite field.

Three of the biotites analyzed (samples 1, 2, and 3) are coarse-
grained phenocrystic varieties formed during cyrstallization of biotite
granodiorite porphyry and granodiorite, and three (4, 5, and 6) are
secondary or "deuteric" types which pseudomorph hornblende in quartz
diorite. Samples of biotite of hydrothermal origin include fine-grained
reddish-brown biotite (7) from a quartz diorite(?) sill intruding Naco
Limestone south of the stock; coarse biotite (8) from a biotite-chlorite
vein in biotite granodiorite porphyry; and biotite (9) from basalt in
the zone of strong biotitization.

All of the micas analyzed show incomplete occupancy of octahedral
sites by Y group cations indicating some departure from the ideal tri-

Table 11. Iron analyses for biotites from Christmas. Ferrous iron by volumetric method; total iron by spectrophotometric method. Analyst: Sarah T. Neil.

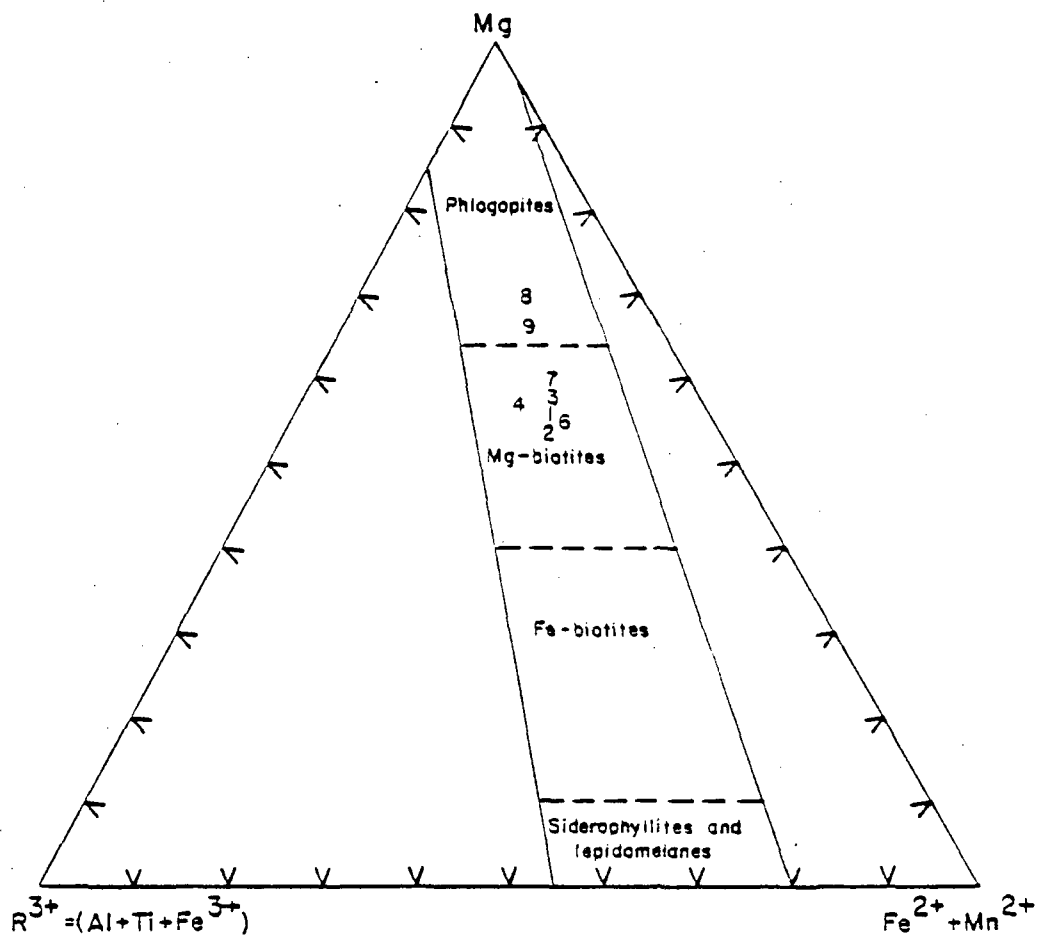| Sample number	Total Fe as percent Fe_2O_3	Percent FeO	$Fe^{3+}/Fe^{3+}+Fe^{2+}$	Fe^{3+} in octahedral coordination
D256-148	16.74	13.00	0.14	0.23
UG-16-7	17.47	13.39	.15	.26
AB77F73	16.93	12.77	.16	.28
D99-430	16.10	11.58	.20	.32
AB78I73	17.64	13.90	.12	.22
D248-328	15.92	12.18	.15	.24
CC-21-75	12.43	9.83	.12	.14
CC-42-75	12.86	9.83	.15	.14

Figure 36. Classification of Christmas biotites based on occupation of octahedral (Y) positions. Triangular diagram modified from Foster (1960). Numbers refer to analyzed samples in Table 10.

octahedral mica structure. Twelve-coordinated cations (K, Ca, Na, and Ba) occupy 1.61-1.95 of the ideal 2.00 interlayer sites per formula. K represents 95-97 percent of the total large cation constituency in all samples.

The compositions of coarse-grained phenocrystic and fine-grained deuteric biotites from the stock are nearly indistinguishable. Although the Mg/Mg + Fe ratios are comparable to those for biotites from several mineralized and unmineralized stocks in the Basin and Range province (Jacobs and Parry, 1976; Moore and Czamanske, 1973), the consistency of values is contrary to the Mg-enrichment of biotite replacing hornblende documented at Bingham, Utah (Moore and Czamanske, 1973) and Butte, Montana (Roberts, 1973). However, Jacobs and Parry (1976) found only a slight mole-fraction phlogopite increase in biotite pseudomorphing hornblende at Santa Rita, New Mexico.

TiO_2 contents of magmatic and deuteric biotites in Table 10 are rather high, ranging from 5.0 to 6.4 weight percent. This compares with TiO_2 contents of 2.6-3.5 percent for biotites from hornblende-biotite tonalite and granodiorite complexes from northern Portugal (de Albuquerque, 1973), and 2.5-4.2 percent for biotites from granitic rocks of the Sierra Nevada batholith (Dodge and others, 1969). Jacobs and Parry (1976), however, analyzed biotites containing up to 6 weight percent TiO_2 from intermediate mineralized and unmineralized plutons in the western United States.

When compared to magmatic and deuteric biotites, samples of hydrothermal biotite in Table 10 have higher values of Mg/Mg + Fe

(although the biotite from altered basalt is only slightly more phlogopitic), as well as lower Ti and Ba. The correlation between increasing mole-fraction phlogopite and decreasing Ti in alteration biotites is also evident in the other porphyry copper deposits mentioned above.

The two phlogopites analyzed in this study (samples 7 and 8) are further characterized by high F contents. Banks (1976) has also reported that hydrothermal biotite from mineralized Laramide intrusive rocks in the Ray, Arizona porphyry copper deposit has higher F than igneous biotite from equivalent but unmineralized intrusive rocks outside the deposit.

The similarity in composition of phenocrystic and secondary biotites from the Christmas stock is supportive of an essentially magmatic origin for the latter variety. That is, the pervasive replacement of hornblende by biotite occurred under late magmatic or "deuteric" conditions in the presence of fluids with Mg/Fe ratios, oxygen fugacities, and other chemical parameters analagous to those for fluids attending the crystallization of biotite phenocrysts. In an alternative view, the compositional homogeneity of these biotite varieties may be the result of reequilibration of primary biotite during later deuteric or hydrothermal events. However, the lack of recrystallization effects in magmatic biotites and the presence of hornblende in the samples of granodiorite and biotite granodiorite porphyry seem to preclude the readjustment of phenocrystic biotite compositions.

The contrasting compositions of hydrothermal biotites signify the chemical evolution of the fluid phase. For example, more magnesian compositions may have resulted from higher oxygen fugacities in the cooler hydrothermal fluids. Additional analyses are planned to further define space-time chemical variations in biotites of orthomagmatic, deuteric, and hydrothermal origin at Christmas.

REFERENCES CITED

de Albuquerque, Carlos A. R., 1973, Geochemistry of biotites from granitic rocks, northern Portugal: Geochim. et Cosmochim. Acta, v. 37, p. 1779-1802.

Banks, Norman G., 1976, Halogen contents of igneous minerals as indicators of magmatic evolution of rocks associated with the Ray porphyry copper deposit, Arizona: Jour. Research U.S. Geol. Survey, v. 4, p. 91-117.

Banks, N. G., Cornwall, H. R., Silberman, M. L., Creasey, S. C., and Marvin, R. F., 1972, Chronology of intrusion and ore deposition at Ray, Arizona: Econ. Geology, v. 67, p. 864-878.

Banks, N. G., and Krieger, M. H., 1977, Geologic map of the Hayden quadrangle, Gila and Pinal Counties, Arizona: U.S. Geol. Survey Geol. Quad. Map GQ-1391, scale 1:24,000 (in press).

Banks, N. G., and Stuckless, J. S., 1973, Chronology of intrusion and ore deposition at Ray, Arizona--Part II, fission track ages: Econ. Geology, v. 68, p. 657-664.

Barnes, H. L., and Ellis, A. J., 1967, Ionization in aqueous solutions, in Barnes, H. L., ed., Geochemistry of hydrothermal ore deposits: New York, Holt, Rinehart, and Winston, Inc., p. 636-649.

Barrett, Larry F., 1972, Igneous intrusions and associated mineralization in the Saddle Mountain mining district, Pinal County, Arizona: Univ. Utah, Salt Lake City, Utah, M.S. thesis, 90 p.

Beane, Richard E., 1974, Biotite stability in the porphyry copper environment: Econ. Geology, v. 69, p. 241-256.

Best, Myron G., 1969, Differentiation of calc-alkaline magmas, in McBirney, A. R., ed., Proceedings of the andesite conference: Oregon Dept. Geology and Mineral Industries Bull. 65, p. 65-75.

Bikerman, Michael, and Damon, P. E., 1966, K-Ar chronology of the Tucson Mountains, Pima County, Arizona: Geol. Soc. America Bull., v. 77, p. 1225-1234.

Blanchard, Roland, 1968, Interpretation of leached outcrops: Nevada Bur. Mines Bull. 66, 196 p.

Blount, C. W., and Dickson, F. W., 1969, The solubility of anhydrite ($CaSO_4$) in $NaCl-H_2O$ from 100° to 450°C. and 1 to 1000 bars: Geochim. et Cosmochim. Acta, v. 33, p. 227-245.

Bowen, N. L., 1928, The evolution of the igneous rocks: New York, Dover Publications, 332 p.

Brown, J. B., 1971, Jarosite-goethite stabilities at 25°C., 1 atm.: Mineralium Deposita, v. 6, p. 245-252.

Bryant, D. G., 1968, Intrusive breccias associated with ore, Warren (Bisbee) mining district, Arizona: Econ. Geology, v. 63, p. 1-12.

Burnham, C. W., 1967, Hydrothermal fluids at the magmatic stage, in Barnes, H. L., ed., Geochemistry of hydrothermal ore deposits: New York, Holt, Rinehart, and Winston, Inc., p. 34-76.

Burnham, C. W., and Davis, N. F., 1969, Energy relations in water-bearing magmas (abs.): Geol. Soc. America Abs. with Programs, v. 1, no. 7, p. 26.

Camus, Francisco, 1975, Geology of the El Teniente orebody with emphasis on wall-rock alteration: Econ. Geology, v. 70, p. 1341-1372.

Coney, Peter J., 1972, Cordilleran tectonics and plate motion: Am. Jour. Sci., v. 272, p. 603-628.

Coney, Peter J., 1976, Plate tectonics and the Laramide Orogeny, in Woodward, L. A., and Northrop, S. A., eds., Tectonics and mineral resources of southwestern North America: New Mexico Geol. Soc. Spec. Pub. 6, p. 5-10.

Cornwall, H. R., and Krieger, M. H., Geologic map of the El Capitan quadrangle, Gila County, Arizona: U.S. Geol. Survey Geol. Quad. Map GQ-1442, scale 1:24,000 (in press).

Creasey, S. C., 1966, Hydrothermal alteration, in Titley, S. R., and Hicks, C. L., eds., Geology of the porphyry copper deposits, southwestern North America: Tucson, Univ. of Arizona Press, p. 51-74.

Creasey, S. C., and Kistler, R. W., 1962, Age of some copper-bearing porphyries and other igneous rocks in southeastern Arizona, in Geological Survey research, 1962: U.S. Geol. Survey Prof. Paper 450-D, p. D1-D5.

Dalyrymple, G. Brent, and Lamphere, Marvin A., 1969, Potassium-argon dating: San Francisco, W. H. Freeman and Company, 250 p.

Damon, P. E., Livingston, D. E., and Erickson, R. C., 1962, New K-Ar
    dates for the Precambrian of Pinal, Gila, and Coconino Counties,
    Arizona: New Mexico Geol. Soc. Guidebook, 13th Field Conference,
    p. 56-67.

Damon, P. E., and Mauger, R. L., 1966, Epeirogeny-orogeny viewed from
    the Basin and Range province: Soc. Mining Engineers Trans.,
    v. 235, p. 99-112.

Deer, W. A., Howie, R. A., and Zussman, J., 1962, Rock forming minerals,
    Vol. 3--Sheet silicates: London, Longman Group Ltd., 270 p.

Deer, W. A., Howie, R. A., and Zussman, J., 1963, Rock forming minerals,
    Vol. 2--Chain silicates: London, Longman Group Ltd., 379 p.

Dodge, F. C. W., Smith V. C., and Mays, R. E., 1969, Biotites from
    granitic rocks of the central Sierra Nevada batholith,
    California: Jour. Petrology, v. 10, p. 250-271.

Drewes, Harald, 1971, Mesozoic stratigraphy of the Santa Rita Mountains,
    southeast of Tucson, Arizona: U.S. Geol. Survey Prof. Paper
    658-C, 81 p.

Eastlick, J. T., 1968, Geology of the Christmas mine and vicinity,
    Banner mining district, Arizona, in Ridge, J. D., ed., Ore
    deposits of the United States, 1933-1967 (Graton-Sales Vol.):
    New York, Am. Inst. Mining, Metall., and Petroleum Engineers,
    v. 2, p. 1191-1210.

Fisher, R. V., 1966, Rocks composed of volcanic fragments and their
    classification: Earth Sci. Rev., v. 1, p. 287-298.

Foster, M. D., 1960, Interpretation of the composition of trioctahedral
    micas: U.S. Geol. Survey Prof. Paper 354-B, p. 11-49.

Fournier, R. O., 1967, The porphyry copper deposit exposed in the
    Liberty open-pit mine near Ely, Nevada: Part I. Syngenetic
    formation: Econ. Geology, v. 62, p. 57-81.

Fournier, R. O., 1976, Exchange of Na^+ and K^+ between water vapor and
    feldspar phases at high temperature and low vapor pressure:
    Geochim. et Cosmochim. Acta, v. 40, p. 1553-1561.

Gilluly, James, 1946, The Ajo mining district, Arizona: U.S. Geol.
    Survey Prof. Paper 209, 112 p.

Gustafson, Lewis B., and Hunt, John P., 1975, The porphyry copper
    deposit at El Salvador, Chile: Econ. Geology, v. 70, p. 857-912.

Hart, S. R., 1964, The petrology and isotopic-mineral age relations of a contact zone in the Front Range, Colorado: Jour. Geology, v. 72, p. 493-525.

Hayes, P. T., 1970, Cretaceous paleogeography of southeastern Arizona and adjacent areas: U.S. Geol. Survey Prof. Paper 658-B, 42 p.

Hemley, J. J., and Jones, W. R., 1964, Chemical aspects of hydrothermal alteration with emphasis on hydrogen metasomatism: Econ. Geology, v. 59, p. 538-569.

Hyndman, Donald W., 1972, Petrology of igneous and metamorphic rocks: New York, McGraw-Hill Book Co., 533 p.

Irvine, T. N., and Baragar, W. R. A., 1971, A guide to chemical classification of common volcanic rocks: Canadian Jour. Earth Sci., v. 8, p. 523-548.

Jacobs, David C., and Parry, William T., 1976, A comparison of the geochemistry of biotite from some Basin and Range stocks: Econ. Geology, v. 71, p. 1029-1035.

James, A. H., 1971, Hypothetical diagrams of several porphyry copper deposits: Econ. Geology, v. 66, p. 43-47.

James, Laurence P., 1976, Zoned alteration in limestone at porphyry copper deposits, Ely, Nevada: Econ. Geology, v. 71, p. 488-512.

Kelly, W. C., and Goddard, E. N., 1969, Telluride ores of Boulder County, Colorado: Geol. Soc. America Mem. 109, 237 p.

Kiersch, G. A., 1949, Structural control and mineralization at the Seventy Nine mine, Gila County, Arizona: Econ. Geology, v. 44, p. 24-39.

Knapp, Richard B., and Knight, Jerry E., 1977, Differential thermal expansion of pore fluids: Fracture propagation and microearthquake production in hot pluton environments: Jour. Geophys. Research, v. 82, p. 2515-2522.

Krieger, M. H., 1968, Geologic map of the Saddle Mountain quadrangle, Pinal County, Arizona: U.S. Geol. Survey Geol. Quad. Map GQ-671, scale 1:24,000.

Krieger, M. H., 1974, Geologic map of the Winkelman quadrangle, Pinal and Gila Counties, Arizona: U.S. Geol. Survey Geol. Quad. Map GQ-1106, scale 1:24,000.

Kuno, H., 1960, High alumina basalt: Jour. Petrology, v. 1, p. 121-145.

Kuno, H., 1968, Differentiation of basalt magmas, in Hess, H. H., and Poldervaart, A., eds., Basalts: The Poldervaart treatise on rocks of basaltic composition, Vol. 2: New York, John Wiley and Sons, p. 623-688.

Lindgren, Waldemar, 1905, The copper deposits of the Clifton-Morenci district, Arizona: U.S. Geol. Survey Prof. Paper 43, 375 p.

Liou, J. G., 1971a, P-T stabilities of laumontite, wairakite, lawsonite, and related minerals in the system $Ca_2Al_2Si_2O_8-SiO_2-H_2O$: Jour. Petrology, v. 12, p. 379-411.

Liou, J. G., 1971b, Stilbite-laumontite equilibrium: Contr. Mineralogy and Petrology, v. 31, p. 171-177.

Lowell, J. D., 1968, Geology of the Kalamazoo orebody, San Manuel district, Arizona: Econ. Geology, v. 63, p. 645-654.

Lowell, J. D., and Guilbert, John M., 1970, Lateral and vertical alteration-mineralization zoning in porphyry ore deposits: Econ. Geology, v. 65, p. 373-408.

McCurry, W. G., 1971, Mineralogy and paragenesis of the ores, Christmas mine, Gila County, Arizona: Arizona State Univ., Tempe, Arizona, M.S. thesis.

Metz, Robert A., and Rose, Arthur W., 1966, Geology of the Ray copper deposit, in Titley, S. R., and Hicks, C. L., eds., Geology of the porphyry copper deposits, southwestern North America: Tucson, Univ. of Arizona Press, p. 177-188.

Meyer, C., and Hemley, J. J., 1967, Wall rock alteration, in Barnes, H. L., ed., Geochemistry of hydrothermal ore deposits: New York, Holt, Rinehart and Winston, Inc., p. 166-235.

Mitcham, T. W., 1974, Origin of breccia pipes: Econ. Geology, v. 69, p. 412-413.

Moore, Alan C., 1976, Intergrowth of prehnite and biotite: Mineralog. Mag., v. 40, p. 526-529.

Moore, William J., and Czamanske, Gerald K., 1973, Compositions of biotites from unaltered and altered monzonitic rocks in the Bingham mining district, Utah: Econ. Geology, v. 68, p. 269-280.

Moore, William J., and Nash, J. Thomas, 1974, Alteration and fluid inclusion studies of the porphyry copper orebody at Bingham, Utah: Econ. Geology, v. 69, p. 631-645.

Nash, J. Thomas, 1976, Fluid-inclusion petrology--data from porphyry copper deposits and applications to exploration: U.S. Geol. Survey Prof. Paper 907-D, p. D1-D16.

Nash, J. Thomas, and Theodore, Ted G., 1971, Ore fluids in the porphyry copper deposit at Copper Canyon, Nevada: Econ. Geology, v. 66, p. 385-399.

Nielsen, R. L., 1968, Hypogene texture and mineral zoning in a copper-bearing granodiorite porphyry stock, Santa Rita, New Mexico: Econ. Geology, v. 63, p. 37-50.

Orville, P. M., 1963, Alkali ion exchange between vapor and feldspar phases: Am. Jour. Sci., v. 261, p. 201-237.

Peirce, H. Wesley, 1976, Elements of Paleozoic tectonics in Arizona: Arizona Geol. Soc. Digest, Vol. X, p. 37-57.

Perry, D. V., 1968, Genesis of the contact rocks at the Christmas mine, Gila County, Arizona: Univ. Arizona, Tucson, Arizona, Ph.D. thesis, 229 p.

Perry, D. V., 1969, Skarn genesis at the Christmas mine, Gila County, Arizona: Econ. Geology, v. 64, p. 255-270.

Perry, V. D., 1961, The significance of mineralized breccia pipes: Mining Eng., v. 10, p. 367-376.

Peterson, Nels P., and Swanson, Roger W., 1956, Geology of the Christmas copper mine, Gila County, Arizona: U.S. Geol. Survey Bull. 1027-H, p. 351-371.

Phillips, Evan R., and Rickwood, Peter C., 1975, The biotite-prehnite association: Lithos, v. 8, p. 275-281.

Phillips, W. J., 1973, Mechanical effects of retrograde boiling and its probable importance in the formation of some porphyry ore deposits: Inst. Mining and Metallurgy Trans., v. 82, sec. B, p. B90-B98.

Piwinskii, A. J., and Wyllie, P. J., 1968, Experimental studies of igneous rock series: A zoned pluton in the Wallowa batholith, Oregon: Jour. Geology, v. 76, p. 205-234.

Ransome, F. L., 1919, The copper deposits of Ray and Miami, Arizona: U.S. Geol. Survey Prof. Paper 115, 192 p.

Ransome, F. L., 1923, Description of the Ray quadrangle: U.S. Geol. Survey Geol. Atlas Folio 217, 24 p.

Rehrig, W. A., and Heidrick, T. L., 1972, Regional fracturing in Laramide stocks in Arizona and its relationship to porphyry copper mineralization: Econ. Geology, v. 67, p. 198-213.

Rehrig, W. A., and Heidrick, T. L., 1976, Regional tectonic stress during the Laramide and Late Tertiary intrusive periods, Basin and Range province, Arizona: Arizona Geol. Soc. Digest, Vol. X, p. 205-228.

Reid, A. M., 1966, Stratigraphy and paleontology of the Naco Formation in the southern Dripping Spring Mountains near Winkelman, Gila County, Arizona: Univ. Arizona, Tucson, Arizona, M.S. thesis.

Roberts, Steven A., 1973, Pervasive early alteration in the Butte district, Montana, in Guidebook for the Butte field meeting, Soc. Economic Geologists, p. HH-1-HH-8.

Robinson, R. F., and Cook, Annan, 1966, The Safford copper deposit, Lone Star mining district, Graham County, Arizona, in Titley, S. R., and Hicks, C. L., eds., Geology of the porphyry copper deposits, southwestern North America: Tucson, Univ. of Arizona Press, p. 250-266.

Roedder, Edwin, 1971, Fluid inclusion studies on the porphyry-type ore deposits at Bingham, Utah, Butte, Montana, and Climax, Colorado: Econ. Geology, v. 66, p. 98-120.

Rose, A. W., 1970, Zonal relations of wall rock alteration and sulfide distribution at porphyry copper deposits: Econ. Geology, v. 65, p. 920-936.

Ross, Clyde P., 1925, Ore deposits of the Saddle Mountain and Banner mining districts, Arizona: U.S. Geol. Survey Bull. 771, 72 p.

Ross, Donald C., 1976, Prehnite in plutonic and metamorphic rocks of the northern Santa Lucia range, Salinian block, California: Jour. Research U.S. Geol. Survey, v. 4, p. 561-568.

Sales, R. H., and Meyer, C., 1948, Wallrock alteration at Butte, Montana: Am. Inst. Mining Engineers Trans., v. 178, p. 9-35.

Sheppard, Simon M. F., and Gustafson, Lewis B., 1976, Oxygen and hydrogen isotopes in the porphyry copper deposit at El Salvador, Chile: Econ. Geology, v. 71, p. 1549-1559.

Sheppard, Simon M. F., Nielsen, Richard L., and Taylor, Hugh P., Jr., 1971, Hydrogen and oxygen isotope ratios in minerals from porphyry copper deposits: Econ. Geology, v. 66, p. 515-541.

Sillitoe, Richard H., 1973, The tops and bottoms of porphyry copper
    deposits: Econ. Geology, v. 68, p. 799-815.

Sillitoe, Richard H., 1975, Subduction and porphyry copper deposits
    in southwestern North America--A reply to recent objections:
    Econ. Geol., v. 70, p. 1474-1477.

Silver, L. T., 1963, The use of cogenetic U-Pb isotope systems, in
    Radioactive dating and methods of low-level counting: Radio-
    active Dating Symposium, Internat. Atomic Energy Agency,
    Vienna, Proc., p. 779-787.

Simons, Frank S., 1964, Geology of the Klondyke quadrangle; Graham and
    Pinal Counties, Arizona: U.S. Geol. Survey Prof. Paper 461,
    173 p.

Tainter, S. L., 1948, Christmas copper deposit, Gila County, Arizona:
    U.S. Bur. Mines Rept. Inv. No. 4293.

Taylor, H. P., Jr., 1974, The application of oxygen and hydrogen
    isotope studies to problems of hydrothermal alteration and
    ore deposition: Econ. Geology, v. 69, p. 843-883.

Theodore, Ted G., and Priego de Wit, Miguel, 1976, Porphyry type
    metallization and alteration at La Florida de Nacozari, Sonora,
    Mexico: U.S. Geol. Survey Open File Report 76-760, 28 p.

Theodore, Ted G., Silberman, Miles L., and Blake, David, 1973,
    Geochemistry and potassium-argon ages of plutonic rocks in
    the Battle Mountain mining district, Lander County, Nevada:
    U.S. Geol. Survey Prof. Paper 798-A, 24 p.

Thornton, C. P., and Tuttle, O. F., 1960, Chemistry of igneous rocks:
    I. Differentiation index: Am. Jour. Sci., v. 258, p. 664-684.

Titley, Spencer R., 1966, Preface to Titley, S. R., and Hicks, C. L.,
    eds., Geology of the porphyry copper deposits, southwestern
    North America: Tucson, Univ. of Arizona Press, p. IX-X.

Titley, S. R., 1972, Some geological criteria applicable to the search
    for southwestern North American porphyry copper deposits: Am.
    Inst. Mining and Metallurgy Preprint G12, p. 1-16.

Titley, S. R., 1973, "Pyrometasomatic"--An alteration type: Econ.
    Geology, v. 68, p. 1326-1329.

Turner, Francis, J., and Verhoogen, John, 1960, Igneous and metamorphic
    petrology: New York, McGraw-Hill Book Co., 694 p.

Waters, A. C., and Krauskopf, K. B., 1941, Protoclastic border of the Colville batholith: Geol. Soc. America Bull., v. 52, p. 1355-1418.

Willden, Ronald, 1964, Geology of the Christmas quadrangle, Gila and Pinal Counties, Arizona: U.S. Geol. Survey Bull. 1161-E, 64 p.

Wright, A. E., and Bowes, D. R., 1963, Classification of volcanic breccia: A discussion: Geol. Soc. America Bull., v. 74, p. 79-86.

Yakowitz, H., Myklebust, R. L., and Heinrich, K. F. J., 1973, FRAME, an on-line correction procedure for quantitative electron probe microanalysis: Natl. Bur. Standards Technical Note 796, 46 p.